STUDIES ON THE ON-LINE IDENTIFICATION AND OPTIMAL CONTROL OF BIOREACTORS

Thesis by
Ka-yiu San

In Partial Fulfillment

of the Requirements for the Degree of

Doctor of Philosophy

California Institute of Technology

Pasadena, California
1984

(Submitted 4 January 1984)

To my parents for their continuous encouragement and support

ACKNOWLEDGEMENTS

I would like to take this opportunity to express my appreciation to my advisor, Professor Gregory N. Stephanopoulos. I am also thankful for his guidance as well as the freedom he allowed in reseach.

My interaction with other members of Dr. Stepanopoulos Group was especially enjoyable. I am also thankful for my office-mates Nam Sun Wang and Ron Grosz for not only tolerating with me but also serving as a source of new ideas during my stay at Caltech.

I am also indebted to Brian Davison for introducing me to the culture growing technique and also serving as a very helpful lab-mate. I would also like to thank Kurt Fickie for helping me putting the micro-computer together.

Finally, I would like to thank Caltech and NSF for the financial support during my tenure at Caltech.

ABSTRACT

An integrated approach is presented for the on-line estimation of the state of a biochemical reactor from presently attainable real-time measurements. Elemental and macroscopic balances are used for the determination of the total rate of growth and state-of-the-art estimation techniques are subsequently employed for the elimination of process and measurement noise and the estimation of the state variables and unknown culture parameters. The proposed approach is very flexible in that as new sensors become available they can be easily incorporated within the present framework to estimate new variables or improve the accuracy of the old ones. The method does not require any model for the growth kinetics and is very sucessful in accurately estimating the above variables in the presence of intense noise and under both steady state and transient conditions. Computer simulation as well as experimental results obtained from this study clearly demonstrate the superb performance of such estimation methodology. State estimates obtained by the proposed method can be used for the development of adaptive optimal control schemes as well as for basic studies of the characteristic properties of microbial cultures.

TABLE OF CONTENTS

LIST OF FIGURES

LIST OF TABLES

PART I. STUDIES ON THE ON-LINE IDENTIFICATION OF BIOREACTOR

CHAPTER 1

INTRODUCTION

1.1 INTRODUCTION

With recent breakthroughs in the area of genetic engineering and recombinant DNA, there are reasons to believe that in the near future more sophisticated and efficient biocatalysts can be isolated and/or manufactured. Such biocatalysts can be tailored into a custom-designed fashion to produce desired products. The success of transferring such knowledge from bench-top into large scale production will depend heavily on the ability to operate satisfactorily the bioreactor in a stable and yet efficient manner. However, due to some unique characteristics of microbial systems, which will be addressed later in this chapter, controlling a bioreactor is much more involved and complicated than controlling a ordinary chemical reactor. And it is the aim of this work to derive an on-line estimation scheme which can be applied to the study and control of such bioreactors.

Before presenting the difficulties involved with such bioreactors, it will be instructive to define several terms which will be used repeatedly in this work. Thus, the *state* of a bioreactor system is defined as the set of dependent variables which adequately describe the situation in the reactor at any point in time. It must be recognized at this point that besides temperature and pH, which are always among the *state variables*, the other components of the state vector depend on the nature of the model of the biological process considered. If a nonsegregated, non-structured approach is taken, then the state vector $\mathbf{x}$ will have as its other components lumped parameters such as the biomass concentration, b, the limiting-substrate concentration, s, the product concentration,

p, the level of dissolved oxygen, $[\ O_2]_{dis}$ and the concentrations of other substances that are of interest either as products or as factors affecting the rate of microbial growth. If one introduces structure in the model of microbial growth, the state vector will have to be augmented to include the concentrations of key intracellular intermediates. Furthermore, if the segregation of the biological processes in distinct cell units is recognized, all the above variables have to be replaced by the distribution functions of the corresponding variables in the cell population. In the estimation studies which are presented in the sequel, a non-segregated, nonstructured approach will be taken basically for two reasons: first, most of the mechanisms underlying a structured model are largely uncertain at this point and the parameters involves uncertainties even in the order of magnitude, and, second, structure and/or segregation are often characterized by a complexity that renders the corresponding models impractical for control purposes, which is one of the main uses of on-line estimates of microbial cultures. Furthermore, the variables involved in a lumped description of a growth process, when properly estimated, can be very informative about the state of microbial growth and other reactor characteristics.

Operating parameters are those parameters which can be manipulated at the will of the user so that optimal operation is achieved. The dilution rate, D, and the concentration of the limiting substrate in the feed, s_f, are such parameters in the case of continuous or fed-batch reactors. Other operating parameters include the speed of agitation, the flow rate of aeration gases through the reactor, the rate of addition of an alkali used to maintain a constant pH and the flow rate and properties of a coolant stream used to maintain a constant temperature. If so desired the pH and temperature can also be varied in a predetermined manner that results in optimal reactor operation.

Culture parameters or *growth parameters* are the parameters that describe the state of growth of microorganisms as well as the state of the other processes associated with the process of growth. Such parameters are the specific growth rate, μ, the various yields, Y, the mass transfer rate of O_2 and CO_2 in the liquid phase (in particular, the factor $K_L a$ – the product of the mass transfer coefficient by the interfacial area per unit volume), and others.

One can write conservation equations for mass and energy to relate the state variables to the operating and culture parameters. Under transient conditions, these equations have the form of differential equations expressing the time rate of change of the state variables as functions of the operating and culture parameters. This system of differential equations will be self-contained provided that the culture parameters can be expressed as functions of the state variables through models of growth or empirical correlations. Numerious such models have appeared in the literature relating μ to s, p, b, etc. (Fredrickson and Tsuchiya, 1977), Y to s (Crooke *et al.*) and $K_L a$ to the power input and broth properties (Bailey and Ollis, 1977). The various parameters involved in these models will be called *model parameters*.

1.2 IMPORTANCE OF ON-LINE ESTIMATION

Although the above mentioned models were rather successful in some cases and served their purpose well, they are quite limited in scope and applicability because they were developed for very specific systems, and their extension to other system is, as of now, questionable. Also, such models are incapable of accounting for the effect on the corresponding culture parameters of all possible factors, many of which (toxins, promoters, etc.) are not and cannot be even included in the list of state variables. Moreover, these kinetic models of growth and product formation are mostly empirical, not globally or uniformly valid,

cannot account for all the phenomena observed, and involve parameters which are subject to change during the course of growth (for example, yield) or are poorly determined from batch growth experiments (*e.g.*, K_s constant of the Monod model). More detailed structured models can be constructed, but the uncertainty introduced by the large number of model parameters precludes their use for the proposed estimation of state variables or control . Also contributing to the complexity of the problem is the sensitivity of the microbial culture to the environment in which it is growing.

The above mentioned difficulties clearly indicate the need to develop an on-line estimation methodology to yield information on the level of cell biomass, specific growth rates, yields, concentrations of substrate and product, and others without using models and at various operating conditions.

Not only does the on-line estimation of the above parameters provide for an extended array of parameters that can be monitored thus describing more completely the biological process, but it also yields continuous information thus eliminating the uncertainty and speculation about the events that took place between two consecutive samples. Finally, the filtering of measurements, which is a part of the estimation process, eliminates any random noises and yields smooth reliable estimates.

The second use of on-line estimates is for control purposes. To date, the control of bioreactors is limited to pH and temperature regulation realized by local analog controllers. In some cases the level of dissolved oxygen is also controlled through the manipulation of agitation rate and/or gas flow rate. Although it does not seem possible that computer implemented direct digital control will replace the above controllers, some other changes are almost certain to put in place as the complexity of the reactor system increases to meet

continuously expanding requirements.

First, in batch operation, the profiling of some state variables (especially temperature and pH) has been shown to increase productivity (Constantinides *et al*, 1970). Second, fed-batch reactors are being introduced because of the ability of these reactors to maintain an optimal substrate level throughout the course of fermentation by properly controlling the feed rate. In the above case, if reliable growth models are available, the optimal profiles of the state variables (pH, temperature) and operating parameters (flow rate in a fed-batch reactor) can be obtained as the solution to an optimal control problem. However, as is more often the case, when no models can be used, the optimal operation of the above reactor depends on how accurately the remaining state variables can be estimated from the available data. Third, future biological processes engaging in large volume applications will be strongly bent toward continuous operation. These continuous flow applications, in the form of suspended cultures or immobilized cell reactors, will be subject to a great variety of operating perturbations and culture instabilities thus requiring effective controls for satisfactory operation. Before the potential of continuous operation is realized, definite improvements will have to be made in their operability and control, and central to this activity is the development of efficient schemes for the accurate on-line estimation of the bioreactor state. Finally, digital set-point control is gaining popularity, and one can envision many situations where the available computers will be used for this purpose, as in programmed start-up procedures, automated variation of set-points to implement an optimal policy, predetermined response to various perturbations and others. Clearly, the determination of a new set-point will rely on the accurate knowledge of the bioreactor state, and state estimators will be indispensable for this purpose as well.

1.3 AIM AND SCOPE OF THIS WORK

It is the ambition of this work to produce a general, on-line estimation theory which is model independent in that it does not assume or require any kind of specific relationships between the culture parameters (such as μ, Y, *etc.*) and the state variables (such as s, p, b, *etc.*) The proposed approach consists of augmenting the state vector to include, in addition to the state variables, those of the culture parameters which are not desirable to be expressed by models, and expressing the dynamics of these parameters by differential equations obtained from adaptive estimation theories. Coupled to the so-derived state dynamics are measurements attainable with presently available sensors. The overall objective of the approach proposed herein is to utilize the above formulation to obtain reliable, noise-free estimates of the state variables and culture parameters, on-line and under both steady-state and transient dynamic conditions. Such estimates will be essential for on-line adaptive control schemes and can also be used for basic investigations of the culture under consideration.

NOTATION

b	biomass concentration
D	dilution rate
$K_L a$	volumetric mass transfer coefficient
p	product
s	limiting - substrate concentration
s_f	limiting - substrate concentration in the feed
$\mathbf{x}$	general state vector
Y	yield

GREEK LETTERS

μ	specific growth rate

CHAPTER 2

THEORY

2.1 INTRODUCTION

As it was discussed in the previous chapter there is a need for the development of an on-line identification methodology which can estimate the bioreactor state variables and culture parameters without making use of any models and from a limited numbers of available measurements. In this chapter, the general framework of such a methodology utilizing the available macroscopic and elemental balances and appropriate state-of-the-art estimation techniques will be presented.

The essence of this approach is to represent a biological growth process with or without product formation by a chemical reaction. The coefficients of this chemical reaction (which are related to the yields), are not usually constant during the growth process especially during transient conditions. Therefore, the identification problem requires that such coefficients be determined continuously. It will be shown later in this chapter that by employing the concept of macroscopic and elemental balances, together with the appropriate measurements, enough equations may be generated to evaluate the various coefficients.

The approach described above produces an estimate of the total rate of growth, which is the product of the specific growth rate, μ, and the biomass concentration, b. In order to obtain an estimate on b and μ separately, we take the approach to model the specific growth rate as a time-varying parameter of the system which is to be estimated from the measurements. In this chapter, the development and implementation of such estimator into the general estimation

scheme will be presented.

2.2 BALANCES

The available balances will be best utilized if the possible measurements that can be taken in a bioreactor are first identified. The recognition of the need for on-line measurements discussed earlier spurred a noticeable activity on the development of sensors for the on-line measurement of substances of interest in the operation of biochemical reactors (Hikuma *et al.*, 1979; Danielsson *et al.*, 1979; Hendy and Gray, 1979; Gondo *et al.*, 1980; Kjellen and Neujahr, 1980; Lee and Lim,1980; Kulys and Kadziauskiene, 1980) Most of these sensors, however, seem to suffer from convergence and slow response problems, and they are not as yet fully tested and commercially available. Consequently, the estimation studies proposed herein will be based on the measurement of O_2 and CO_2 concentrations in the off-gases because the corresponding sensors (IR, paramagnetic analysers, mass spectrometers) are commercially available and are also characterized by fast response and high reliability. Other sensors, such as dissolved oxygen, pH, and temperature probes, are also available and their use, in connection with the estimation of additional state variables and culture parameters, will be examined in a later section after the basic ideas have been presented in this and the following sections, It should be also emphasized at this point that any new measurements which may become available in the future can be easily incorporated within the proposed framework for the determination of other useful parameters or for the improvement of the accuracy of the ones that can be estimated presently with the available sensors. In this regard, these estimation studies can also serve to establish a hierarchy in the sensor development activity.

The first attempt for the indirect but on-line measurement of cell biomass

and growth rate was based on a macroscopic balance over the fermentor and was first proposed by Yamashito *et al.*(1969). According to this approach, provided that no secondary metabolites are formed, the *total* rate of biomass growth R (in gr/cm^{3}s) is determined by

$$R = \frac{Y}{V}(F_{in} - F_{out}) \tag{2.1}$$

where V is the volume of the fermentor, Y the yield of biomass with respect to the component under consideration, (gr biomass/ gr component), and F_{in}, F_{out} the rates (in gr/s) at which a component that is consumed during the fermentation is supplied and removed from the fermentor, respectively.

The above approach involved the assumption of a constant Y which is questionable for a large number of fermentations and certainly not valid under transient conditions. This problem was bypassed by coupling the above equation with the four elemental balances for C, H, O and N, and this allowed for a continuous estimate of Y, to be obtained. The use of the elemental balances was proposed by Jefferis and Humphrey(1979), and Cooney *et al.*(1977) and was demonstrated in the production of baker's yeast (Cooney *et al.*, 1979), and single-cell protein from ethanol (Ziegler and Humphrey, 1979). See also Bravard *et al.*(1979), Madron(1979), and Ho(1979) for other related studies. The basic feature of this method is to represent the process of growth by a chemical reaction in which substrate is converted, in the presence of oxygen and ammonia, to biomass, carbon dioxide and water, according to the following reaction:

$$aC_xH_yO_z + bO_2 + cNH_3 \longrightarrow C_\alpha H_\beta O_\gamma N_\delta + dH_2O + eCO_2 \tag{2.2}$$

If the empirical formulae of the carbon-energy source and cell biomass are assumed to be known and constant during fermentation (a reasonable assumption), then the only unknowns in the above scheme are the five

stoichiometric coefficients a,b,c,d, and e (five and not six, since they can be normalized with respect to the coefficient of cell mass). One can write four elemental balances for C, H, O and N involving these coefficients. A fifth equation can be obtained by utilizing the on-line measurements of O_2 and CO_2 concentrations in the gas stream that flows continuously through the fermentor. These five equations fully determine the values of the five stoichiometric coefficients of Eq. (2.2) as described in more detail below.

The four elemental balances are:

$$C \;:\; xa = \alpha + e \tag{2.3a}$$

$$H \;:\; ya + 3c = \beta + 2d \tag{2.3b}$$

$$O \;:\; za + 2b = \gamma + d + 2e \tag{2.3c}$$

$$N \;:\; c = \delta \tag{2.3d}$$

One can eliminate a,c and d among the above equations to obtain a relationship between b and e. This relationship, which is equivalent to the balance of the degree of reductance obtained by making an electron balance (Erickson *et al.*,1978), can be written in terms of the yields of O_2 consumption, Y_{O_2}, and CO_2 formation, Y_{CO_2}, for the latter can be expressed in terms of b and e simply by:

$$Y_{O_2} = \frac{(MW)_b}{32b} \quad \text{and} \quad Y_{CO_2} = \frac{(MW)_b}{44e} \tag{2.4}$$

where MW_b in the last equation denotes the molecular weight of biomass. The resulting relationship between Y_{O_2} and Y_{CO_2} then is:

$$4x\frac{(MW)_b}{32Y_{O_2}} + (2z - y - 4x)\frac{(MW)_b}{44Y_{CO_2}} = 2\gamma x + y\alpha + 3x\delta - x\beta - 2z\alpha \tag{2.5}$$

Two components which can be easily measured are oxygen and carbon dioxide concentrations in the off-gas. If the concentrations C, of these two gases are measured at the entrance and the exit of the fermentor, two equations similar to Eq. (2.1) can be written involving Y_{O_2} and Y_{CO_2}, namely:

$$R = \frac{32 Y_{O_2}}{V}(Q_{in} C_{O_2,in} - Q_{out} C_{O_2,out}) = \frac{44 Y_{CO_2}}{V}(Q_{out} C_{CO_2,out} - Q_{in} C_{CO_2,in}) \quad (2.6)$$

where Q_{in} and Q_{out} are the volumetric gas flow rates at the entrance and exit of the fermentor. Now Eqs (2.5) and (2.6) constitute a system of two equations in two unknown, Y_{O_2} and Y_{CO_2}. If the measurements of the flow rates and concentrations of O_2 and CO_2 are available, these equations can be solved to determine, on-line, all the yields and, through them, the rates of microbial growth, substrate consumption, etc.

The above approach can produce estimates of the yields and *total rates* of growth, substrate uptake, etc., if no metabolic product is formed in appreciable quantities. It is, however, desirable to obtain estimates of the concentration of biomass, substrate, products etc., as well as estimates of specific rates of growth, substrate uptake, etc., from these measurements, for these parameters describe the situation in a bioreactor fully. This can be achieved by coupling to the above elemental balances and macroscopic balances with respect to the gases, the unsteady state macroscopic balances with respect to the biomass, substrate and product. The method with which one obtains such estimates will be presented shortly, after certain points which are usually overlooked are first discussed. These points are related to the validity of Eq. (2.6), the formation of products, and the presence of noise in the measurements.

2.3 VALIDITY OF EQUATION (2.6)

Equation (2.6) is the steady state design equations of a continuous stirred tank reactor (CSTR). Since many bioreactors do not operate at a steady state mode, (batch, fed-batch), and, since, even under steady state operation one would need to detect trends that may upset the reactor, it is desirable that state variables and culture parameters be estimated under transient, as well as steady state, conditions. The use of Equation (2.6) under transient conditions with respect to the biological processes presupposes that the reactor operates at a quasi-steady state with respect to the O_2 and CO_2 dynamics. This assumption will be valid provided that (a) the residence time of the gas stream is much smaller than the characteristic time of growth (for example, the reciprocal of the specific growth rate at all time for batch or fed-batch, or the reciprocal of the dilution rate for continuous operation) and (b) the buffering capacity of the abiotic medium in O_2 and CO_2 is small.

The first of the above requirements is very often satisfied in most fermentation processes because of the large volume of gases required for aeration. Similarly, the capacity of most fermentation broths in O_2 is very small due to the very small solubility of O_2 in such solutions. More attention is needed with CO_2 because of possible interference of pH changes with its dynamics. This becomes clear if one considers the ionic interactions of dissolved CO_2 in a fermentation medium:

$$\begin{array}{l} B \longrightarrow H_2CO_3^* \underset{\leftarrow}{\rightarrow} HCO_3^- + H^+ \\ \quad\quad\quad\quad \uparrow \downarrow \\ \quad\quad\quad\quad CO_{2\,gas} \end{array} \qquad (2.7)$$

According to this scheme, CO_2 produced by the biological process (B) appears in the medium in the dissolved (CO_{2aq}) or hydrated (H_2CO_3) form. These forms are usually combined together and represented as a single entity, $H_2CO_3^*$.

This dissolved/hydrated CO_2 can escape as CO_2 gas or undergo dissociation to form bicarbonate ions and protons.

At a true steady state (with respect to pH and H_2CO_3, besides biomass and substrate), the CO_2 evolution rate is directly proportional to the rate at which CO_2 is formed as a result of microbial metabolism and Eq. (2.6) is valid. However, changes in the pH can cause changes in the amount of CO_2 evolved which may be interpreted incorrectly as changes of the rate of growth. Furthermore, if a buffer solution is used for pH control, the dissociation constant of the weak electrolytes that constitutes the buffer will have to be compared to the equilibrium constants of Eq. (2.7), and mainly K_1, to insure that any changes in $[H^+]$ will be absorbed quickly by the buffer and will not affect the rate of CO_2 evolution. If a pH controller is employed to maintain a constant pH by adding an alkali to the medium, small oscillations of CO_2 concentration will result from the successive additions of the alkali. The amplitude of these oscillations depends on the range the pH is allowed to vary and the level of pH at which the oscillation is occurring. A 10% variation in $C_{CO_2,out}$ is typical of pH variations within 0.1 of a pH unit at pH 7. With regard to this complication, one may try to (a) minimize the variation by controlling the pH very tightly, (b) take this effect into consideration in the calculation of the CO_2 evolution rate, or (c) utilize these pH and CO_2 excursions to obtain information in K_La, the level of dissolved CO_2 and other parameters.

In conclusion, the physiochemical properties of the broth will have to be examined carefully if CO_2 measurements in the gas phase are to be associated reliably with the process of growth in the way indicated by Eq. (2.6). If this is not possible, the dynamics of CO_2 evolution must be taken into consideration as determined by the process of growth, the ionic equilibrium and the mass transfer process from the liquid to the gas phase. Further discussion on this

point is provided in a later section.

2.4 PRODUCT FORMATION

In the case of product formation, Eq. (2.2) must be modified to account for the formation of the product:

$$a C_6H_{12}O_6 + bO_2 + cNH_3 \rightarrow C_\alpha H_\beta O_\gamma N_\delta + dH_2O + eCO_2 + f C_{\alpha'} H_{\beta'} O_{\gamma'} N_{\delta'} \quad (2.8)$$

In the above equation $C_{\alpha'}H_{\beta'}O_{\gamma'}N_{\delta'}$, represents the chemical formula of the product. Clearly, the presence of a product introduces one more unknown, and an extra, on-line measurement is needed for the determination of the unknown stoichiometric coefficient. It will be shown in Chapter 5 that the measurement of the amount of alkali/acid added to control the pH could serve this purpose.

If more products are formed more sensors will be required unless a known stoichiometric relationship exists between the various metabolic products. Clearly, if such relationships are not sufficient, it is possible that the availability of proper sensors will limit the types of fermentations which can be studied this way.

2.5 NOISE IN THE MEASUREMENTS

Despite claims to the contrary, the procedure outlined earlier produces an estimate of only the *total* rate of growth, R, which is the product of the specific growth rate, μ, and the biomass concentration, b, and not μ and b severally. Since μ and b are important elements in defining the state of a fermentor, various attempts were made for their estimation. One effort consists of integrating the governing differential equation with known initial conditions. For a batch reactor, for example, b was estimated by integrating

$$\dot{b} = R(t) \quad ; \quad b\,(0) = b_o \quad (2.9)$$

where b_0 is the initial concentration and $R(t)$ the measured rates; μ was subsequently estimated as the ratio R/b. Similar method were employed for continuous and fed-batch reactors.

The main criticism of these methods is that no consideration was given to random errors and noises which are always present both in the process and the measurements, In a continuous system, for example, mixing assumptions need to be made which are not always satisfied, the level of the working volume may fluctuate, wall growth may occur, and, furthermore, errors are involved in the measurement of the dilution rate, the flow rate of the gases, and, to a lesser extent, in the measurement of O_2 and CO_2 concentrations. Averaging the measurements reduces the intensity of the noises but does not eliminate the problem, may introduce other complications, and does nothing about the process noise.

The above indicate that the obtained values of R and Y are corrupted by measurement and process uncertainties and cannot be used directly in Eq. (2.9) for the estimation of the bioreactor state. Integrating Eq. (2.9) by using direct measurements of R is equivalent to attempting the estimation of the final position of an object from the measurements of its initial position and its velocity at subsequent time instants, and such an estimate is not possible to obtain accurately. In fact, it can be shown (Stephanopoulos and San, 1981) that the variance of the estimates of b obtained this way increases continuously with time if a batch reactor is employed. The implication of this is that even if one starts with a very accurate estimate of the inoculum concentration, there will come a time at which the variance of (and, therefore, the uncertainty associated with) the estimate of b have grown unacceptably high. Unless the measurements are absolutely noise-free, the estimates of b, μ, etc. will eventually become unreliable. Similar results can be obtained for a fed-batch reactor, and the conclusion

reach earlier (Wang *et al*, 1977) regarding the need for reinitialization of the biomass concentration estimate after several integration steps of Eq. (2.9) can be considered as a manifestation of the above assertion. For a continuous bioreactor the variance tends to a constant but high value, and still large measurement errors tend to produce large estimation errors. It will be shown below how proper estimation theories can be employed to eliminate noise and produce accurate estimates of the state variables and culture parameters.

2.6 THE GENERAL ESTIMATION PROBLEM

A brief presentation of the basic features of the general estimation problem is attempted below. A linear system is first considered because exact solutions are available of these systems. The nonlinear case is discussed later.

In a biochemical reactor system, as is often the case with state estimation problems, the state of the system (b, s, p) is not directly measurable but it is observable through the measurement of other parameters (output) of the system, such as O_2 and CO_2 concentrations and, through them, R and the yields. The state estimation problem then can be generally stated as follows, if the state $\mathbf{x}$ of a dynamical system satisfies the following linear equation

$$\dot{\mathbf{x}} = \mathbf{A}\mathbf{x} + \mathbf{B}\mathbf{u} + \zeta(t) \tag{2.10}$$

which is forced by the nonrandom input (the control) $\mathbf{u}$ and the random disturbance $\zeta(t)$, how does one develop an algorithm for determining the state $\mathbf{x}(t)$ at time t from the observations of an output $\mathbf{y}$ of the system, contaminated with random errors $\xi(t)$ and related to the state $\mathbf{x}$ by

$$\mathbf{y} = \mathbf{H}\mathbf{x} + \xi(t) \tag{2.11}$$

Because of the errors ξ in the measurement, $\mathbf{x}$ can never be found, and we have to settle for an estimate $\hat{\mathbf{x}}$. In the presence of the random noises $\zeta(t)$ and

$\xi(t)$, the estimation problem will have to be understood in the sense of finding an estimate $\hat{\mathbf{x}}$ of the state $\mathbf{x}$ such that the uncertainty, or the variance, of the estimation error is minimized. The process of constructing $\hat{\mathbf{x}}$ is called filtering because it is essentially one of extracting the signal form the noise. A distinction, however, must be made here between the above filter and usual R-C filters (such as averaging). The latter would be adequate if all that were required were an output smoothing. However, the key function performed by the filters to be discussed below is the estimation of unmeasured states and imprecisely known parameters, a very useful function that a simple filter cannot perform. It is instructive to notice, in this regard, that when the dimension of the output $\mathbf{y}$ is smaller than that of the state $\mathbf{x}$ and when the matrix $\mathbf{H}$ is such that all the components of the state contribute to the output $\mathbf{y}$, (observable system), the state can still be reconstructed. If averaging were to be used for $\mathbf{y}$, one would be left with less equations than unknowns to estimate $\mathbf{x}$ and would have to resort to unwarranteed *ad hoc* procedures for this purpose.

The theory of filtering is too involved to go into in detail but can be found in Jazwinski (1970). We shall be content with a brief presentation of the results and basic features here. If the noise $\zeta(t)$ and $\xi(t)$ can be modelled by white noise processes then the estimate $\hat{\mathbf{x}}$ can be found as the solution of the following filter equation (Kalman-Bucy filter):

$$\dot{\hat{\mathbf{x}}} = \mathbf{A}\hat{\mathbf{x}} + \mathbf{B}\mathbf{u} + \mathbf{K}(\mathbf{y} - \mathbf{H}\hat{\mathbf{x}}) \tag{2.12a}$$

with $\mathbf{K}$, the filter gain, given by

$$\mathbf{K} = \mathbf{P}\mathbf{H}^T\mathbf{R}^{-1} \tag{2.12b}$$

and the variance of the estimation error (a measure of the uncertainty in the estimate of $\mathbf{x}$), $\mathbf{P} = E[(\mathbf{x} - \hat{\mathbf{x}})(\mathbf{x} - \hat{\mathbf{x}})^T]$, given by

$$\dot{\mathbf{P}} = \mathbf{AP} + \mathbf{PA}^T + \mathbf{Q} - \mathbf{PH}^T\mathbf{R}^{-1}\mathbf{HP} \qquad (2.12c)$$

The matrices $\mathbf{Q}$ and $\mathbf{R}$ (positive-definite matrices) are measures of the intensity of the noises ζ and ξ, respectively; $\mathbf{Q}\delta(t-\tau) = E(\zeta(t)\zeta^T(\tau))$, $\mathbf{R}\delta(t-\tau) = E(\xi(t)\xi^T(\tau))$. (E[.] is the expected value operator).

The characteristic features of the above estimation algorithms can be best presented by considering the schematic of Figure 2.1. Let the true values of the state $\mathbf{x}$ be represented by the solid curve so marked and the state estimate at time t be as indicated. If no account of the measurement noise is taken, the state estimate at t+1, $\mathbf{x}_{t+1}$, is obtained by integrating $\dot{\mathbf{x}} = \mathbf{A}\hat{\mathbf{x}} + \mathbf{Bu}$ with $\hat{\mathbf{x}}(t) = \hat{\mathbf{x}}_t$ as initial condition. The actual deviation of this estimate from the true value is not known; what can be determined is the variance of $\hat{\mathbf{x}}_{t+1}$ which is obtained by integrating $\dot{\mathbf{P}} = \mathbf{AP} + \mathbf{PA}^T + \mathbf{Q}$, and which will be certainly high and increasing with time. If, however, the filter equations (2.12 a-c) are used, the dynamic equation of the estimate must be corrected by a term proportional to the difference between the actual measurement $\mathbf{y}_{t+1}$ and the prediction of the output based on $\mathbf{x}_{t+1}$, $\mathbf{Hx}_{t+1}$, as indicated by equation (2.12a). Notice that the proportionality constant $\mathbf{K}$ depends proportionally on the variance of the estimate and inversely proportionally on the intensity of the noise of the measurement. Thus, the higher the accuracy of the current state estimate and the lower the intensity of the measurement noise, the more heavily the correction will be weighed in readjusting the dynamics of $\hat{\mathbf{x}}$. With this adjustment, a better estimate for the state is obtained, (indicated by $\hat{\mathbf{x}}_{t+1}$ in Fig. 2.1), and with significantly lower variance than that of $\mathbf{x}_{t+1}$. This latter result is derived from the presence of the term $\mathbf{PH}^T\mathbf{S}^{-1}\mathbf{HP}$ in the variance equation (2.12c) which tends to decrease the variance against the opposite effects of the accumulated state uncertainties and process noise as represented by $\mathbf{AP} + \mathbf{PA}^T$ and $\mathbf{Q}$, respectively, in the variance equation. If the above filtering algorithms are not used then the compounding of

accumulated state uncertainties and process noise will eventually make the estimates unreliable.

To implement these filters one needs to integrate simultaneously the system of ordinary differential equations (2.12) with initial conditions $\hat{\mathbf{x}}(0)$ and $\mathbf{P}(0)$, the a priori estimates of the state $\mathbf{x}(0)$ and the variance or the uncertainty associated with this estimate. If $\mathbf{x}(0)$ is known exactly, say $\mathbf{x}_0$, then $\hat{\mathbf{x}}(0) = \mathbf{x}_0$ and $\mathbf{P}(0) = 0$. If not, even crude estimates of $\hat{\mathbf{x}}(0)$ will suffice, provided the variance $\mathbf{P}(0)$ is chosen sufficiently large to reflect the uncertainty proportionately. Then, integration of Eqs (2.12) will give the best estimates for $\mathbf{x}$ in the sense that the sum of the squares of the estimation errors is minimum.

Uncertain parameters, π, may also be estimated in the same way by treating them as additional state variables with appropriate dynamic equations. Usually $\dot{\pi} = 0$ is chosen, and this gives accurate estimates if the unknown parameters do not change substantially with time. In the estimation problem under consideration, μ and Y will be treated as additional state variables. These culture parameters, however, may experience significant variations during the course of a fermentation so that more sophisticated equations, based on adaptive estimation theories, had to be developed for their estimation. These equations are presented in the following section.

Equations (2.12) described the evolution of the estimate $\hat{\mathbf{x}}$ and its variance $\mathbf{P}$ with time for a linear system. Most systems of practical interest, however, are nonlinear and are of general form:

$$\dot{\mathbf{x}} = \mathbf{f}(\mathbf{x}) + \zeta(t) \qquad ; \qquad \dot{\mathbf{y}} = \mathbf{h}(\mathbf{x}) + \xi(t) \qquad (2.13)$$

For such systems, a variety of filtering algorithms have been advanced, one of which is the extended Kalman filter, obtained by linearizing the nonlinear equations around the current estimate and applying Eqs (2.12) to the linearized

equations:

$$\dot{\hat{\mathbf{x}}} = \mathbf{f}(\hat{\mathbf{x}}) + \mathbf{K}(\mathbf{y} - \mathbf{h}(\hat{\mathbf{x}})) \tag{2.14a}$$

$$\mathbf{K} = \mathbf{P}\mathbf{h}_{\mathbf{x}}^{T}(\hat{\mathbf{x}})\mathbf{R}^{-1} \tag{2.14b}$$

$$\dot{\mathbf{P}} = \mathbf{f}_{\mathbf{x}}(\hat{\mathbf{x}})\mathbf{P} + \mathbf{P}\mathbf{f}_{\mathbf{x}}^{T}(\hat{\mathbf{x}}) + \mathbf{Q} - \mathbf{P}\mathbf{h}_{\mathbf{x}}^{T}\mathbf{R}^{-1}\mathbf{h}_{\mathbf{x}}(\hat{\mathbf{x}})\mathbf{P} \tag{2.14c}$$

the above equations apply to the case when the measurements are taken continuously with time. This, of course, is neither necessary nor convenient, and filter equations exist for the case of intermittent measurements also.

2.7 ESTIMATION OF PURE CULTURE

With this background to the state estimation theory we now turn to the specific problem of estimating the state of a bioreactor which is employed for the propagation of a pure culture. Assume, initially, that no metabolic product is formed.

First, the set of variables that can be measured and the set of variables that compose the state vector must identified. As indicated in a previous section, the measurement of the O_2 and CO_2 concentrations at the entrance and exit of the bioreactor, together with the four elemental balances, allows for the determination of the total rate of growth, R, and the yield with respect to the substrate, Y_s. Therefore, R and Y_s will be the measured variables. Of the state variables, one would certainly like to monitor the biomass and substrate concentrations, b and s, but also the specific growth rate, μ, and the yield, Y_s which are culture parameters. Since it is not desirable to use a model for the dependence of μ and Y_s on b and s, both of them will have to be treated as state variables. The state vector will then comprise four variables, namely, b, s, μ and Y_s.

The measured variables are related to the state variables as follows:

$$R = \mu b + \xi_1(t) \tag{2.15a}$$

$$Y_{s,ms} = Y_s + \xi_2(t) \tag{2.15b}$$

where ξ_1 and ξ_2 are two white-noise processes of intensity equal to $\sigma_i^2, i = 1,2$, which account for the uncertainties and measurement errors involved in the determination of R and Y_s.

Equations (2.15 a-b) relate the two measurements R and Y_s to the state variables μ, b, and Y_s and, in this sense, they are the equivalent to the measurement equation (2.11) of the general case. To complete the formulation, equations for the dynamics of the state must also be supplied. This is straightforward for b and s, for their dynamic equations are given by the conservation balances over the bioreactor, namely:

$$\dot{b} = \mu b - Db \tag{2.16a}$$

$$\dot{s} = D(s_f - s) - \frac{1}{Y_s}\mu b \tag{2.16b}$$

where s_f is the feed concentration and D is zero for a batch reactor, the dilution rate for a continuous reactor, and equal to $\frac{\dot{V}}{V}$ for a fed-batch reactor. For lack of appropriate information no process noise was considered but can easily be added when such information becomes available.

A note on the observability of the concentration of the substrate, (and if a product is formed, that of the product), is in order here. Since the measured variables are the rates of change of b and s only, the latter is not observable from Eqs (2.16 a-b) in the strict sense of the word. This is not true for the concentration of biomass because the measured variable R does depend in the values of b and, in the sense of the usual observability criteria, changes in the values of b will cause changes in the measured value of R thus contributing to

the observability of this state variable. To bypass the problem that arises from the non-observable nature of s, (and p), these state variables were estimated by direct integration of the corresponding dynamic equations after, the filtered and noise free estimates of μ, Y_s and b had been substituted in for Eq. (2.16 b).

For μ there is no balance that one can use. As indicated previously, the usual approach is to set $\dot{\mu} = 0$, and this gives good convergent results for time-invariant parameters. The performance of the estimator, however, for time-varying parameters, such as μ, was found to be unsatisfactory. Several approaches were investigated for improving the estimates of time-varying specific growth rates. One possibility is to employ an adaptive estimation method and write for μ : $\dot{\mu} = \zeta(t)$ with $\zeta(t)$ a white-noise process with variable intensity, σ_ζ^2. The basic idea here is to improve the estimates of μ and the other state variables basically through changes in the variance equation and, in particular, through adaptive changes of the term Q. Recall that the matrix $Q\delta(t-\tau)$ equals $E[\zeta\zeta^T]$ and is therefore a function of σ_ζ^2. By changing σ_ζ^2 according to the value of the current estimate and measurement, the dynamic of the variance, and through it, μ, are affected. A sensible way of changing σ_ζ^2 is to check the residual between the predicted and measured values of the measurable variable at time $t + dt$ and set σ_ζ^2 equal to zero if the residual is within one standard deviation of the measurement noise, because, in this case, the measured variable is consistent with the statistics under null hypothesis that no change in μ occurred between t and $t + dt$. Otherwise, a proper correction is set for σ_ζ^2 so as to "open" the estimation algorithm to incoming observations (Jazwinski, 1970).

The above approach gives good but slow response for time varying μ. The algorithm can be further improved by treating ζ as a color noise, implemented by:

$$\dot{\mu} = C + \eta(t) \tag{2.17a}$$

$$\dot{C} = \eta'(t) \tag{2.17b}$$

with $\eta(t)$, $\eta'(t)$ white-noise processes having the same properties as $\zeta(t)$ above, with $\sigma_{\eta'}^2 = \sigma_{\eta}^2$. The response is quicker but a tendency to overshoot was detected so that a damping force was added to the equation for C above. Similar investigation regarding Y_s, led to the following equations for the adaptive estimation of μ and Y_s:

$$\dot{\mu} = \eta_1(t) + C \tag{2.16c}$$

$$\dot{C} = -CD + \eta_1'(t) \tag{2.16d}$$

$$\dot{Y}_s = \eta_2(t) \tag{2.16e}$$

The above equations (16 a-e) were tested in a variety of cases characteristic of the operation of biochemical reactors and were found to produce excellent estimates of the state. Most of these numerical studies and supporting experimental results are presented in later chapters. Because of the excellent agreement between true and estimated value of μ, b, s, and Y_s, it is proposed that the scheme of Eqs. (2.16c-e) for the dynamics of μ and Y_s be adopted for the on-line estimation of bioreactors. The previously presented estimation algorithms then can be applied to the state equations (2.16 a-e) and measurement equations (2.15 a,b), to generate state estimates under various operating conditions.

The implementation of the estimation algorithms (2.14 a-c) to the bioreactor system described by Eqs. (2.15 a,e) and (2.16 a-e) requires:

(i) Proper initial conditions which will depend upon the accuracy with which the state is known initially.

(ii) Expressions for the matrices Q and R in terms of the intensities of the white-noise processes η_1, η_2, ξ_1, and ξ_2.

Recalling the definitions of Q and R one can write the following for equations (16 a-e):

$$Q = \begin{bmatrix} 0 & 0 & 0 & 0 & 0 \\ 0 & 0 & 0 & 0 & 0 \\ 0 & 0 & \sigma_{\eta_1}^2 & \sigma_{\eta_1}^2 & 0 \\ 0 & 0 & \sigma_{\eta_1}^2 & \sigma_{\eta_1}^2 & 0 \\ 0 & 0 & 0 & 0 & \sigma_{\eta_2}^2 \end{bmatrix} \tag{2.18}$$

and

$$R = \begin{bmatrix} \sigma_1^2 & 0 \\ 0 & \sigma_2^2 \end{bmatrix} \tag{2.19}$$

In writing Equations (2.18) and (2.19) it has been assumed that the white-noise processes ξ_1 and ξ_2 as well as η_1 and η_2 are independent and that ξ_1 and ξ_2 have intensity equal to σ_1^2 and σ_2^2, respectively. The adaptive intensities of η_1 and η_2 are given by the following expressions:

$$\sigma_{\eta_1}^2 = \begin{cases} 0 & \text{if} \quad \Phi_1 \leq 0 \\ \Phi_1 = \dfrac{1}{\kappa_1}\left[\left(R - \hat{\mu}\hat{b}\right)_{t+1}^2 - \left(P_\mu \hat{b}^2 + 2P_{\mu b}\hat{\mu}\hat{b} + P_b\hat{\mu}^2\right)_{t+1} - \sigma_1^2\right] & \text{if} \quad \Phi_1 > 0 \end{cases} \tag{2.20}$$

$$\sigma_{\eta_2}^2 = \begin{cases} 0 & \text{if} \quad \Phi_2 \leq 0 \\ \Phi_2 = \dfrac{1}{\kappa_2}\left[\left(Y_{s,ms} - \hat{Y}_s\right)^2 - \left(P_{Y_s}\right)_{t+1}^2 - \sigma_2^2\right] & \text{if} \quad \Phi_2 > 0 \end{cases} \tag{2.21}$$

where $P_\mu = E\left[\left(\mu - \hat{\mu}\right)^2\right]$, $P_{\mu b} = E\left[\left(\mu - \hat{\mu}\right)\left(b - \hat{b}\right)\right]$, $P_b = E\left[\left(b - \hat{b}\right)^2\right]$, and $P_{Y_s} = E\left[\left(Y_s - \hat{Y}_s\right)^2\right]$, all elements of the covariance matrix P, known at the time instant t. The two constant κ_1 and κ_2 determined through computer simulation

are introduced to optimize the dynamics of the response. The values used in this paper are $\kappa_1 = \kappa_2 = \frac{1}{3}$. Notice that the units of κ_1 and κ_2 are $[b^2 t]$ and $[t]$, respectively. Also notice that as far as the consistency of Eqs. (2.20) and (2.21) is concerned, σ_1^2 and σ_2^2 should be written as $\sigma_1^2 \delta(t-\tau)$ and $\sigma_2^2 \delta(t-\tau)$, respectively, but in the actual implementation of the algorithm, σ_1^2 and σ_2^2 are taken as the square of the measurement error.

(iii) Simultaneous integration of the estimation equation (2.14) using the on-line obtained measurement of R and Y_s.

An important adaptive feature of the above estimation algorithm is revealed by a close examination of the three terms involved in the expression for the variable intensity $\sigma_{\eta_1}^2$ in Eq (2.20). The first term is the residue between the measured and predicted value of R, the second is the uncertainty associated with the available estimates of μ and b at time t, and the third reflects the uncertainty of the measurements of R. If, $\Phi_1 < 0$; i.e., if the residue is less than the combined uncertainties of the estimates and measurements, the observed discrepancy between measurement and prediction is attributed to random errors and is essentially ignored as far as the dynamics of μ is concerned. If, on the other hand, the residue exceeds the uncertainties of the estimate and measurement, a systematic trend is detected in the values of μ and the estimation algorithms are adjusted accordingly by opening the filter to incoming measurements. Similar observations hold for Eq. (2.21).

2.8 DISCUSSION

The analysis presented above section covers the case of a pure culture growing in a bioreactor with no product formation, when only O_2 and CO_2 measurements are available. There are, however, some other types of measurements that can be taken with presently available sensors. The potential use of these

measurements and the case of product formation are discussed below.

Measurement of Dissolved Oxygen: This measurement can be readily obtained by a dissolved oxygen electrode. Although it cannot be used for the estimation of another state variable, such as the product concentration if there is product formation, it can serve to enhance the accuracy of the other estimates, as well as to estimate the useful mass-transfer parameter, $K_L a$. For this purpose, the set of measurable parameters and the state vector are augmented to include several additional variables as indicated in Table 2.1 which contains the complete set of measurement and state equations in this case.

Numerical experiments conducted to test the effectiveness of the above scheme showed that, (a) the accuracy of the estimates of μ, b, s, and Y_s was definitely improved over the case without dissolved O_2 measurements, and (b) the agreement between the estimated and true values of $K_L a$ was very good. Consequently, the mass-transfer parameter, $K_L a$, can be estimated, on-line, and under real growth conditions, to be used for modelling, design, or control purposes. Furthermore, the efficiency with which these estimates can be obtained points out to the possibility of using the above approach to determine $(K_L a)_o$ under varying conditions of agitation, growth, vessel configuration, broth viscosity, etc. This information would be very useful in checking the validity of existing correlations for $(K_L a)_o$ obtained under non-growth conditions.

Estimation of Dissolved CO_2: This can be achieved by adding to the measurement equation of Table 2.1:

$$Y_{CO_2,ms} = Y_{CO_2} + \xi_6 \qquad (2.22a)$$

Also the following equations for the dynamics of dissolved CO_2 , $[CO_2]_{dis}$ must be added to the state equations:

$$[\dot{CO_2}]_{dis} = \frac{\mu b}{Y_{CO_2}} - (K_L a)_c \left[[CO_2]_{dis} - [CO_2^*] \right] \tag{2.22b}$$

$$\dot{Y_{CO_2}} = \eta_5 \tag{2.22c}$$

where $[CO_2^*]$ is the CO_2 concentration at equilibrium with $C_{CO_2,out}$ and $(K_L a)_c$ the volumetric mass transfer coefficient for CO_2. According to the CO_2 production scheme of Eq. (2.7), Eq. (2.22b) is valid for the description of small perturbations of the concentration of dissolved CO_2 about a steady state. For transients of longer duration the equilibrium with the bicarbonate ion must be considered. This equilibrium is affected by the proton concentration and, through it, by the production of acidic or basic products and their interaction with the buffer. The situation becomes more involved and its analysis will be presented in Chapter 5.

If the estimation equations that correspond to the system of Table 2.1 and Eqs. (2.22) are integrated with on-line measurements of gas phase O_2, CO_2 concentrations, and $[O_2]_{dis}$, on-line estimates of $[CO_2]_{dis}$ will be obtained along with estimates of $(K_L a)_o$, $[O_2]_{dis}$, b, s, μ, and the yields. It is possible, also to use prior estimates of $(K_L a)_o$ and then integrate the estimation equations corresponding to the basic system of Eqs. (2.15) and (2.16) augmented by Eqs. (2.22 a-c). A package of lower dimensions will thus result requiring less integration time for its implementation. It is assumed above that $(K_L a)_o$ and $(K_L a)_c$ are related in the same way as the diffusion coefficients of O_2 and CO_2 respectively in the fermentation medium. If this is not so then equations for the estimation of $(K_L a)_c$ similar to those in Table 2.1 for $(K_L a)_o$ will have to be added.

Product Formation: When a metabolic product is formed during fermentation, the same approach described above for the pure culture can be applied to include the product in the chemical reaction representation of the growth process. However, the number of unknown stoichiometric coefficients in

Eq. (2.8) increases to six, and the four elemental balances together with the measurement of the respiratory quotient are not sufficient for their on-line determination. If, as quite often is the case, a pH variation results from the biological processes of growth and product formation, then some pH-control related measurement can yield valuable information for the closure of the equations that determine the unknown stoichiometric coefficients. Detailed analysis based on the pH measurement to yield extra information about the process will be presented in Chapter 5.

Other Measurements: Central to the development of the previous estimation methods is the ability to determine on-line the stoichiometric coefficients of Eqs. (2.2) or (2.8), and, through them, the total growth rate per unit volume, R. With this in mind, the impact of a new measurement that may become available in the future, can be easily assessed. In a growth situation where R and the yields can be determined on-line from existing measurements, the addition of a new measurement, will increase the accuracy of the estimates and the speed of convergence of the algorithm, a useful improvement. Furthermore, the observability of the entire system will be significantly enhanced, for, in this case, a direct feedback mechanism will be available to compare estimates and measurements and provide the necessary corrections when significant deviations between the two are detected. This new measurement is incorporated in the previous structure by adding

$$Z_{ms} = Z + \xi_8 \tag{2.27a}$$

and

$$\dot{Z} = D(Z_f - Z) + \frac{1}{Y_Z}\mu b \tag{2.27b}$$

in the measurement and state equations, respectively, with Z standing for

b, s, p, or any other product or substrate that can be measured directly on-line.

If on the other hand, R and the yields cannot be determined on-line, developing a new measurement to achieve this is of utmost importance. In this context, a measurement of the rate of consumption or formation, rather than the concentration, of a substrate or product will be most useful, for such a rate measurement can be employed directly for the determination of R and the yields. If this is not possible and only the concentration is provided by the new measurement, an extra equation for R is, apparently

$$R = Y_Z\left(Z_{t+\delta t} - Z_t\right)\frac{1}{\delta t} \tag{2.28}$$

and the same structure, as previously, can be employed for state estimation.

In conclusion, an integrated approach for the on-line estimation of state variables and culture parameters of biochemical reactors has been presented in this chapter. Computer simulation and experimental results indicated that the obtained on-line estimates are in good agreement with the true values and the off-line measurements, respectively. These results will be presented in Chapter 3 and Chapter 4 respectively.

$$\dot{x} = Ax + Bu + \zeta(t)$$

$$y = Hx + \xi(t)$$

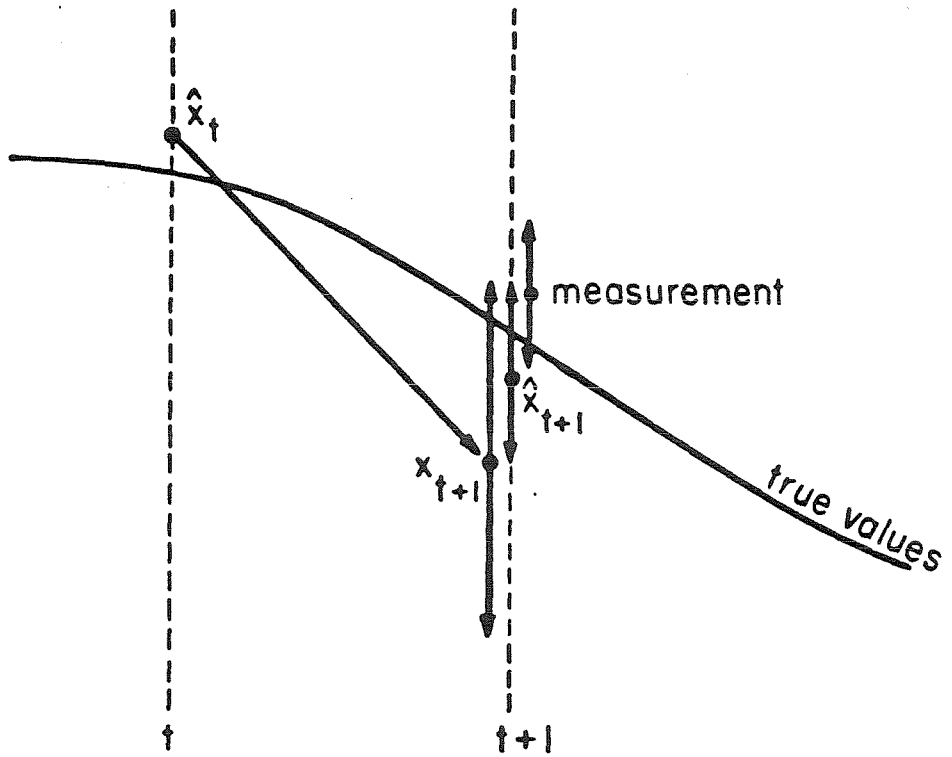

$$\dot{\hat{x}} = A\hat{x} + Bu + K(y - H\hat{x}) \; ; \qquad K = PH^T R^{-1}$$

$$\dot{P} = AP + PA^T + Q - PH^T R^{-1} HP$$

Fig. 2.1 Schematic showing the adaptive filtering algorithm

TABLE 1

MEASUREMENT OF DISSOLVED OXYGEN

Measurement Equations		State Equations	
R	$= \mu b + \xi_1$	$\dot{b}$	$= \mu b - Db$
$Y_{s,ms}$	$= Y_s + \xi_2$	$\dot{s}$	$= D(s_f - s) - \frac{1}{Y_s}\mu b$
$Y_{O_2,ms}$	$= Y_{O_2} + \xi_3$	$\dot{\mu}$	$= C + \eta_1$
$[O_2]_{dis,ms}$	$= [O_2]_{dis} + \xi_4$	$\dot{C}$	$= -CD + \eta_1$
R_{O_2}	$= (k_L a)_0\left[[O_2^*] - [O_2]_{dis}\right] + \xi_5$	$\dot{Y}_S$	$= \eta_2$
where the volumetric oxygen uptake rate is given by		$\dot{[O_2]}_{dis}$	$= (k_L a)_0\left[[O_2^*] - [O_2]_{dis}\right] - \frac{1}{Y_{O_2}}\mu b$
$R_{O_2} = \frac{1}{V}\left[Q_{in}C_{O_2,in} - Q_{out}C_{O_2,out}\right]$		$\dot{(k_L a)_0}$	$= \eta_3$
$\left[[O_2^*]\right.$ is at equilibrium with $\left.C_{O_2,out}\right]$		$\dot{Y}_{O_2}$	$= \eta_4$

NOTATION

A,B	matrix in the description of the state dynamics
a,b,c	gmole of carbon source, oxygen and ammonia, respectively, consumed per gmole of cell biomass produced
a	interfacial area per unit volume
b	biomass concentration
c	concentration of O_2 and CO_2 at the entrance and exit of the reactor
$[CO_2^*]$	concentration of CO_2 in the liquid phase at equilibrium with $[CO_2]_{out}$
$[CO_2]_{dis}$	concentration of dissolved carbon dioxide
D	dilution rate
d,e,f	gmole of H_2O, CO_2 and product , respectively, formed per gmole of cell biomass produced
f	function for the state dynamics
F	rate at which a component is supplied or removed from the fermentor
F_{NH_3}	time rate of ammonium addition (gmole/time)
H	measurement matrix
h	measurement equation
K	filter gain
$(K_L a)_i$	volumetric mass transfer coefficient; o:oxygen, c:carbon dioxide
MW_b	molecular weight of biomass
$[O_2^*]$	concentration of O_2 in the liquid phase at equilibrium with $[O_2]_{out}$
$[O_2]_{dis}$	concentration of dissolved oxygen
P	covariance matrix
Q	volumetric flow rate of gases
Q	measure of the process noise intensity
R	total rate of growth per unit volume
R	measure of the noise intensity of the measurement

s	limiting - substrate concentration
s_f	limiting - substrate concentration in the feed
$\mathbf{u}$	general control vector
V	reactor volume
$\mathbf{x}$	general state vector
x, y, z	number of C,H and O, respectively, in a molecule of carbon source
y	measurement defined in Eq. (2.11)
Y_i	yield of biomass with respect to component i, $i=p, s, O_2, CO_2$
$Y_{i,ms}$	measured value of yield Y_i
Z	additional measurement defined in Eq. (2.27)

GREEK LETTERS

$\alpha,\beta,\gamma,\delta$	numbers of atoms of C,H,O and N , respectively, in cell biomass
$\alpha',\beta',\gamma',\delta'$	numbers of atoms of C,H,O and N in a molecule of product
ζ	random disturbance of process
η	white-noise process, define in Eqs. (2.17)
κ_i	constants defined in Eqs. (2.20) and (2.21)
μ	specific growth rate
ξ	random errors in the measurements
σ_i^2	intensity of the white-noise processes ξ_i, $i=1,2$
$\sigma_{\eta_1}^2$	intensity of the white-noise process ζ_1 (Eq. (2.27))
Φ_i	defined by Equations (2.20) and (2.21)

CHAPTER 3

COMPUTER SIMULATIONS

3.1 INTRODUCTION

Results obtained from the numerical studies that were carried out in order to evaluate the estimation methodology as presented in the previous chapter will be discussed in this chapter. The objective of these numerical studies was threefold: a) to examine the ability of the estimator to produce the correct parameter values from inaccurate initial guesses, b) to investigate the possibility of using the estimation scheme as a mechanism for detecting abrupt or gradual changes in the culture parameters, and c) to study the general dynamic properties of the estimator by comparing the "true" values to the estimates obtained under a variety of operating conditions.

3.2 NUMERICAL SIMULATIONS

A series of numerical simulations was carried out with the purpose of evaluating the general properties of the proposed estimator and fine-tuning the time constants that appear in the dynamic equations for the culture parameters. In Eqs. (2.15 a-b) and (2.16 a-e) there is only one such time constant which was set equal to the inverse of the dilution rate in Eq. (2.16d). This does not have to be necessarily so, however. For a different choice of the time constant, Eq. (2.16d) should be written in general as:

$$\dot{C} = -\frac{C}{\tau} + \eta_1(t) \tag{3.1}$$

The criteria for choosing the time constant τ are rapid detection of any changes

and good convergence properties for the state variables and culture parameters. In the absence of any information about the effect of τ, the latter can be given the value of a characteristic time of the system such as the inverse of the dilution rate for a continuous or fed-batch reactor or the inverse of the maximum specific growth rate for a batch reactor. These choices produced, in general, very satisfactory results in our simulations.

The numerical simulations were performed as follows: Models were assumed for the dependence of the specific growth rate μ and the substrate yield Y_s on the bioreactor state variables, namely b and s. The bioreactor design equations, (Eqs. 2.16 a,b), were then integrated for various values of the operating parameters to yield the variation of the state variables b and s as a function of time. From the resulting values of b and s, the values of the total rate of growth, R $(=\mu b)$, and the yield, Y_s, were determined and subsequently corrupted with an additive random white noise that represents 15% measurement error by employing a random number generator. The so obtained values of R and Y_s were used as raw data in the measurement equations (2.15 a-b) and then the estimation algorithm was employed for the reconstruction of the state and culture variables. The algorithm is described by Eqs. (2.14 a-c) as these equations apply to the measurement and process equations (2.15 a-b) and (2.16 a-e), respectively. It should be noted that a direct comparison between the estimated and the "true" values is possible and can be used to evaluate the efficiency of the estimator.

3.3 RESULTS AND DISCUSSION

Results characteristic of the estimator performance obtained from the numerical studies are shown in Figs. 3.1-3.5. For the results of Figs. 3.2,3.3, and

3.5, the Monod model was employed for $\mu(s)$ with $\mu_{max} = 0.5\ hr^{-1}$ and $K_s = 0.05$ gr/ l together with a constant substrate yield Y_s of 0.5 gr of biomass/ g of substrate. No model was used in the simulations of Figs. 3.1 and 3.4. Instead, constant values for μ and b were assumed in the results of Fig. 3.1 and the raw data R were constructed by corrupting the product μb with the aforementioned noise. Figure 3.4 depicts the situation of a chemostat operating at a constant dilution rate and suffering a gradual decrease in time in the specific growth rate μ. The value of b was obtained by integrating $\dot{b} = \mu b - Db$, using the shown time variation of μ, and the value of R were afterwards similarly constructed as μb.

Figure 3.1 shows the approach to the true values of b and μ when the initial guesses of these variables were incorrect. It can be seen that the estimates converge to the true values ($10\ g/cm^3$ and $0.7\ hr^{-1}$) in a short time period when the algorithm is initiated at the incorrect values of $9\ g/cm^3$ and $0{,}65\ hr^{-1}$, respectively. These results indicate that the performance of the estimator is independent of the accuracy with which the parameters to be estimated are known initially. Furthermore, other simulations indicated that other initial guesses, significantly different from the true values, will eventually converge but they require a longer period of time.

The response of the true and estimated values of b and μ to a series of step changes of the dilution rate of a chemostat is shown in Fig. 3.2. Again, a very good agreement is observed suggesting that a similar experiment could be applied to a chemostat in order to study the properties of the specific growth rate under steady-state and dynamic conditions. It should be noticed that μ converges to the value of the maximum specific growth rate, μ_{max}, following a step increase of the dilution rate to a value larger than μ_{max}, suggesting that μ_{max} can be conveniently estimated by a washout chemostat experiment.

A constant substrate yield was assumed in the above simulations. This need not be so, however, and Fig. 3.3 shows the estimates of μ and b as functions of time when Y_s is not constant but depends on μ in a manner similar to that depicted in Fig. 3a of Wang *et al.*, 1970. Figure 3.3 shows the estimates of the specific growth rate and cell biomass concentration following a step change in the dilution rate from 0.25 to 0.55 hr^{-1}. The response to a stepwise change is similar to that of Figs 3.2.

An important feature of a good estimator is the ability to reliably detect changes or variations in the values of the important culture parameters as they may develop during the course of a fermentation. In this case a control scheme can be based on such an estimator in order to maintain the optimal operation of the bioreactor in the presence of undesirable disturbances. In order to test the proposed estimator in that regard the operation of a chemostat was simulated under conditions in which the specific growth rate was initially kept constant and subsequently decreased linearly with time. The results are shown in Fig. 3.4. It can be seen there that after an initial period of less than one hour the drop in the specific rate is reliably detected and followed closely by the estimator for the entire period of variation. The estimator can be modified to estimate almost instantaneously changes in the specific growth rate or other culture parameters. This can be achieved by employing a scheme similar to that of Eqs. (2.17 a-b) for the dynamics of μ. However, in this case the estimates almost invariably tend to overshoot the true value of μ especially after the linear drop of the "true" μ is terminated and stabilized at another lower value. A control structure based on an estimator with such dynamic behavior will tend to be unstable so the scheme of Eqs. (2.16 a-e) is proposed as the one with the best overall dynamic features.

In another simulation the estimator was tested during a chemostat washout experiment. Figure 3.5 shows the results in a situation where the chemostat is initially at steady state and at time t = 2 hr., the dilution rate is raised to a value large than μ_{max}. Again the agreement between true and estimated values for all three of μ, b and s is very satisfactory. Shown in Fig. 3.5 are also the smoothed estimates of the above variables. Fixed interval smoothing (Gelb, 1979) is a non-real-time data processing scheme which utilizes all the measurements in a fixed time interval 0 to t. It consists of a suitable combination of a forward filter that processes all the data before time t to give an estimate $\hat{x}_f(t)$, and a backward filter that processes all the data after time t to find an estimate $\hat{x}_b(t)$. The smoothed estimate $\hat{x}_s(t)$ is then obtained as

$$\hat{x}_s(t) = P_s(t)\left[P_f^{-1}(t)\hat{x}_f(t) + P_b^{-1}(t)\hat{x}_b(t)\right] \tag{3.2}$$

where

$$P_s(t) = \left[P_f^{-1}(t) + P_b^{-1}(t)\right]^{-1} \tag{3.3}$$

and P_f, P_b and P_s are the variances of the forward, backward and the smoothed estimates, respectively. As seen in Fig. 3.5 the smooth estimates are in excellent agreement with the true values.

Results presented in this chapter are a representative cross-section of a variety of numerical simulations that were carried out in order to study the proposed estimation methodology. The excellent behavior that was invariably observed is indicative of the capabilities of the estimator for on-line identification of bioreactors. In order to test the estimator with a real system, the method was applied to the identification of a fed-batch reactor employed for the propagation of and ethanol formation by a culture of *Saccharomyces cerevisiae*. The results of this experimental work will be presented in the next chapter.

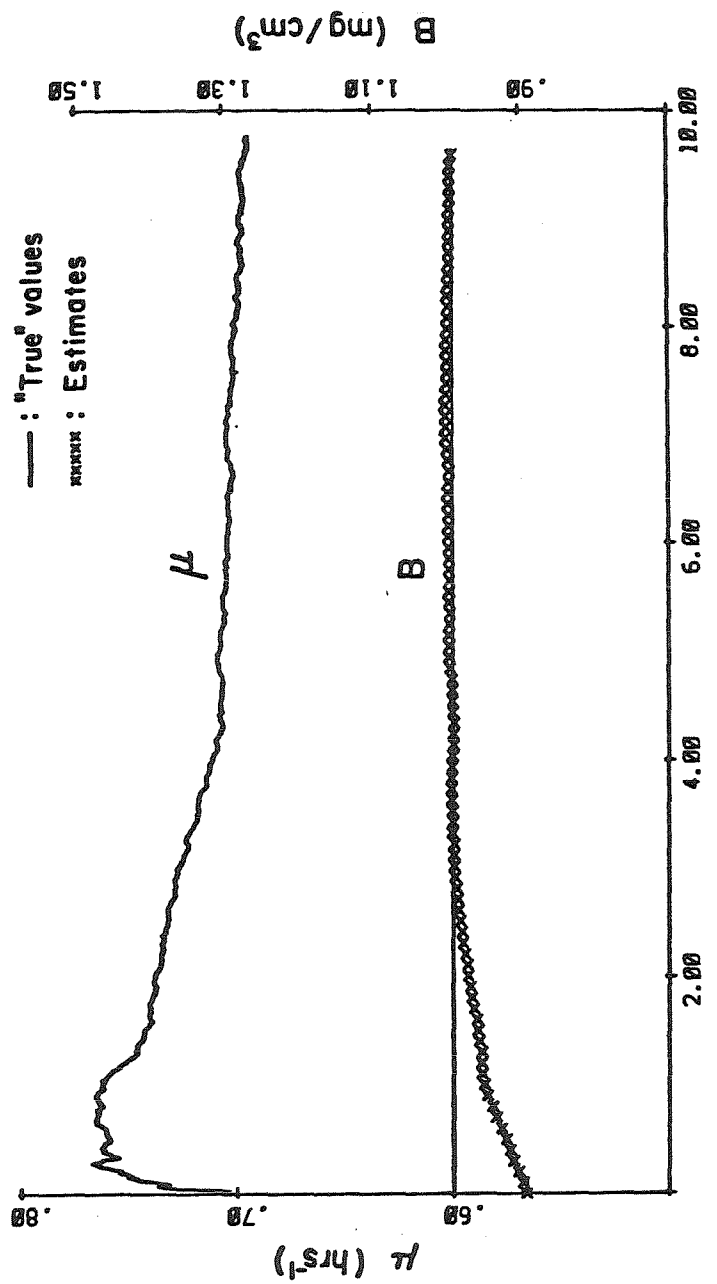

Fig. 3.1 Comparison between the estimates and true values for incorrect initial condition

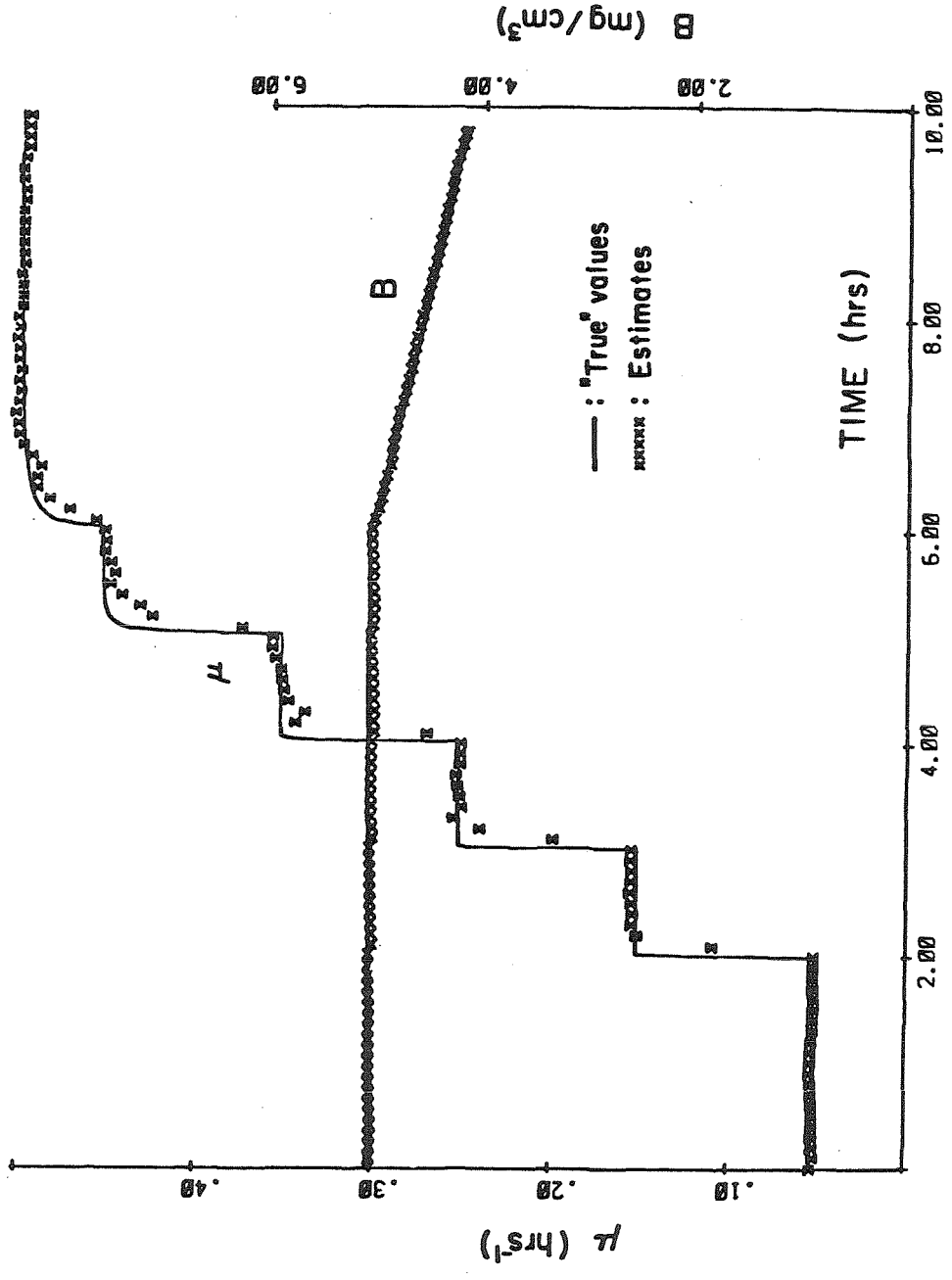

Fig. 3.2 Response of estimator to a series of step changes in the dilution rate for continuous reactor with a constant yield

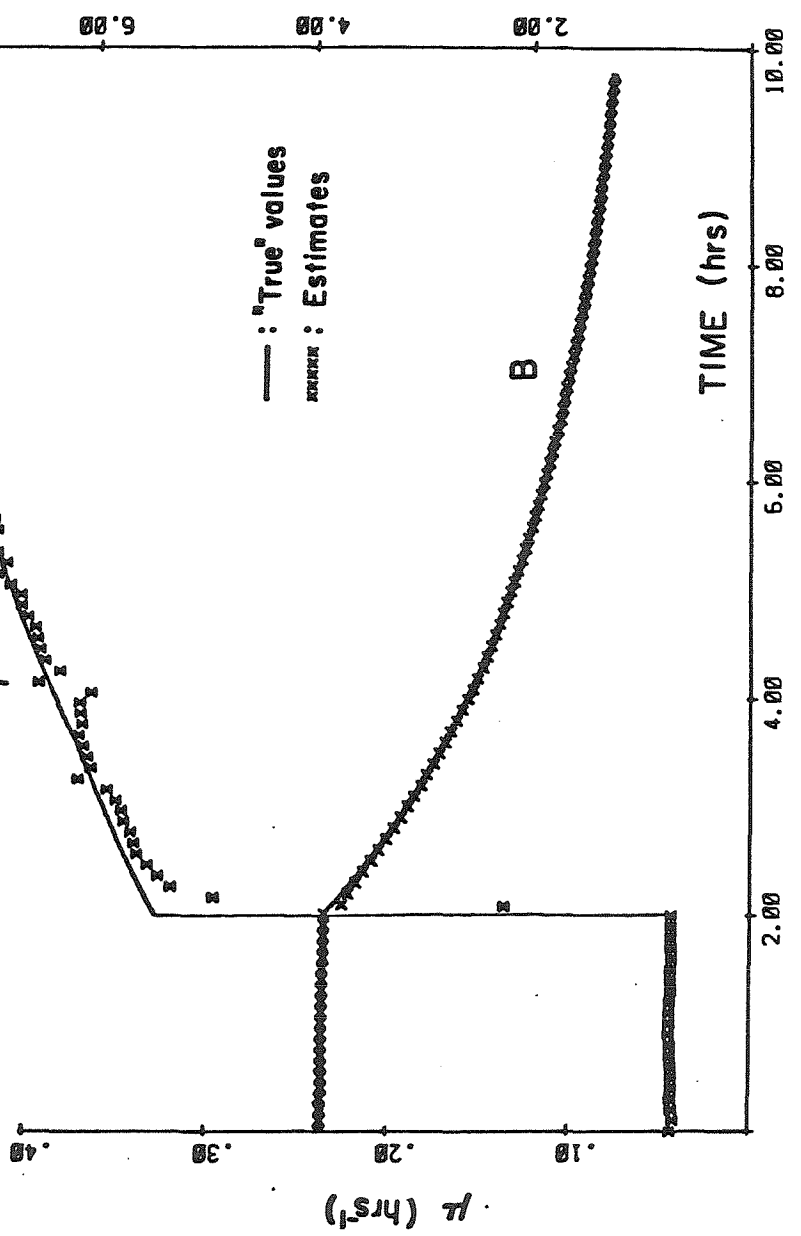

Fig. 3.3 Response to a similar set of changes as in Fig. 3.2 but with a time-varying yield

Fig. 3.4 Comparison between estimates and true values for a chemostat culture with a constant dilution rate and specific growth reate decreasing linearly with time

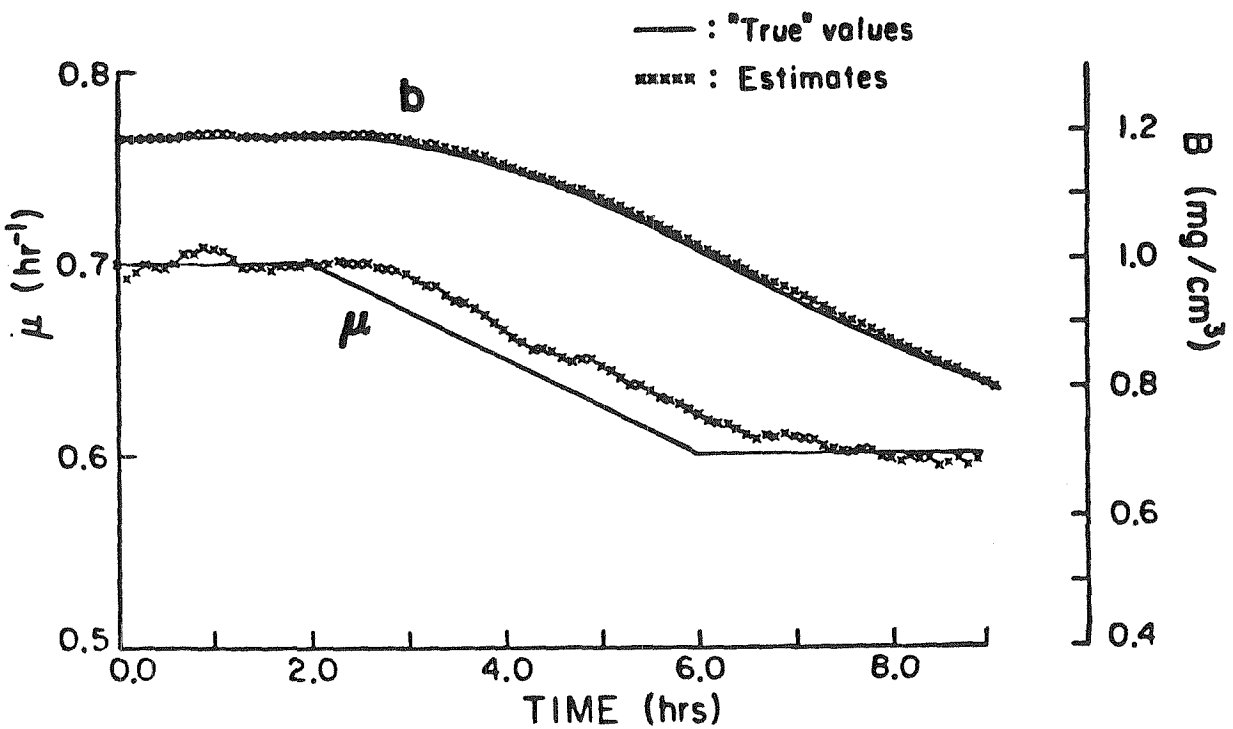

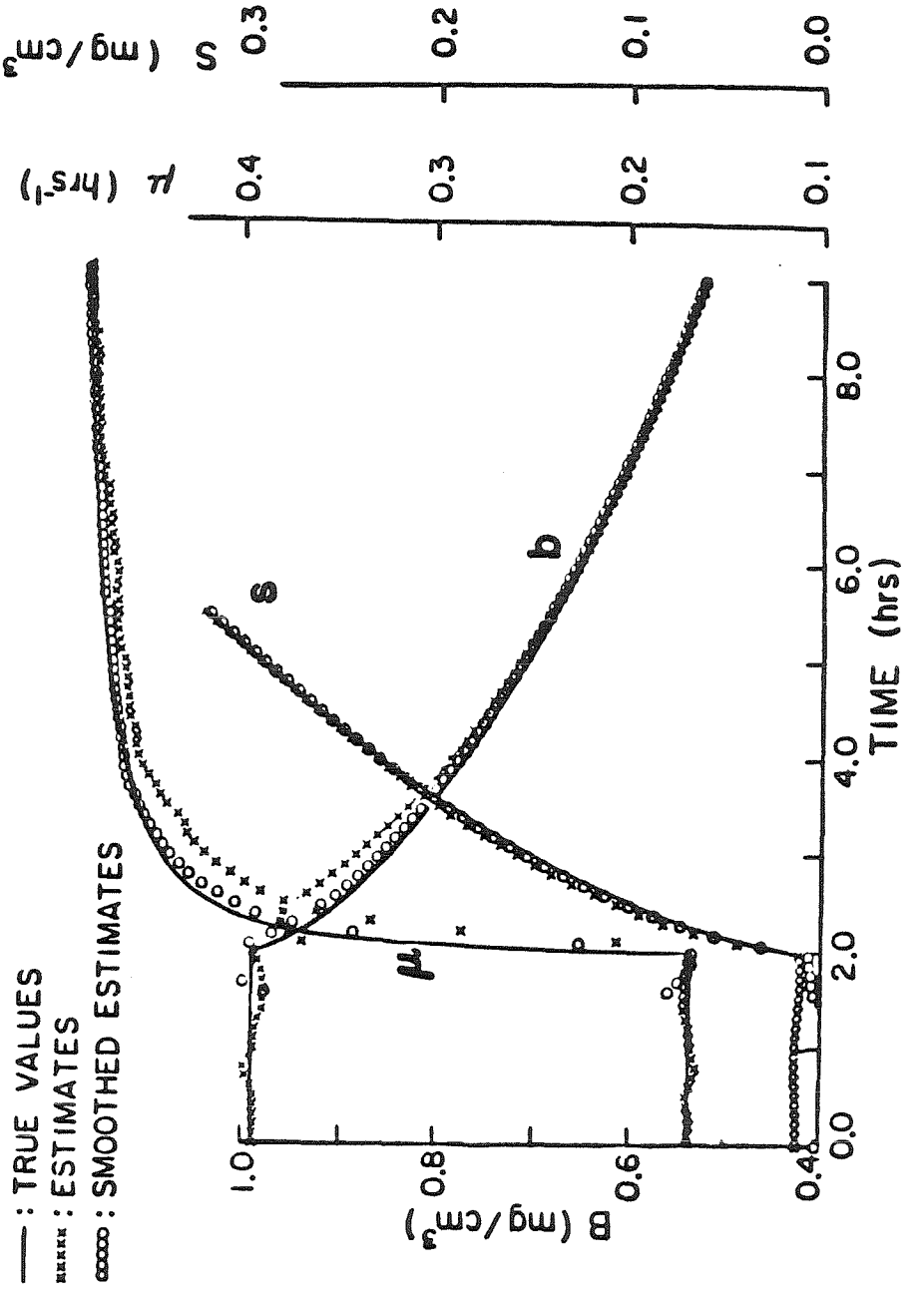

Fig. 3.5 Comparison between the estimates and true value for a washout simulation of a chemostat culture

NOTATION

b	biomass concentration
C	dummy variable defined in equation 3.1
D	dilution rate
K_s	constant defined in Monod model
P	covariant matrix
R	total rate of growth per unit volume
S	substrate concentration
t	time
Y_s	substrate yield

GREEK LETTERS

μ	specific growth rate
μ_{max}	maximum specific growth rate
τ	time constant in equation 3.1
η	white noise process associated with equation 3.1

CHAPTER 4

EXPERIMENTAL STUDIES

4.1 INTRODUCTION

A methodology for the on-line state and parameter estimation of a bioreactor has been presented in Chapter 2. This method first employs the concept of elemental and macroscopic balances together with presently available real-time measurements to solve for the coefficients of Eq. (2.1); adaptive filtering techniques are subsequently applied to provide good estimates of the state and culture parameters of the bioreactor. Furthermore, successful computer simulations of such a methodology have also been presented in chapter 3. In order to test this estimator in a real system, the method was applied for the on-line identification of yeast fermentation of ethanol from glucose in a fed-batch reactor.

In this chapter, a detailed description of the experimental set-up and procedure will be presented. The experimental system can be divided into three parts. The first part is concerned mainly with the fermentation process which consists of a NBS 14-litre Microferm fermentor with other accessories, such as two 13-litre medium jars, a waste jar, an antifoam jar, etc. The second part is instrumentation, which include a pH controller regulating the pH of the fermentor at a prescribed set-point, a mass flow controller controlling the flowrate of air into the fermentor, the oxygen and carbon dioxide gas analyzers measuring the O_2 and CO_2 gas concentration in the exhaust air stream. The third part is a data acquisition system based on a Z-80 microprocessor. The analog signals from the above mentioned instruments are converted into digital signals and stored on a floppy disk for later data analysis.

Also presented in this chapter are the results obtained by applying the estimation methodology to the on-line identification of *S. cerevisiae* grown on

glucose in a fed-batch reactor. On-line estimates of the concentrations of cell biomass, glucose, and ethanol concentrations, the specific growth rate, and the substrate and product yields are compared with off-line measurements of the same quantities. As shown in later sections, the agreement was very good and confirmed the ability of the estimator to provide accurate on-line state and parameter estimates under conditions applicable to bioreactor operation. The generally very good characteristics of the identification methodology as witnessed by these experiments point out that the proposed estimator can be profitably used for on-line identification and control of biochemical reactors.

The sensitivity problems related to this estimation scheme with respect to the respiration quotient will also be discussed.

4.2 PRELIMINARY STUDIES

The fermentation of *S. cerevisiae*, strain ATCC #18790 was studied in an NBS Microferm fermentor operated in a fed-batch mode. Ethanol is the main product formed during this fermentation. Acetic acid and some other organic acids are also formed. However, the rates of formation are very small compared to that of ethanol so these products are ignored in formulating the elemental balances for carbon, hydrogen, oxygen, and nitrogen. Following the formulation of Chapter 2, the processes of growth and ethanol formation with glucose as the carbon-energy source can be represented by the following overall reaction:

$$aC_6H_{12}O_6 + bO_2 + cNH_3 \longrightarrow C_\alpha H_\beta O_\gamma N_\delta + dH_2O + eCO_2 + fC_2H_6O \qquad (4.1)$$

In order to determine the elemental composition of biomass, a batch fermentation was performed. Cells were withdrawn from the reactor at various times during the course of the fermentation and analyzed for C, H, and N content. The sample was centrifuged at 1000 RPM for 15 minutes at 4^oC. The cells were twice washed with distilled water at 4°C and were centrifuged. Then, the pellets were dried in a preweighed aluminum dish at 100°C for 24 hrs and

analyzed for C, H, and N, oxygen being determined by the difference.

The results of these analyses are summarized in Table 4.1. This table shows the calculated elemental chemical formulae of cell biomass that correspond to the various samples and corresponding molecular weights based on one carbon atom per mole of biomass in accordance with the formulation of Chapter 2. Based on the results of Table 4.1 an average formula of $CH_{1.666}O_{0.51}N_{0.168}$ was used for the cells of *S. cerevisiae* in exponential growth under the conditions of the described experiments.

Because of the formation of ethanol, the measurement of the respiratory quotient is not sufficient for the determination of the six unknown stoichiometric coefficients in Eq. (4.1). The additional measurement that was employed in order to close the system was the rate of ammonia addition for pH control. The nitrogen needs of the cells are satisfied by the uptake of ammonia which is provided with the medium in the form of ammonium sulfate. The protons liberated because of this ammonia uptake process cause a decrease in the pH, and the amount of ammonium hydroxide (NH_4OH) added for pH control per unit time and per unit volume of reactor, R_{NH_3}, is related to the total rate of growth R by a proton balance which , for a fed-batch reactor, as will be shown in Chapter 5, is approximately given by the following expression when the time interval between two consecutive ammonium hydroxide additions is small:

$$\frac{1}{c}R_{NH_3} = R = \frac{1}{b}OUR = \frac{1}{e}CER \tag{4.2}$$

where *OUR* is the oxygen uptake rate and *CER* is the carbon dioxide evolution rate. Detailed discussion on the application of pH control as an additional measurement that can be incorporated into the general framework of bioreactor identification will be presented in chapter 5.

4.3 INSTRUMENTATION

A schematic of the experimental apparatus is shown in Fig. 4.1. The fermentor is a standard 14-litre NBS Microferm fermentor with 11 litres of working volume and has a built-in temperature and agitation rate controllers. Detailed description on the set-up and operation procedures of such fermentor can be found in the operation manual and will not be discussed here.

The pH of the fermentor was monitored with an Ingold combination pH electrode and was maintained at a prescribed set-point by means of a pH controller (Chemtrix, Inc). When the pH controller is operated at the expanded scale, one can control the pH in the fermentor to within 0.03 pH unit. Since during yeast fermentation ammonia is taken up by the culture and protons are released, the pH always decreases in the absence of any control action. When the pH in the fermentor falls below the lower set-point, the controller activates a small peristaltic pump to add NH_4OH into the fermentor from a flask containing NH_4OH solution of known concentration. The alkali solution is added until the pH is restored to the original set-point.

To measure the time interval during which the pH control action is on or off (Δt_1 and Δt_2 as shown in Fig. 5.1), the DC side of the electrical relay inside the pH controller is tapped off and the voltage across it is monitored by the A/D converter of the microcomputer. When the controller is on, it activates the pump to add NH_4OH into the fermentor by supplying a DC voltage of approximately 2.8 V across the DC side of the relay. Therefore, Δt_2 can be obtained by timing the period during which the voltage is greater than 2 V. with the help of the real time clock. As a word of caution, if the A/D converter in the microcomputer system is set up as single-ended configuration, that is, all input signal is referenced to a common ground, the negative end from the relay cannot be connected directly to the ground input of the converter. This is because in doing so the voltage of negative end will be pulled to ground and thus will change the circuitry of the pH controller. The problem can be solved by monitoring both the

negative and positive end of the relay by *two* separate channels with reference to the ground and taking the difference of the channels. If the difference is greater than 2 V, the pump is on; otherwise, it is off.

Air flowing into the fermentor was supplied by a cylinder of compressed air available from Caltech Central Warehouse. The flowrate of air was controlled by a mass flow controller (Tylan). In order to ensure proper control action of such flow controller, the upstream pressure has to be maintained at a pressure higher than 20 psig with a pressure regulator (Linde Specialty Gas or Matheson) connected to the cylinder. Before air was passed into the fermentor, it was saturated with water vapor with a humidifier and was filtered by passing through a gas filter of 0.2 μm.

The exhausted air from the fermentor was dried by passing through two columns of anhydrous calcium chloride pellets. It was then split into two streams and was filtered by a Matheson gas filter before passing through the oxygen and carbon dioxide gas analyzers. The amount of gas passing through the analyzers was monitored by an air flow-meter (Linde Specialty Gas).

The concentration of oxygen in the gas stream was measured by a Beckman Model 755 Paramagnetic Oxygen Analyzer. The measurement principle is based on the fact that oxygen is strongly paramagnetic and most other gases, are weakly diamagnetic. The paramagnetism of oxygen may be regarded as the capability of an oxygen molecule to become temporarily magnetic when placed in a magnetic field. Therefore, the oxygen content, in the form of partial pressure, in the gas stream can be obtained by measuring the magnetic susceptibility of the gas.

The fact that the oxygen analyzer measures the partial pressure of oxygen in the gas stream and that it is operated with zero suppressed range (concentration range 19-21%) makes it extremely sensitive to external pressure fluctua-

tions. The effect of such pressure variation on the read-out of the analyzer is best illustrated by the following example.

For the case of zero suppressed mode with operating range of 19-21% oxygen, assume the barometric pressure change after calibration is 1%, that is, the barometric pressure went down from 760mm Hg to 752.4mm Hg and assume the instrument reading is 20% oxygen. But since the pressure has changed and the read-out error is given by

$$-0.01 \times 20\%O_2 = -0.2\%O_2$$

Therefore, the true oxygen concentration should be 20.2%, which is equivalent to 10% relative error.

In order to correct for any barometric pressure fluctuations, a pressure transducer (Setra System) was added at the exit stream of the oxygen analyzer. The barometric pressure was then continuously monitored and correction can be made by applying ideal gas law.

The carbon dioxide concentration in the gas stream was measured by a Horiba Model PIR-2000 infrared gas analyzer. Since most molecules absorb infrared radiation of a specific wavelength, the degree of absorption is proportional to the concentration at constant pressure. However, the signal output in response to different gas concentration is not linear; a calibration curve is thus required to convert the read-out from the analyzer to the actual concentration.

The calibration curve is obtained by introducing different concentration of carbon dioxide gas, prepared by mixing different combination of carbon dioxide gas of known concentration with pure nitrogen, into the analyzer. The composition of the carbon dioxide gas is determined by the relative flowrate of each component controlled by a mass flow controller (Tylan). Note that since most of the flow controller module in the laboratory is calibrated for air, a correction

must be made for different gas flow in order to obtain the correct flow rate. Detailed discussion on this topic and applicable formulae can be found from the operator manual supplied by the manufacturer.

4.4 DATA ACQUISITION SYSTEM

A microcomputer system was set up to automate data acquisition and to communicate with other mini-computers, mainly VAX 11/780, around the campus. The microcomputer was built around a mainframe which was equipped with the required power supply and eight empty slots of S-100 data bus. Such approach allows more flexibility and simplicity in tailoring the functions of the microcomputer. New features or functions can be added on by simply inserting appropriate boards into the empty slot and can be interfaced easily to the whole microcomputer system by writing appropriate supporting software. A general computer architecture of such system is shown in Fig. 4.2. At present, we have a CPU board, a memory board with 64K dynamic memory, a real time clock, a floppy disk controller board, a A/D converter and a I/O board. The user interacts with the microcomputer through a Televideo Model 925 terminal. Other supporting peripherals include a μ-science 83A printer and a Bausch and Lomb plotter. The book written by Adam Osbone provided a discussion on the general theory and structure of a microcomputer. Another good reference book on the subject of interfacing of a microcomputer is written by Murray Sargent III and L. Shoemaker, 1981.

The CPU board is the main brain of the microcomputer system which has a Z-80 microprocessor (CPU) running on a 2 MHz clock. The clock is generated by a oscillator together with the CTC counter residing on the same board. The Z-80 microprocessor provides the major control signals required to read and write to memory and I/O ports. A 16-bit address bus and an eight bit bi-directional data bus is generated by the microprocessor. The CPU has an arithmetic unit

which can perform operations such as addition, complement, compare, shift, move, etc., on quantities contained in the registers. The CPU also has a program counter which keeps track of the current locations in the executing program. Detail description on the structures and functions of such Z-80 microprocessor will not be described here.

An important integral part of the microcomputer system is the memory which provides the necessary instructions and/or working space. There are two kinds of memory. The first kind is known as ROM (Read Only Memory) in which, as indicated by the name, the information residing inside the memory can only be retrieved (read) by the microprocessor but cannot be changed. In our system, such ROM resides in the disk controller board which has the program to " bootstrap " the computer, that is, to get the computer started from the state of amnesia when the power is first turned on. The other kind is the RAM (Random Access Memory) which is a read-write memory. The microprocessor can read as well as change the information (write) stored inside the memory. The memory board we have is a 64K dynamic RAM which can be directly addressed by the microprocessor. Dynamic RAM refers to the kind of memory which requires constant refresh mechanism; otherwise the information stored inside will be destroyed. The other kind which does not require constant refresh mechanism is known as the static RAM; this kind of RAM can hold the information even when the power is down.

The disk controller board consists of two main parts: hardware and the software which controls the hardware. The hardware allows the computer to control the drive selection, head loading, track seeking, formatting and reading and writing operations. The software directs the hardware in each of these operations. At present, we have three single-sided double-density disk interfaced with the microcomputer, each of these drives has a memory capacity of 470K.

The A/D converter board (Techmar, Inc) is the heart of the data-acquisition system. The board accepts 16 single ended inputs or 8 channels of true differential inputs, and can be used to perform analog to digital conversion for data throughputs up to 25 KHz with 12 bits accuracy and excellent linearity. For example, at 30 KHz operation, the relative and absolute accuracies are ± 0.025% full scale, that is, ± 1 LSB (least significant bit). The input range can be selected from -10 to +10 V , -5 to +5V, 0 to 10V or 0 to 5V. The board is interfaced to the microcomputer as a memory-mapped device which requires four consecutive memory locations.

The following simple procedures illustrate how sampling is carried out by the A/D converter:

1) Store the channel number of the converter at which the sampling is going to take place in port 1 (first memory location).

2) Store anything in port 2 to start conversion

3) Wait until the lower order bit of port 2 become 1 which indicates the completion of conversion

4) Obtain the converted data from the next 2 byte of memory

A sample program written in Pascal is attached in the appendix.

A real time clock (SciTronics, Inc) provides an extremely accurate time for the system. It employs the latest microprocessor clock chip available and is crystal-controlled to ensure an accuracy of 0.002%. A lithium battery provides clock power in the event that system power is removed. It can be easily interfaced to the microcomputer as a memory-mapped device requiring four consecutive address in the memory. Two software programs are required for the interfacing, one is to set the clock and the other one is to read the clock. A sample program written in Pascal is given in the appendix.

Microcomputers spend a lot of time transferring information between the

microprocessor and various other components of the system and, moreover, the microprocessor must also control the operations of these other components. Microcomputers perform these operations by executing programs that are referred to collectively as the operating system. The operating system of our microcomputer is CP/M 80 Version 2.2 one of the most popular operating systems available. By using appropriate CP/M commands, one can transfer data from a diskette to the microcomputer, print data on a printer, or perform any operation which the microcomputer is physically capable of handling. Detailed description on the working of the operating system can be found in the book, CP/M User Guide, by Thom Hogan. Other software supports include an assembly language compiler and a Pascal compiler (MT Plus Pascal Compiler by Digital). These compilers translate the higher level language into machine language which can readily be executed by the microcomputer. All the interfacing programs are written in Pascal.

4.5 EXPERIMENTAL PROCEDURE

4.5.1 PREPARATION

In order to prevent or reduce the chance of contamination, several preventive measures were taken. All connections were made air-tight. For example, the connection between any Nalgene tubing and glass or metal tubing must be clamped tightly either with a plastic clamp or by copper wire. Any attempt to open the system to the air must be done quickly and carefully. For example, when changing the filter in the medium jar, it is advisable to flame the surrounding and then spray the outside of the connecting tubing with ethanol before any changes were attempted. For the autoclaving of empty flasks some water were purposely left inside such that steam can be generated inside the flask during the autoclave cycle. A positive pressure was maintained inside the fermentor at all times, especially during the cool down period after the fermen-

tor has been removed from the autoclave.

The whole fermentation set-up consisted of a NBS 14-litre Microferm fermentor, two 13-litre growth medium jars, a jar containing anti-foam solution (0.2 g/l), and a flask of NH_4OH of known concentration. After making the necessary connections with various pieces of equipment, the whole set-up was steam sterilized in an autoclave at 112°C for 40 minutes.

The composition of the growth medium is given on Table 4.2. The pH of the medium was adjusted to 5.0 by adding KOH pellets. The medium was filter-sterilized by passing it through a sterilized 0.2 μm filter (Gelman Science, Inc.) into a steam sterilized medium reservoir. The filter was changed after each use. The used filter can be steam sterilized and reused for 5 to 6 times. The filtration process was driven solely by gravity force.

4.5.2 CULTURE PREPARATION AND START-UP

Method and techniques for the maintenance of pure culture are described elsewhere (Pelczar and Chan, 1977). An active culture was prepared by transferring a small amount of culture from the plate into a flask containing the growth medium. Then the culture was transferred from flask to flask several times to ensure the culture was acclimated before inoculation.

The reactor was first filled with 4 liters of medium (together with anti-foam) and then inoculated. The agitation rate and the temperature were controlled at 500 RPM and 30°C respectively. Aeration was provided by a filtered air flow of 3 l/min supplied by a cylinder of compressed air. The pH of the fermentor was controlled at 5.00 by a pH controller as described before. The culture was allowed to grow for about 10 hours in batch mode before switching into fed-batch mode.

4.5.3 ACTUAL EXPERIMENT

After enough amount of biomass had been accumulated in the reactor, the fermentation was switched into fed-batch mode by introducing a feed of growth medium at a constant rate of 1.10 litre/ hr into the fermentor by a peristaltic pump (Sage Inc). The oxygen and carbon dioxide concentrations in the exhaust air were monitored by the O_2 and CO_2 analyzers respectively. Data logging of the signals from various instruments was performed by the microcomputer.

Every 30 minutes, about 10 ml of sample was withdrawn from the reactor through the sampling port for off-line measurement. Several precautions in withdrawing the sample from the fermentor were taken. First, the general area around the sample port was flamed with a Bunsen Burner to prevent contamination. Second, before withdrawing any sample, the culture residing inside the sample tube has to be purged back into the reactor; this prevents the error caused by differences in the concentrations of the sampling tube and the broth. Third, after withdrawing the sample, it is advisable to flame the tip of the sampling port before replacing the sampling vial to prevent contamination. Part of the sample obtained was filtered immediately and the filtrate was analyzed for the concentration of glucose and ethanol by enzymatic kits. Another part of the sample was used to determine the turbidity at 660 nm with a spectrophotometer (Bausch and Lomb, Spec 21) and was converted into dry-cell weight by a calibration curve.

4.5.4 OFF-LINE MEASUREMENTS

A calibration curve relating the optical density to the actual dry-cell weight can be obtained by the following procedures. A large sample of cells, about 80 ml, was withdrawn from the reactor. Then the absorbance of the sample at 660 nm was taken and the rest of the sample was centrifuged at 1000 RPM for 15

minutes at 4°C. The cells were twice washed with distilled water at 4°C and were centrifuged. Then, the pellets were dried in a preweighed aluminum dish at 100°C for 24 hrs. Therefore the dry-cell weight of the sample can be obtained. Such procedure was performed twice, once before the fed-batch and once at the end of the fed-batch. Thus, two calibration points were generated.

The concentration of the glucose in the sample was determined by the enzymatic kit (Sigma Chemical Company). The analysis is based upon the conversion of glucose to glucose-6-phosphate by ATP in the presence of hexokinase, coupled with the subsequent reduction of NADP to NADPH. As NADPH has a high absorbance at 340 nm and NADP has no absorbance at this wavelength, the reaction can be followed by measuring the increase in that particular wavelength. The increase in absorbance due to the formation of NADPH is directly proportional to the amount of glucose present. Shown below is the typical reaction:

$$\text{glucose} + \text{ATP} \longrightarrow \text{G–6–P} + \text{ADP}$$

$$\text{G–6–P} + \text{NADP} \longrightarrow \text{6–PG} + \text{NADPH}$$

To determine the glucose concentration in the sample, the following procedures were taken:

1) Add 31 ml of cold distilled water to the assay vial

2) Invert gently to dissolve content

3) Pipet 3.0 ml of enzyme kit into a cuvett

4) Record absorbance at 340 nm (A_o) of the cuvett vs water

5) Add 0.02 ml of sample into the cuvett

6) Read final absorbance (A_f) after about 3 minutes.

The glucose concentration can then be calculated by using the following formula:

$$Glucose\ (g/l) = 4.37 \times (A_f - A_o)$$

The ethanol concentration in the sample was determined by the ethanol kit (Sigma Chemical Company) which is based upon the method of Bonnichsen and Theorell, 1951. This method uses alcohol dehydrogenase (*ADH*) and nicotinamide adenine dinucleotide (NAD). It is simple to perform and relatively specific for ethanol and requires only a small sample.

The enzyme, alcohol dehydrogenase (*ADH*), catalyses the conversion of ethanol to acetaldehyde as follows:

$$C_2H_5OH + NAD \xrightarrow{ADH} CH_3CHO + NADH$$

The formation of acetaldehyde is favoured when the reaction takes place at approximately pH 9. Furthermore, the acetaldehyde formed is trapped with semicarbazide, causing the reaction to proceed nearly to completion (Lundquist, F). The increase in absorbance at 340 nm, which occurs when NAD is converted to NADH, becomes an accurate measure of the amount of ethanol present.

To determine the ethanol concentration in the sample, the following procedures were taken:

1) Add 2.3 ml of cold distilled water to the NAD-ADH Vial

2) Swirl slightly to dissolve content

3) Add 0.2 ml of NAD-ADH solution to a cuvett

4) Add 2.8 ml of Pyrophosphate Buffer Solution

5) Add 0.1 ml of water to serve as blank, then seal

6) Add 0.1 ml of sample to another cuvett, then seal

7) Wait for 10-15 minutes

8) Read and record the absorbance in blank (A_o) and sample (A_s)

The ethanol concentration in the sample can be calculated by applying the following formula:

$$ethanol\ (g/l) = 0.0229 \times (A_s - A_o)$$

4.6 DATA ANALYSIS

The data recorded by the microcomputer were transferred to a Vax 11/780 Mini-computer for data analysis. The voltage read-outs obtained from the oxygen and carbon dioxide analyzers were first converted into concentration unit with the appropriate formulae. The time interval during which the pH controller was on or off together with the amount of NH_4OH added during each cycle were also calculated.

Several corrections and calculations have to be made before the data can be fed into the estimation algorithm. First the oxygen concentration has to be corrected for any barometric pressure fluctuations by applying the ideal gas law with the data obtained from the pressure transducer. Then it has to be corrected for the effect of the interfering gases such as nitrogen and carbon dioxide. The amount of such interference is given in the user's manual provided by the manufacturer.

Note that we only control and measure the flowrate of incoming air into the fermentor; the total flowrate of exhaust air flowing out of the fermentor is not monitored. Nevertheless, this flowrate can be calculated by applying the conservation equation for the inert gases, that is, the amount of inert gases flowing into the fermentor must be equal to that of flowing out because the inert gases are not consumed or produced inside the fermentor. The total outflow of exhaust air is thus given by:

$$Q_{out} = \frac{Q_{in}(1 - C_{co_2,in} - C_{o_2,in})}{(1 - C_{co_2,out} - C_{o_2,out})}$$

where Q_{out} is the total outflow of exhaust air, Q_{in} is the flowrate of incoming air, $C_{co_2,in}$ and $C_{co_2,out}$ are the concentrations of carbon dioxide in the incoming and exhaust air respectively, $C_{o_2,in}$ and $C_{o_2,out}$ are the concentrations of oxygen in the incoming and exhaust air respectively.

With the knowledge of CER, OUR, and R_{NH_3} and together with the four elemental balances for C, H, O, and N, the six coefficient in Eq. (4.1) can be determined by solving the following set of linear equations:

$$\begin{bmatrix} 6 & 0 & 0 & 0 & -1 & -2 \\ 12 & 0 & 3 & -2 & 0 & -6 \\ 6 & 2 & 0 & -1 & -2 & -1 \\ 0 & 0 & 1 & 0 & 0 & 0 \\ 0 & 0 & 0 & 0 & 1 & 0 \\ 0 & 1 & 0 & 0 & 0 & 0 \end{bmatrix} \begin{bmatrix} a \\ b \\ c \\ d \\ e \\ f \end{bmatrix} = \begin{bmatrix} 1 \\ 1.666 \\ 0.511 \\ 0.168 \\ 0.168\ CER/R_{NH_3} \\ 0.168\ OUR/R_{NH_3} \end{bmatrix} \tag{4.3}$$

The bioreactor identification procedure consists of solving the above equations for the unknowns a through f for each of the measured values of OUR, CER, and R_{NH_3} obtained continuously in real-time. The resulting values of R and substrate and product yields, Y_s and Y_p, respectively, are the three measurements relating to the state variables as follows:

$$R = \mu b + \xi_1(t) \tag{4.4a}$$

$$Y_{s,ms} = Y_s + \xi_2(t) \tag{4.4b}$$

$$Y_{p,ms} = Y_p + \xi_3(t) \tag{4.4c}$$

The dynamics of the state vector is given by the following equations similar to Eq. (2.16) of Chapter 2:

$$\dot{b} = \mu b - Db \tag{4.5a}$$

$$\dot{s} = D(s_f - s) - \frac{1}{Y_s}\mu b \tag{4.5b}$$

$$\dot{p} = \frac{1}{Y_p}\mu b - Dp \tag{4.5c}$$

$$\dot{\mu} = C + \eta_1(t) \tag{4.5d}$$

$$\dot{C} = -CD + \eta_1'(t) \tag{4.5e}$$

$$\dot{Y}_s = \eta_2(t) \tag{4.5f}$$

$$\dot{Y}_p = \eta_3(t) \tag{4.5g}$$

where D for a fed-batch reactor is equal to

$$D = \frac{1}{V}\frac{dV}{dt} = \frac{F}{V} \tag{4.6}$$

Equations (4.4) and (4.5) constitute the measurement and state equations, respectively, for the fermentation of *S. cerevisiae* in a fed-batch reactor. They were employed together with the extended Kalman filter equation (2.14), and Eqs. (2.20) and (2.21) for the variable intensities of the random noises η_1, η_1', η_2, and η_3 in order to produce estimates of the state vector during the fermentations. The results are presented on the following section.

4.7 RESULTS

From the stored measurements of O_2 and CO_2 concentrations and weight of ammonium hydroxide, the value of total rate of growth, R, oxygen uptake rate, *OUR*, carbon dioxide evolution rate, *CER*, and rate of ammonium hydroxide addition, R_{NH_3}, were determined at all time instants during the course of the fermentation. From these measurements, using the proposed adaptive estimator, estimates of the concentrations of cell biomass, glucose, and ethanol, as well as estimates of the specific growth rates, and glucose, and ethanol yields were obtained. These estimates, along with the off-line measurements and the associated error bars for the latter are shown in Figs. 4.3 through 4.8. It can be seen in these results that the estimated values of these state variables and cul-

ture parameters are in excellent agreement with the corresponding off-line measurements.

Shown in Figs 4.3 - 4.8 are also the estimates of the state and culture parameters as obtained by using not the extended-adaptive Kalman filter but a moving average of the measurements which is the equivalent of an R-C filter (dashed line). Those estimates were obtained by straight integration of the governing differential equation with the averaged value of data. Each time, a set of 200 data points was averaged before feeding into the differential equation and each subsequent point was the average of a set of 200 new points. The choice of 200 points was rather arbitrary and the effect of changing this number on the quality of the RC filter estimates was not investigated. 200 points roughly corresponded to two full pH cycles.

A comparison between the estimates obtained by the proposed estimator and those by the R-C filter reveals that, for cell biomass, glucose, and ethanol, R-C filter is acceptable if not as accurate as the estimates obtained by the Kalman filter. The reason is that the integration of Eqs. (4.5 a-c), which is carried out in the application of the R-C filter, is equivalent to an additional noise filter for R; thus, resulting in a rather smooth output for b, s, and p. However, since no such additional filtering is involved in the estimation of the specific growth rate and the yields, the R-C estimates for these culture parameters are very noisy compared to those obtained by the Kalman filter. It was mentioned in the introduction of Chapter 2 that the main purpose of on-line state and culture parameter estimation is for the on-line control of fermentation. The specific rates of growth and product formation and the yields are probably the most important indicators of the state of the culture and fermentation. The results presented in Figs. 4.6-4.8 indicate that the R-C estimates of these variables would be totally inappropriate for control purposes for they would lead to an unstable control operation. Kalman filter estimates, on the other hand, are smooth and reliable

and, as extensive simulations indicate, can be employed for the efficient control of the operation of bioreactors.

Some other interesting features of the estimator can be observed in Fig. 4.3 for biomass. It can be seen that the Kalman filter estimates of b become better and extremely accurate at the later stages of the fermentation. The reason is that biomass is observable in the presented scheme; hence, with the progress of time, an increasing amount of information is accumulated about the past behaviour of this state variable, and this additional knowledge contributes substantially to the observed improvement of the estimates. On the other hand, the estimates of the R-C filter begin to deviate significantly from the off-line measurements after about 4 hours of operation. This deviation is in accord with a similar behavior observed by Wang *et at*, (1979) and is attributed to the fact that, for fed-batch operation, the variance of the R-C estimates increases continuously with time and leads eventually to unreliable state estimates as predicated before (Stephanopoulos and San, 1980).

Figures 4.4 and 4.5 offer an additional justification for using the presented estimator. If off-line measurements of the glucose and ethanol were obtained, they might be incorrectly interpreted as some kind of oscillatory behaviour; whereas, no such response is exhibited by the on-line estimates, which, in addition, are smoother and more accurate. Even though both the glucose and ethanol are not observable. The Kalman filter yields more accurate estimates because it is based on better biomass values. Finally, despite the substantial smoothing of the data, the R-C filter was incapable of producing acceptable estimates of rate-type parameters such as the specific growth rate and yields (Figs. 4.6, 4.7, and 4.8).

4.8 DISCUSSION

As stated earlier, the objective of this study is to propose a generalized methodology for the estimation of the important state variables and culture parameters of a bioreactor from measurements attainable by the presently available instruments. The methodology is general enough in that it can incorporate new measurements to improve the accuracy of the estimates or to produce new ones. In this chapter, the results of extensive experimental studies are discussed which support the claim regarding the accuracy of the estimates and the efficiency of the identification process. It is thus proposed that the estimation algorithm be adopted for on-line bioreactor identification.

Central to the estimation scheme is the measurement of the respiration quotient. There are, however, some points that need to be examined carefully with regard to the sensitivity of the estimation scheme with respect to the measurement of the respiration quotient. Further insight into the process that contribute to the measured values of RQ can be obtained by replacing the overall reaction (4.4) with a more detailed account of the processes of substrate dissimilation, energy production through NADH oxidation in the respiratory chain, the detailed biochemistry of product formation, and the overall reaction of biosynthesis. Exact analysis has been presented somewhere else (Grosz *et al.*, 1983). Presented here are the main results of that study which are of importance to the proposed bioreactor identification scheme : (a) If no product formation reaction is taken into consideration small variation in the value of the RQ can be accounted for by large shifts in the relative amounts of the carbon-energy source that is consumed in the dissimilatory or the biosynthetic pathways. This causes a very high sensitivity of the rates and yields with respect to the value of RQ. Therefore, product formation, no matter how small, always should be included in the overall reaction representing the process of growth and product formation. (b) If the amount of $NADH_2$ produced in the product formation reaction is twice the amount of CO_2 evolved by the same reaction then

the estimates are very sensitive to the RQ measurement when the values of the RQ are close to unity. Shown below is an example that singularities may appear when a correlation of the respiratory quotient, RQ, vs the ratio of coefficients (f/b) is being used as an extra linear relationship among the coefficients.

Shown in Figure 4.9 is the plot of (f/b) vs RQ of several fed-batch runs spanning a range of 1.3 to 2.5 for RQ. This plot reveals a fairly linear relationship between the two. However, our attempt to use the correlation in place of the ammonium hydroxide addition measurement and the nitrogen balance in the estimation scheme described above failed because some of the calculated culture parameters were extremely sensitive to small changes in the slope and intercept of the plot in Fig. 4.9. For example, Figure 4.10 shows the calculated trajectory of the biomass concentration in a fed-batch run with 1.02 or 1.04 as the X-intercept of the correlation. The trajectory calculated from the nitrogen balance and nitrogen addition measurement instead of the correlation along with the off-line biomass measurements are also shown. As can be seen, a fortunate choice of 1.04 for the X-intercept can result in a close duplication of the trajectory obtained by the independent means. However, there is no room for error in placing the intercept because 2% change in it can produce completely different results. Implied by this sensitivity is the existence of singularity among the system of equations. Detailed discussion and explanation by examining the metabolic pathway has been presented elsewhere (Grosz *et al.*, 1983). Shown here is another approach that examines the macroscopic equations. The new set of system of equations describing the coefficients of Eq. 4.1 with the use of the correlation is given by:

$$\begin{bmatrix} 6 & 0 & 0 & 0 & -1 & -2 \\ 12 & 0 & 3 & -2 & 0 & -6 \\ 6 & 2 & 0 & -1 & -2 & -1 \\ 0 & 0 & 1 & 0 & 0 & 0 \\ 0 & I & 0 & 0 & m & -1 \\ 0 & RQ & 0 & 0 & -1 & 0 \end{bmatrix} \begin{bmatrix} a \\ b \\ c \\ d \\ e \\ f \end{bmatrix} = \begin{bmatrix} 1 \\ 1.666 \\ 0.511 \\ 0.168 \\ 0 \\ 0 \end{bmatrix}$$

where I and m represent the slope and the X-intercept of the f/b vs RQ curve respectively. It can be shown easily that the determinant of the above system is given by:

$$\Delta = 24 \times (1 - I) + 24 \times RQ\,(m - 1)$$

Since both I and m are numerically very close to 1, the determinant, Δ, is very close to zero and the systems of equations is very sensitive to any change in either I or m. The sensitivity of the coefficients on the values of I and m comes in when one tries to invert the above matrix in which $\frac{1}{\Delta}$ has to be taken.

Fig. 4.1 Schematic of the experimental apparatus

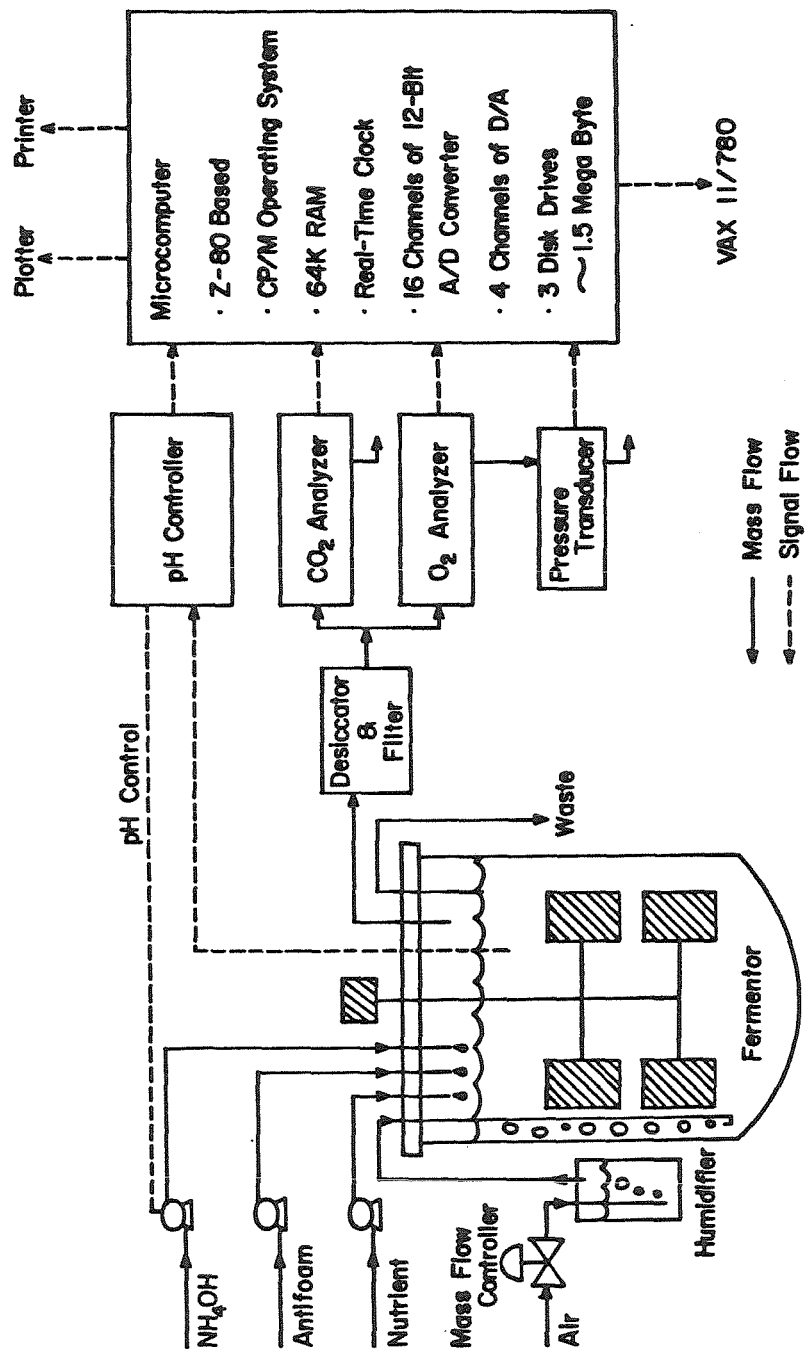

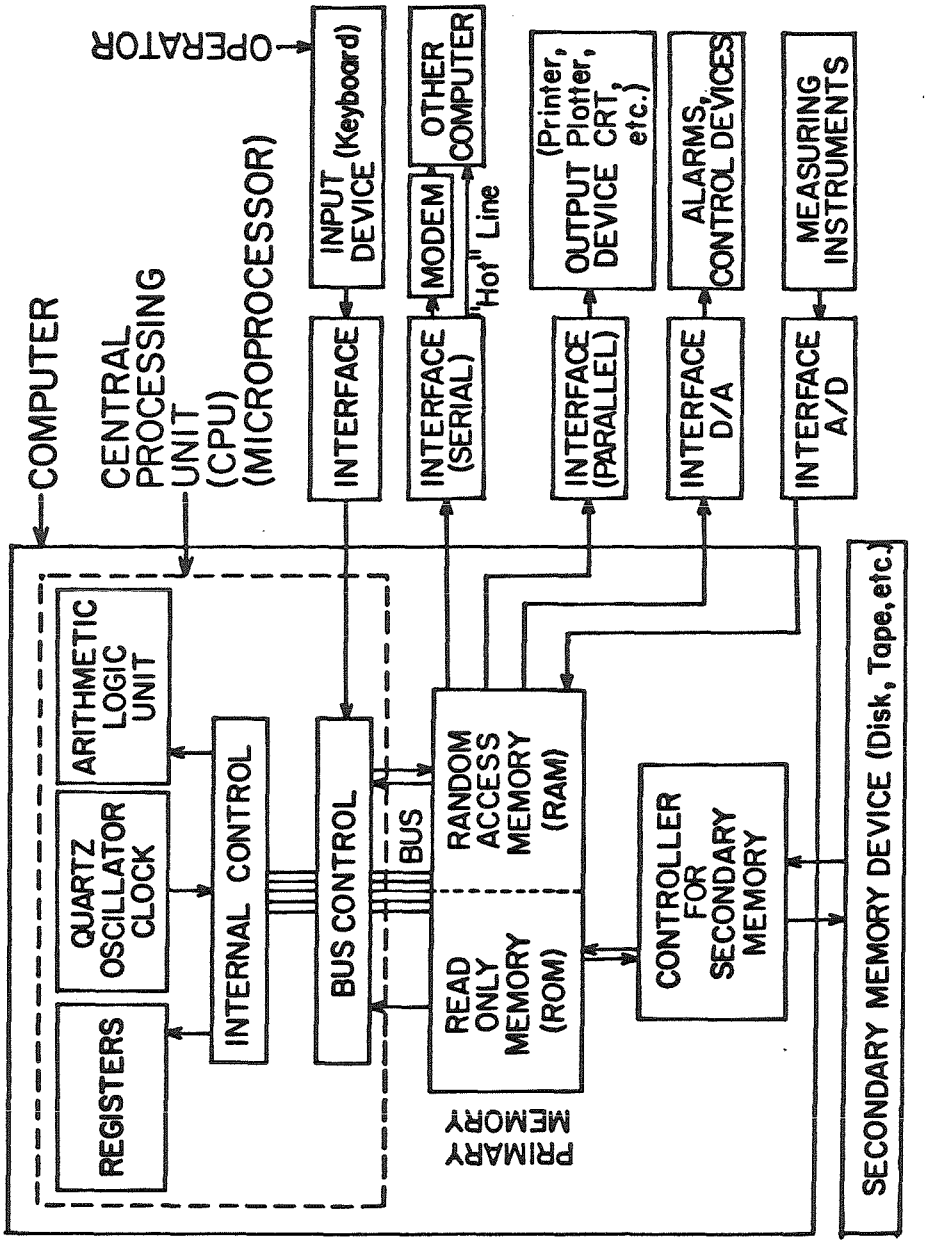

Fig. 4.2 Schematic of a typical microcomputer architecture

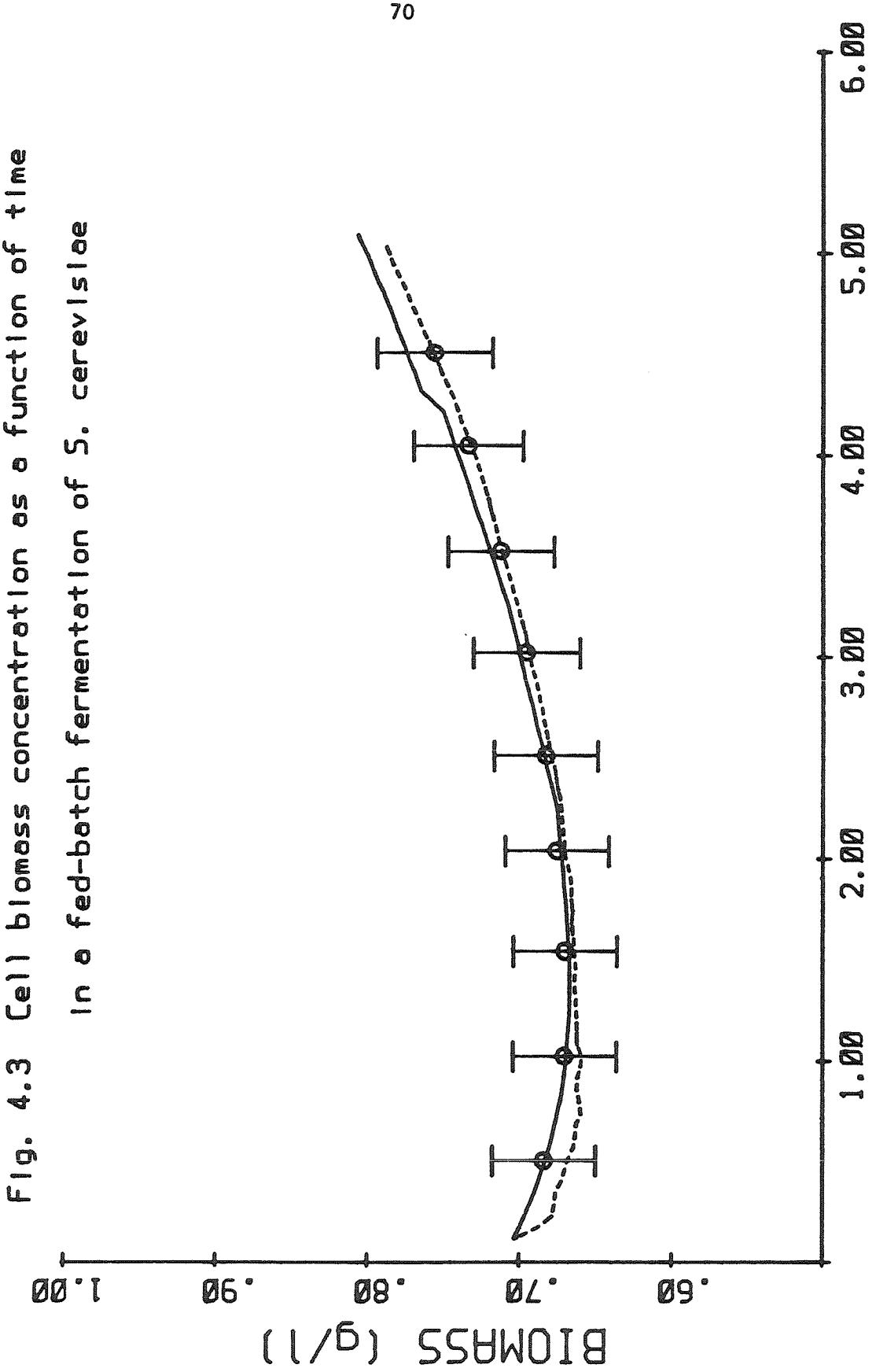

Fig. 4.3 Cell biomass concentration as a function of time in a fed-batch fermentation of S. cerevisiae

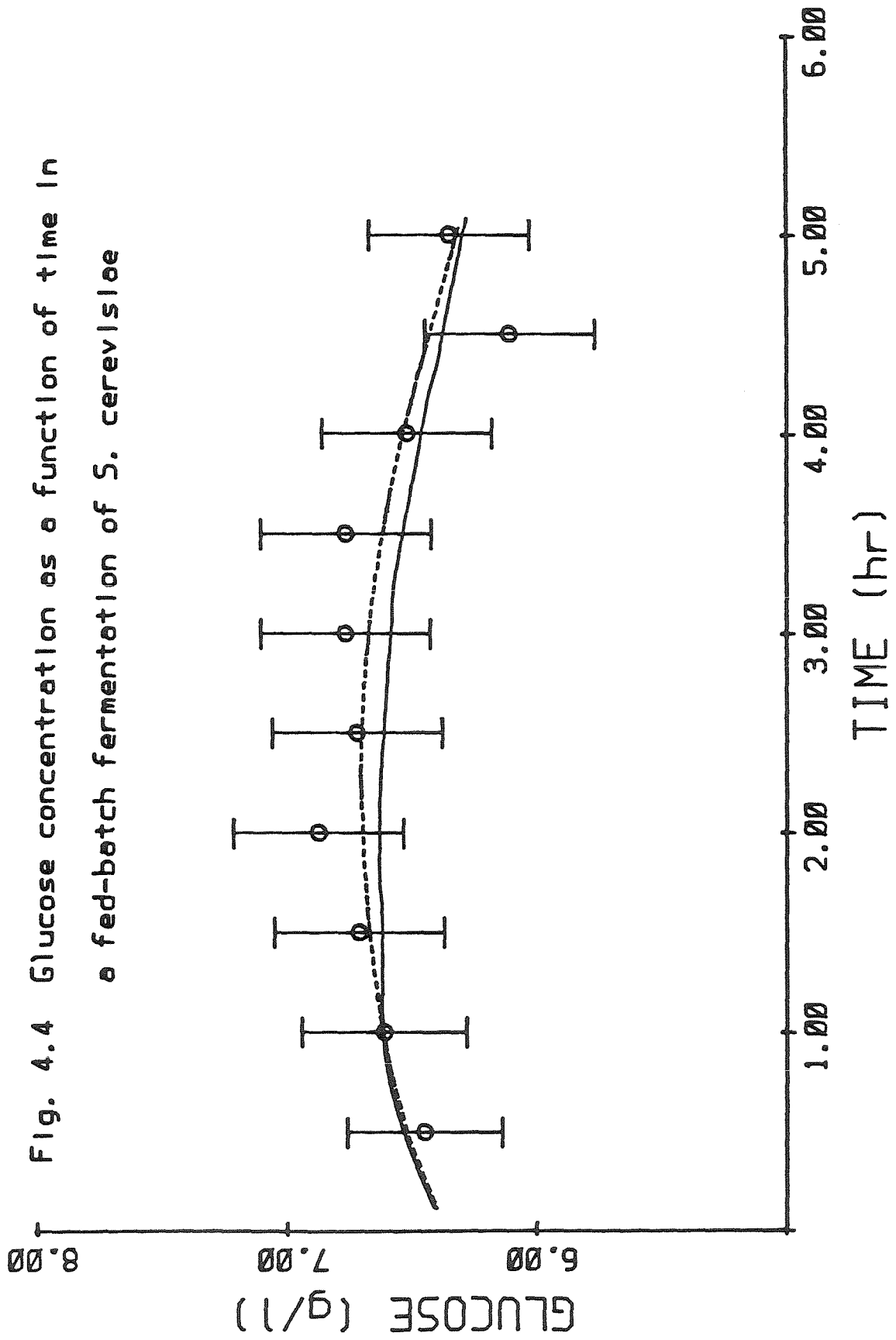

Fig. 4.4 Glucose concentration as a function of time in a fed-batch fermentation of S. cerevisiae

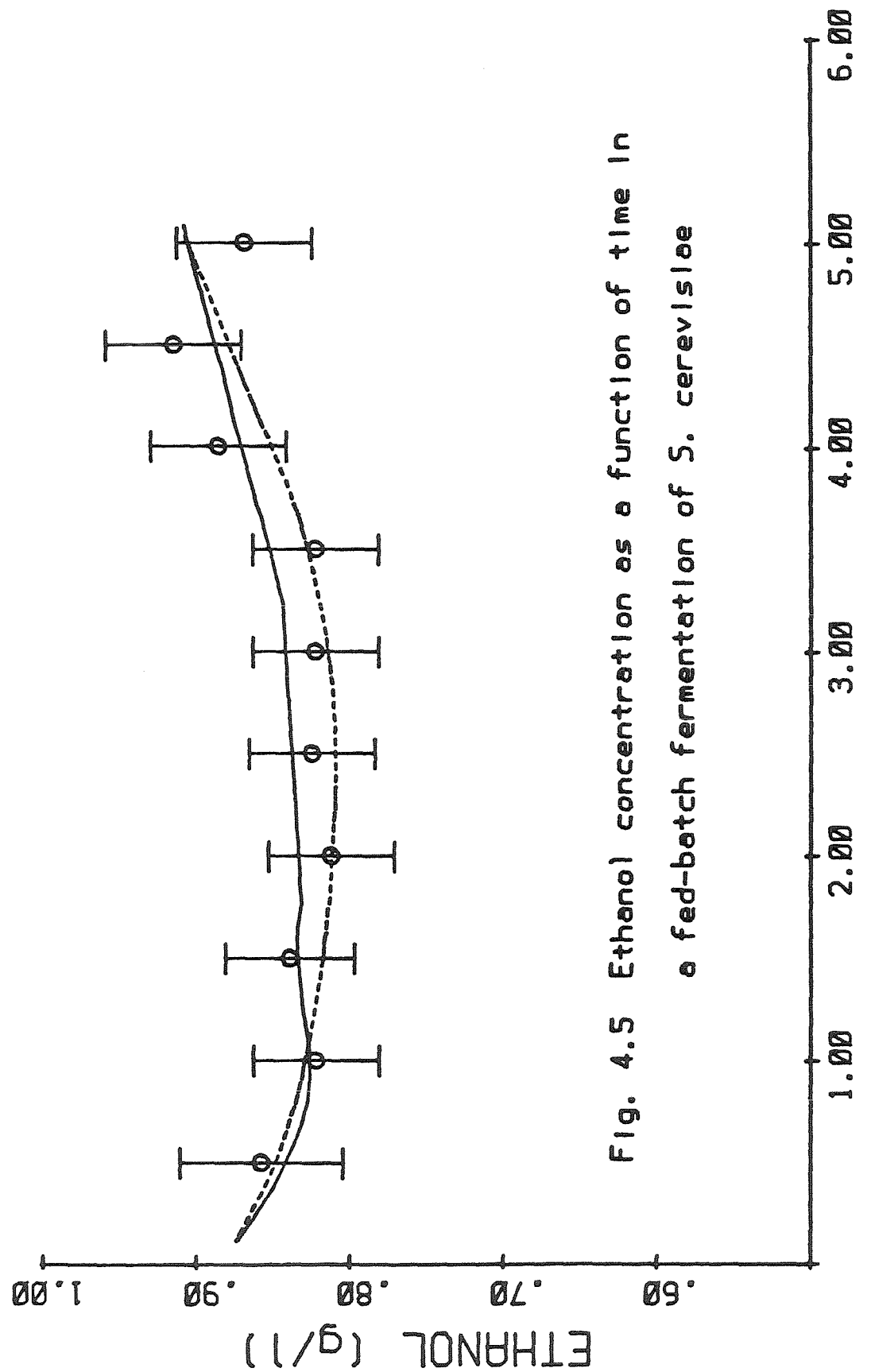

Fig. 4.5 Ethanol concentration as a function of time in a fed-batch fermentation of S. cerevisiae

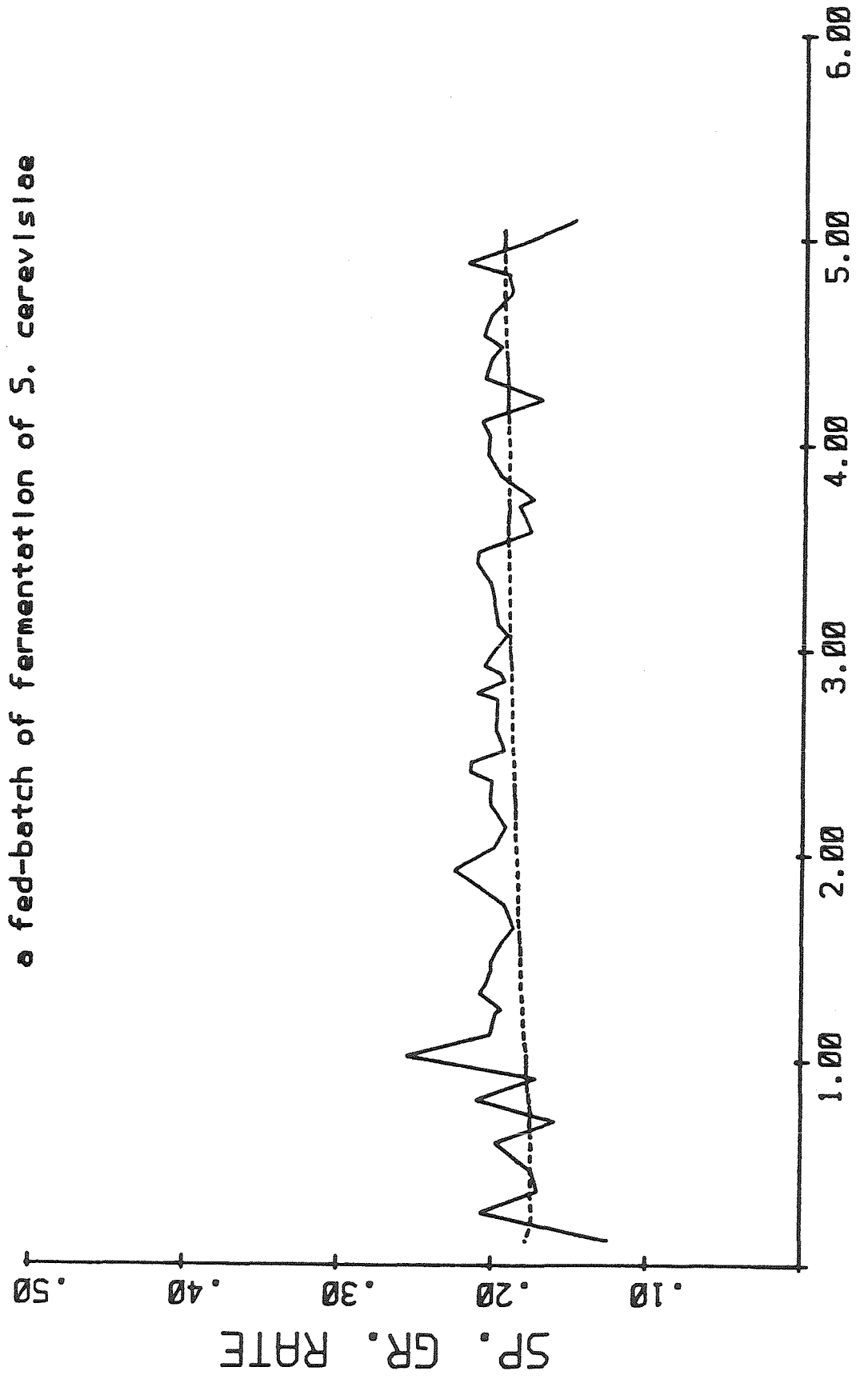

Fig. 4.6 Specific growth rate as a function of time in a fed-batch of fermentation of S. cerevisiae

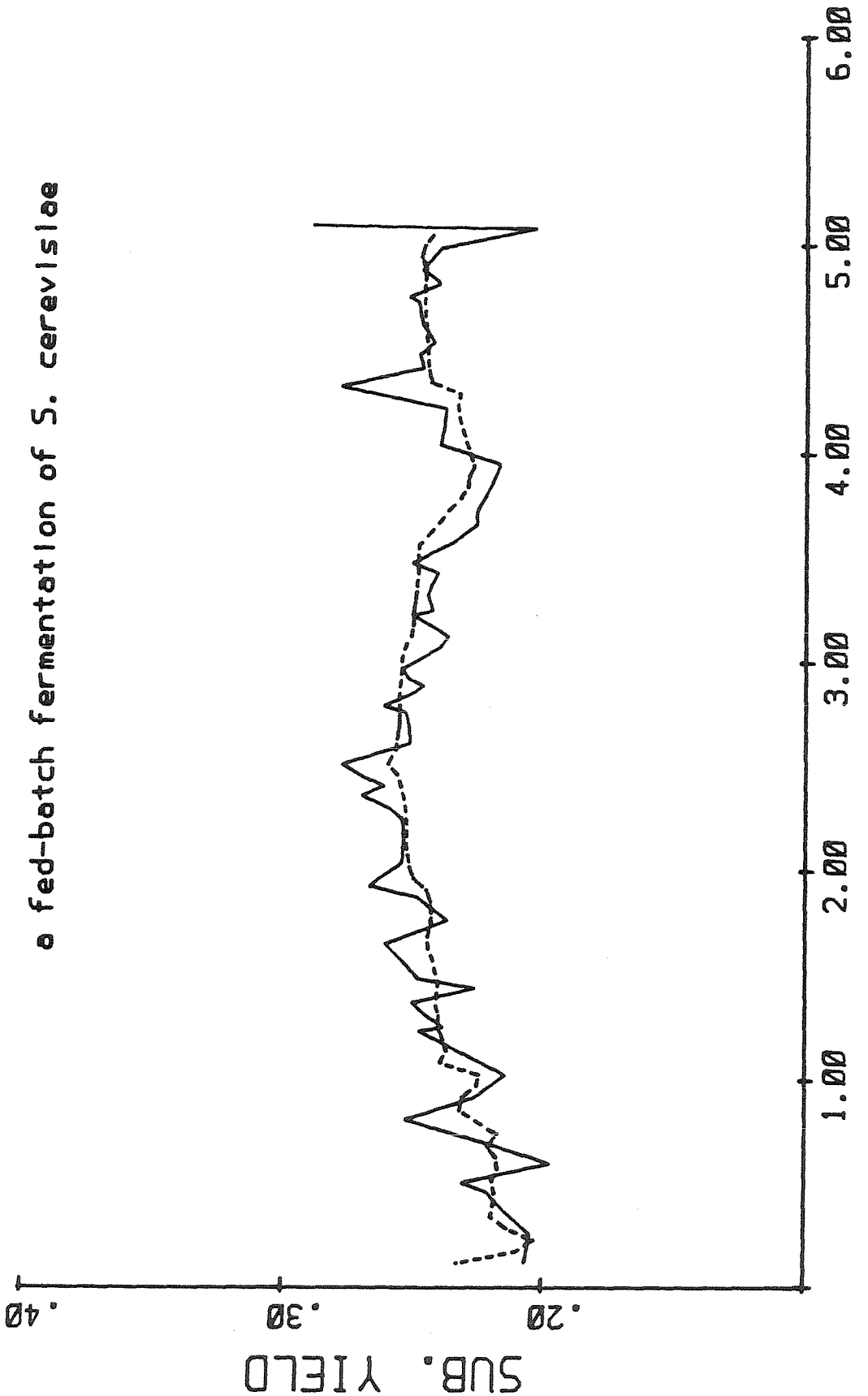

Fig. 4.8 Substrate yield as a function of time in a fed-batch fermentation of S. cerevisiae

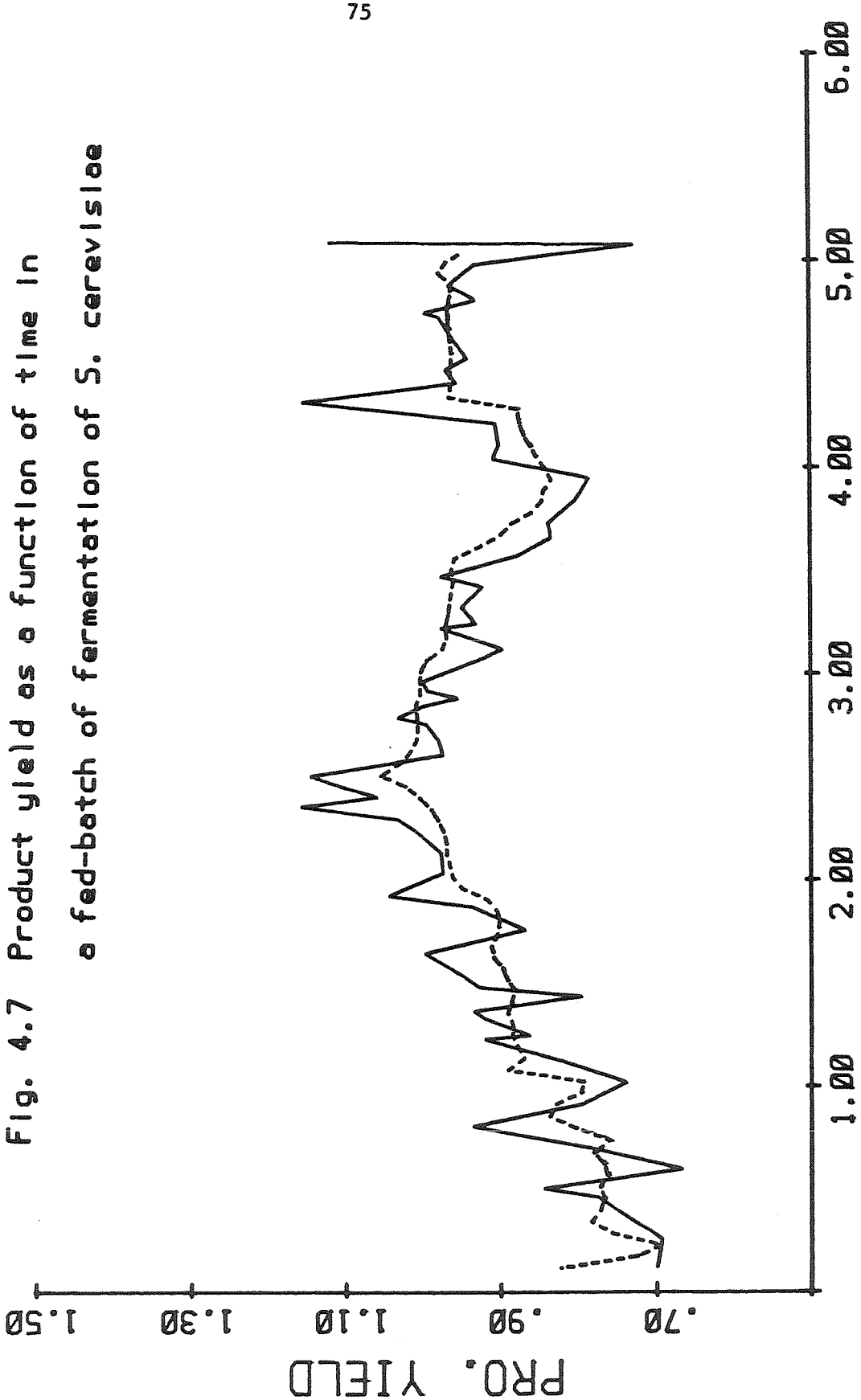

Fig. 4.7 Product yield as a function of time in a fed-batch of fermentation of S. cerevisiae

Fig. 4.9 The linear correlation of f/b vs RQ generated with fed-batch growth data

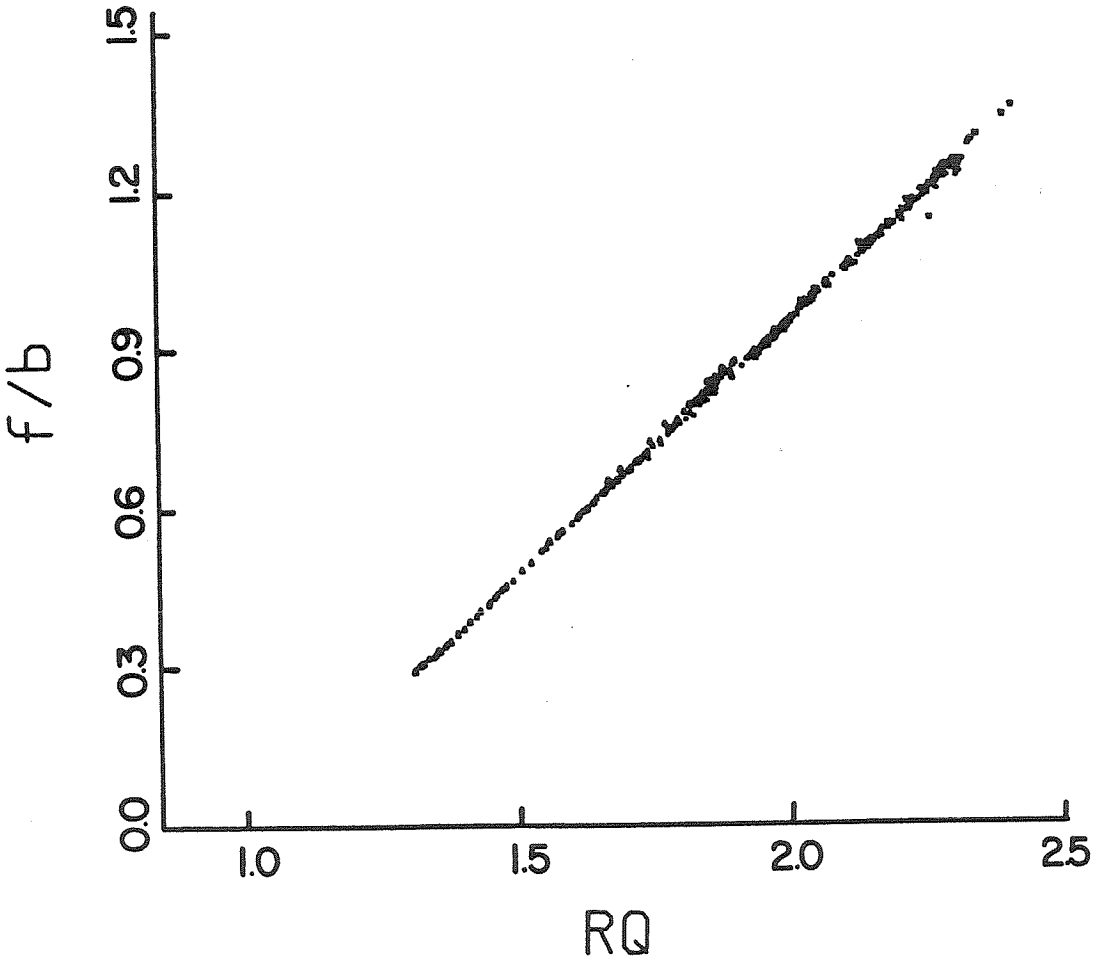

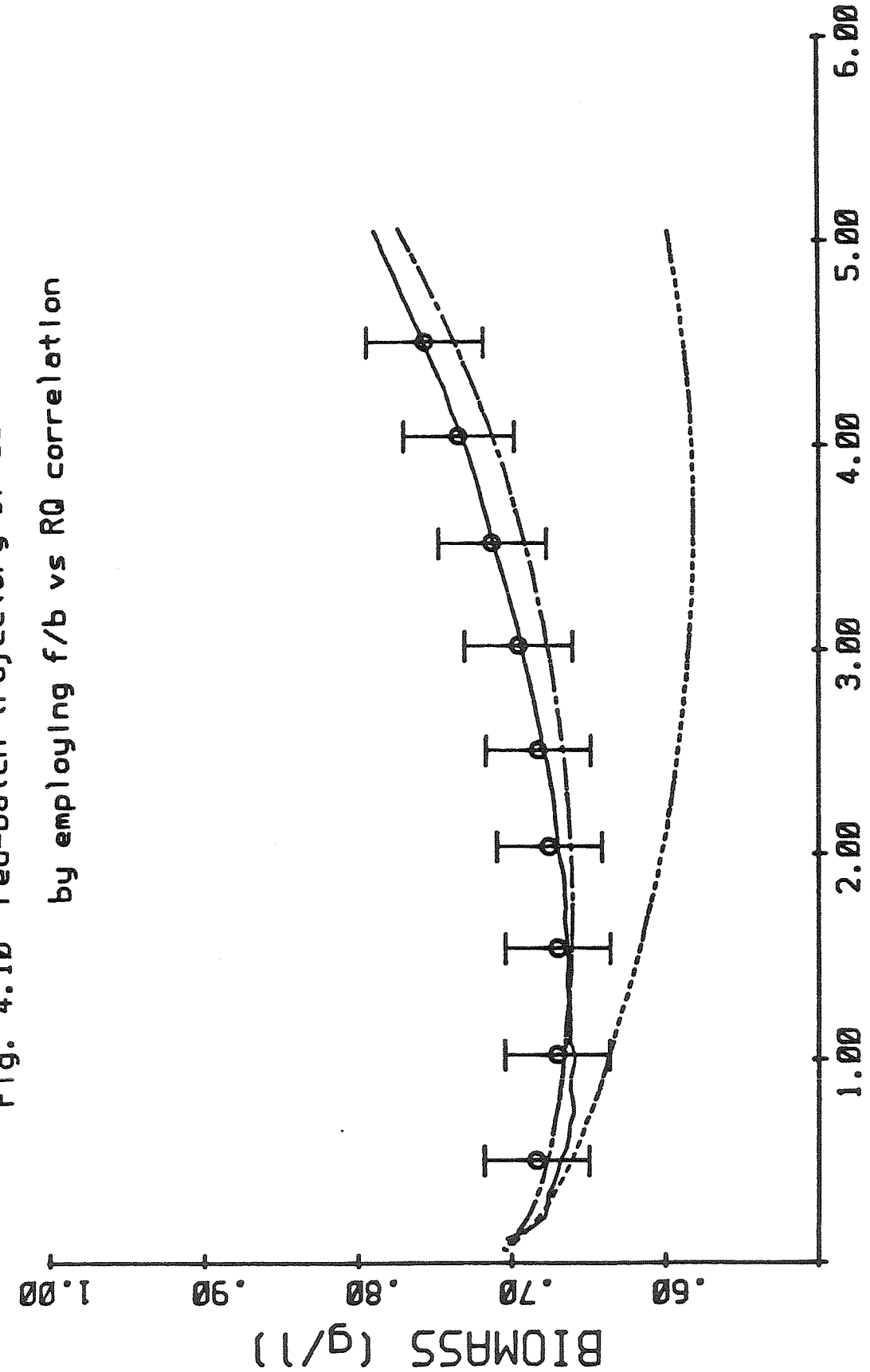

Fig. 4.10 Fed-batch trajectory of cell biomass conc. by employing f/b vs RQ correlation

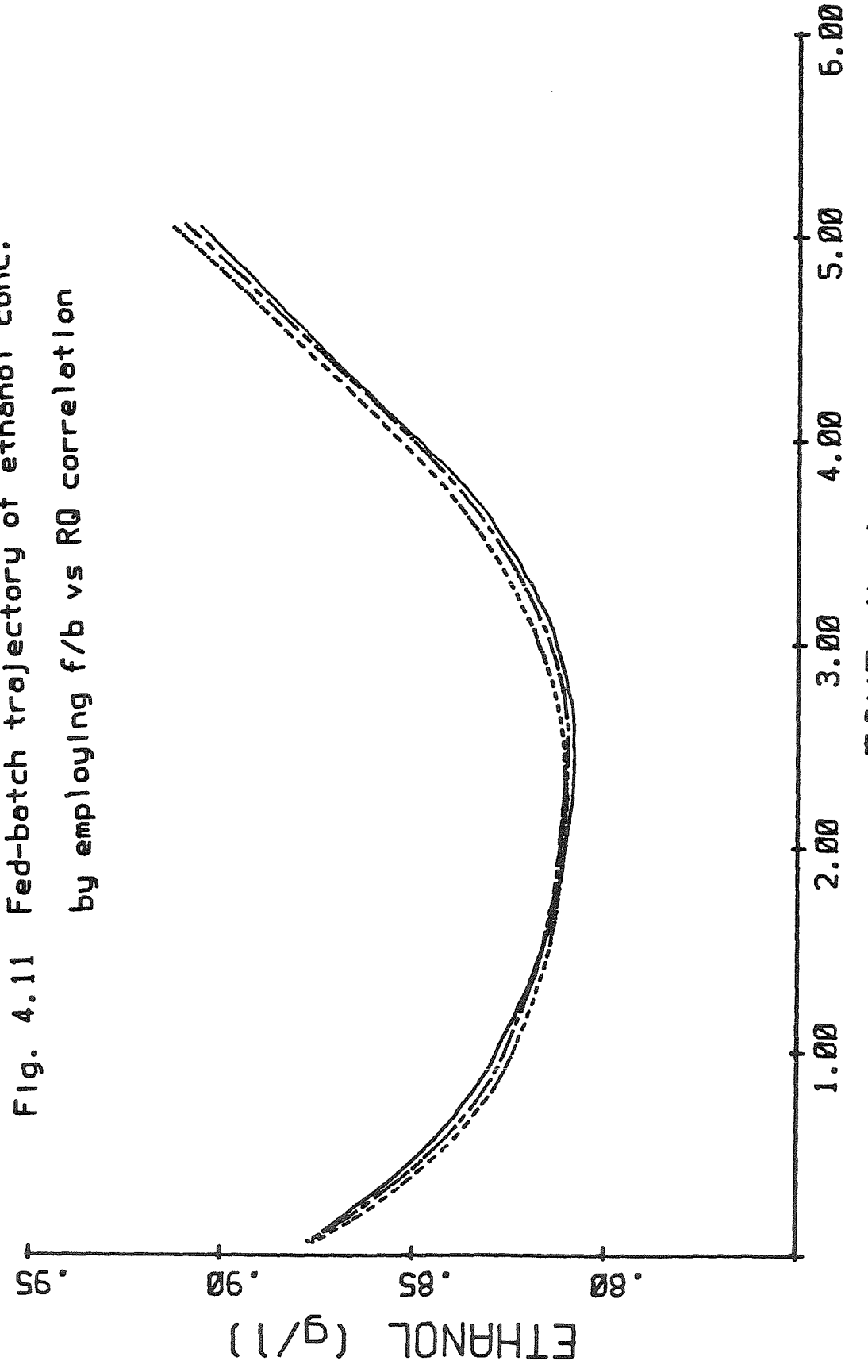

Fig. 4.11 Fed-batch trajectory of ethanol conc. by employing f/b vs RQ correlation

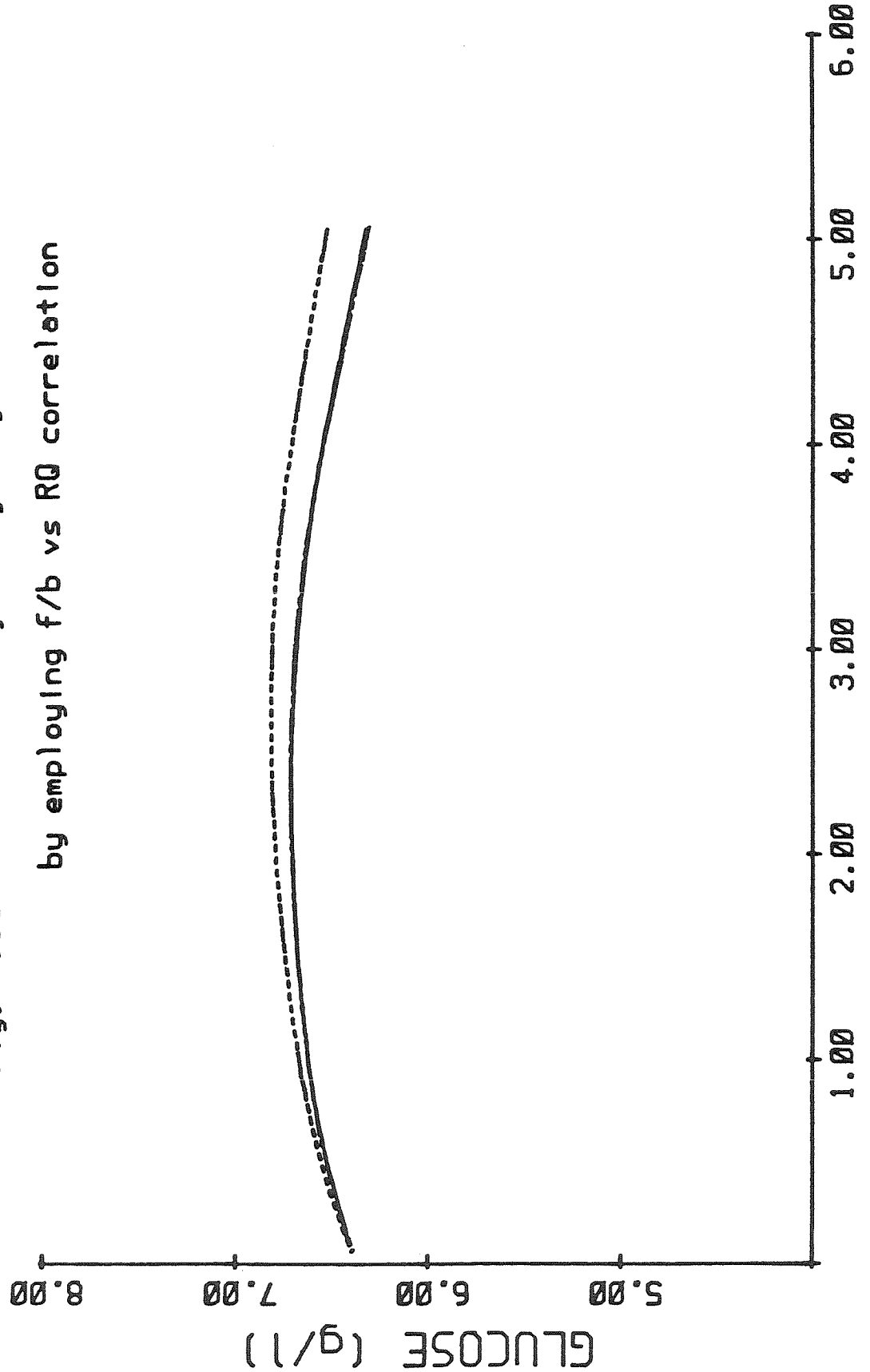

Fig. 4.12 Fed-batch trajectory of glucose conc. by employing f/b vs RQ correlation

Table 4.1 Biomass composition at different growth phases

CELL BIOMASS COMPOSITIONS

POINT	COMPOSITION	MOL. WEIGHT
1	$CN_{0.169}H_{1.690}O_{0.431}$	22.955
2	$CN_{0.168}H_{1.666}O_{0.511}$	24.201
3	$CN_{0.146}H_{1.681}O_{0.474}$	23.309
4	$CN_{0.155}H_{1.675}O_{0.492}$	23.707
5	$CN_{0.149}H_{1.693}O_{0.583}$	25.100

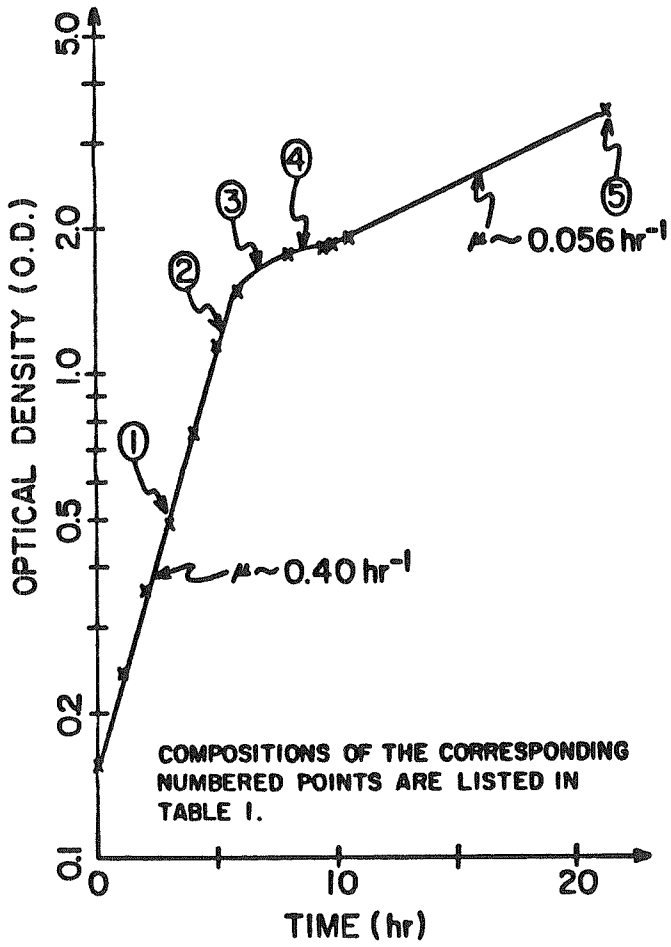

Component	Amount (per litre)
$MgCl_2 \cdot 6H_2O$	0.52 g
$(NH_4)_2SO_4$	12.00 g
H_3PO_4, 85%	1.6 ml
KCl	0.12 g
$CaCl_2 \cdot 2H_2O$	0.09 g
NaCl	0.06 g
$MnSO_4 \cdot H_2O$	3.8 mg
$CuSO_4 \cdot 5H_2O$	0.5 mg
H_3BO_3	7.3 µg
$NaMoO_4 \cdot 2H_2O$	3.3 µg
NiCl	2.5 µg
$ZnSO_4 \cdot 7H_2O$	2.3 µg
$CoSO_4 \cdot 7H_2O$	2.3 µg
KI	1.7 µg
$(FeSO_4)(NH_4)_2SO_4 \cdot 6H_2O$	0.035 g
m-Inositol	125.0 mg
Pyridoxine-HCl	6.25 mg
Ca-D-Pantothenate	6.25 mg
Thiamine-HCl	5.0 mg
Nicotinic Acid	5.0 mg
D-Biotin	0.125 mg

Table 4.2

NOTATION

a,b,c	gmole of carbon source, oxygen and ammonia, respectively, consumed per gmole of cell biomass produced
d,e,f	gmole of H_2O,CO_2 and product formed
A_f	final absorbance in performing the enzyme test
A_o	initial absorbance in performing the enzyme test
b	concentration of biomass per unit volume
C	dummy variable in the parameter estimation equations
$C_{CO_2,in}$	concentration of CO_2 in inlet stream
$C_{CO_2,out}$	concentration of CO_2 in outlet stream
$C_{O_2,in}$	concentration of O_2 in inlet stream
$C_{O_2,out}$	concentration of O_2 in outlet stream
CER	carbon dioxide evolution rate
CPU	central processing unit
D	dilution rate
Δt_1	time interval during which the pH controller is off
Δt_2	time interval during which the pH controller is on
F	flow rate of growth medium into the reactor
Hg	mercury
I	X-intercept in the RQ vs (f/b) plot
m	slop in the RQ vs (f/b) plot
OUR	oxygen uptake rate
p	concentration of product
Q_{out}	flow rate of air flowing out of the fermentor
Q_{in}	flow rate of air flowing into the fermentor
R	total growth rate of biomass per unit volume
R_{NH_3}	rate of ammonium hydroxide added into the reactor
RQ	respiratory quotient

S_f	concentration of the feed
S	feed concentration
V	volume of the reactor
Y	yield

GREEK LETTERS

η	process noise
μ	specific growth rate
ξ	measurement noise

SUBSCRIPT

s	substrate
p	product
1,2,3	noise relate to different state or parameter

CHAPTER 5

UTILIZATION OF pH MEASUREMENT

5.1 INTRODUCTION

As mentioned in Chapter 2, for a fermentation with product formation an additional measurement, besides the oxygen and carbon dioxide, is required for identification purposes. In chapter 3, the measurement of the amount of ammonium hydroxide added to the reactor for pH control was correlated with the total rate of biomass growth. With this additional information, on-line estimates of the biomass, substrate, and product concentrations, the yields, and the specific rates of growth and product formation were obtained for a fed-batch yeast fermentation that compared very satisfactorily with the off-line measurements of the corresponding quantities.

In this chapter, a typical way by which the biological processes in a bioreactor may affect the acidity/alkalinity of the fermentation medium is examined. The objective of the analysis is to correlate any pH-related measurements with important variables of the system and thus fully exploit the above measurements for bioreactor identification purposes.

There is a definite need for correlations of the type described above. Besides the fact that they are based on measurements which are continuously performed on a routine basis in most fermentation systems, such correlations can serve a multitude of purposes related to bioreactor monitoring and control. First, the simple, intuitive relationship between the amount of ammonium hydroxide added for pH control and the amount of biomass formed between two successive ammonium additions is not valid for fed-batch or continuous reactors eventhough it is valid for batch reactors. The rather complex interactions

between the elements of the buffer, the convection through the system, and the biological processes affecting the pH make it necessary that a rigorous analysis be carried out to yield a relationship that can utilize the pH measurements in continuous reactors, as well. It should be noted that in the absence of such a relationship continuous or fed-batch bioreactors without product formation cannot be observed solely from the measurement of the respiratory quotient. Second, the analysis indicates the specific type of neutralizing agent that must be employed with the pH controller so that valuable information on the rates of biomass and product formation is obtained with minimum effort. Finally, as it was pointed out before, various singularities, especially in the absence of product formation, may render the RQ measurement inapplicable in certain fermentations. In these cases, a pH-related measurement may be the only alternative that can supply the information needed, provided, of course, that such measurements are interpreted correctly in terms of the basic parameters that cause the pH changes.

The method of analysis makes use of the powerful concept of reaction invariants which facilitates greatly the description of ionic reaction equilibria. All three types of reactors, batch, fed-batch, and continuous, are examined. Relationships are obtained between the amount of neutralizing agent added and biomass growth rate for the case in which the product formed has no acidic/basic properties. The case of acid/base product formation is also discussed, and a significantly more involved identification method is outlined. The validity of the obtained analytical results was established with fermentation-simulation experiments. Furthermore, on-line estimates obtained in the continuous fermentation of *Saccharomyces cerevisiae* in a glucose limiting medium were in excellent agreement with off-line measurements thus providing direct

confirmation of the applicability of the correlations for on-line bioreactor identification.

5.2 ANALYSIS

The case of bioreactors employed for the propagation of micro-organisms and the formation of products that do not possess acidic/basic properties is addressed in the following discussion. Other more general cases will be examined in later sections. It is assumed that the nitrogen needs of the cells are satisfied by the ammonium salts present in the medium. The protons released during the ammonia uptake process cause the pH in the reactor to decrease and the control of the pH is accomplished by the periodic addition of measurable amounts of ammonium hydroxide. Due to imperfections in the function of the pH controller, the pH of the medium is not exactly constant but fluctuates between a lower and and upper bound as shown schematically in Fig. 5.1. With an expanded pH scale and careful operation, a pH variation of no more than 0.03 pH units can be achieved. The effect of such small pH changes on the concentrations of the bicarbonate and dissolved CO_2 in the medium is minimal and the corresponding fluctuations in the gaseous CO_2 concentrations can therefore be ignored. Also, since the time interval Δt_1 and Δt_2 are usually small and most biological processes are usually characterized by much longer time scales, it will be further assumed that the total rates of biomass growth and product formation remain constant during a full pH cycle.

5.3 BATCH REACTOR

Since the presence of various weak acids or bases affects the concentration of free protons in the medium, the components of the fermentation buffer must be taken into consideration in the analysis. Let M_i^- denote the monoacidic

base of component i of the buffer which is, of course, at equilibrium with the corresponding nondissociated weak acid form M_iH:

$$M_iH \rightleftharpoons M_i^- + H^+ \tag{5.1a}$$

Assuming that the concentration of the M_i^- ions charged initially in the reactor is c_i, one can write the following conservation and equilibrium equations:

$$[M_i^-] + [M_iH] = c_i \tag{5.1b}$$

$$[M_i^-][H^+] = K_i[M_iH] \tag{5.1c}$$

where K_i is the equilibrium constant of reaction (3.1a) and the quantities in square bracket indicate the concentration of the corresponding compounds. If certain components j of the medium are capable of undergoing further dissociation, the additional equilibria must also be considered. For example, in the case of a biacidic base B_j^{2-} the reaction equilibria are:

$$B_jH_2 \rightleftharpoons B_jH^- + H^+ \tag{5.2a}$$

$$B_jH^- \rightleftharpoons B_j^{2-} + H^+ \tag{5.2b}$$

and the conservation and equilibrium equations are, in analogy to Eqs. (5.1b,c), as follows:

$$[B_j^{2-}] + [B_jH^-] + [B_jH_2] = c_j \tag{5.2c}$$

$$[B_jH^-][H^+] = K_{1j}[B_jH_2] \tag{5.2d}$$

$$[B_j^{2-}][H^+] = K_{2j}[B_jH^-] \tag{5.2e}$$

Similar equations can be written for tertiacidic bases. It should be pointed out that from the total initial concentrations, c_i, and a pH measurement, the concentrations of all the buffer components in dissociated and nondissociated forms can be obtained by solving Eqs. (5.1b,c) or (5.2c-e).

In addition to the buffer one also has the reaction for ammonia equilibrium:

$$NH_4^+ \rightleftharpoons NH_3 + H^+ \tag{5.3a}$$

and the corresponding equilibrium relationship

$$[NH_3][H^+] = K_A[NH_4^+] \tag{5.3b}$$

and the overall electroneutrality balance

$$y = [H^+] + [NH_4^+] - [OH^-] - \sum_i [M_i^-] - \sum_j [B_j H^-] - 2\sum_j [B_j^{2-}] = constant \tag{5.4}$$

The constant of Eq. (5.4) is equal to the sum of the concentrations of the strong acids and bases used in the formulation of the buffer, and the specific pH value can be determined from the initial composition of the medium. For the purpose of this discussion, this constant needs not be evaluated. It is important, however, to recognize that the right hand side of Eq. (5.4) is indeed a constant and in this sense Eq. (5.4) is one of the system's reaction invariants to be discussed in the following section.

In a batch reactor there is no addition or removal of any substance so that the concentrations of the components of the buffer, c_i and c_j, remain constant during the course of a fermentation. At the end of a pH cycle, $[H^+]$ is restored to its value at the beginning of the cycle. For constant c_i and c_j, Eqs. (5.1b,c) and Eqs. (5.2c-e), respectively, indicate that the concentrations of the dissociated and nondissociated forms of all buffer components are also restored to their corresponding values at the beginning of the cycle. From Eq. (5.4) it follows that $[NH_4^+]$ is also restored, and finally from Eq. (5.3b) one can see that the ammonia concentration at the end of a cycle will be the same as at the beginning of the cycle. Therefore, the sum of $[NH_3] + [NH_4^+]$ remains unchanged at

the end of a pH cycle, and, consequently, the amount of ammonia added to restore the pH to its set point is exactly equal to the amount taken up by the cells during a complete pH cycle. A straightforward correlation, therefore, results in the case between the amount of ammonium added, m, and the total rate of biomass growth, R:

$$cR(\Delta t_1 + \Delta t_2) = R_a \Delta t_2 = \frac{m}{V} \tag{5.5}$$

where c is the stoichiometric coefficient for ammonia in the overall reaction for biomass growth and product formation,

$$a\,Glucose + b\,O_2 + c\,NH_3 \rightarrow Biomass + d\,H_2O + e\,CO_2 + f\,Product$$

V is the reactor volume and R_a the rate of ammonium hydroxide addition per unit volume of bioreactor, equal to $\frac{m}{V\,\Delta t_2}$.

5.4 REACTION INVARIANTS

The formulation of the conservation equations of fed-batch and continuous reactors is facilitated greatly by the introduction of the concept of reaction invariants. The theory of chemical reaction variants and invariants can be found elsewhere (Fjeld *et al.*, 1974) and has been applied before by Gustafsson and Waller(1983) for the analysis of the function of pH controllers. The basic ideas in the context of bioreactor are present below.

Consider an acid-base reaction process involving all the components of a typical fermentation medium mentioned in the previous section such as aqueous solutions of strong acids and bases, ammonium, mono- and biacidic weak bases, and the corresponding weak acids and ampholytes. The strong electrolytes, of course, fully dissociate but equilibrium reactions are established for the

weak ones as described by Eqs. (5.1a), (5.2a,b), and (5.3). Note that other components that may undergo further dissociation to produce tertiacidic bases may be present in such a system; however, without loss of generality, they have been excluded from this treatment for the sake of simplicity.

For the system described it can be shown (Aris and Mah, 1963) that a set of state variables exists which are invariant to the reactions (5.1a) and (5.2a,b). Avoiding the mathematical analysis which can be found in the cited references, these invariants can be described in physical terms as combinations of the concentrations of the species present, namely, H^+ , OH^-, NH_4^+, NH_3, M_i^- , M_iH , B_j^{2-} , B_jH^- , B_jH_2, and are, generally, of two types. The first type is basically the electroneutrality condition as expressed by Eq. (5.4). This equation can also be viewed as an expression of the *effective* proton concentration present. The second type of invariants is the constancy of the total concentrations of each conjugate acid-base system:

$$c_i = [M_i^-]+[M_iH] \tag{5.1b}$$

$$c_j = [B_j^{2-}] + [B_jH^-] + [B_jH_2] \tag{5.2c}$$

$$c_a = [NH_4^+] + [NH_3] \tag{5.6}$$

It should be noted that any linear combination of invariants yields also an invariant. Furthermore, when two or more acid-base systems are mixed the invariants of the resulting solutions are each weighed by the fraction that each solution contributes to the volume of the resulting mixture. This property, incidentally, is very useful in calculating the pH of a mixture when the compositions of the constituent solutions are known.

Now, in a fed-batch or continuous reactor the state of the medium is continuously changing with time because of convection and the fermentation

processes occurring. The effect of these processes on the aforementioned invariants can be described by discretizing time and by regarding the state of the reactor at the time instant $t + \Delta t$ as the outcome of a series of mixing processes between the bioreactor contents at time t, the amount of nutrient added or removed, and the amounts of components affecting the pH that are produced or consumed during the time interval Δt. Invoking the previously mentioned rule for the invariants of the mixture at $t + \Delta t$, dividing the balance by Δt, and taking the limit as Δt approaches zero, one obtains the time rates of change of the invariants. These balances are employed in the following section for the analysis of open biosystems.

5.5 CONTINUOUS REACTORS

If one ignores the small amount of phosphorous and some other elements taken up by growing cells, the only process that may affect the components of the buffer is convection into and out of the reactor. Similarly the electroneutrality invariant is affected by convection only, resulting in the following balances for c_i, c_j, and y:

$$\dot{c_i} = D(c_{if} - c_i) \quad , \quad i = 1,2,... \tag{5.7}$$

$$\dot{c_j} = D(c_{jf} - c_j) \quad , \quad j = 1,2,... \tag{5.8}$$

$$\dot{y} = D(y_f - y) \tag{5.9}$$

where the subscript f indicates feed conditions and D is the dilution rate, equal to F/V for a continuous and $\dot{V}/V$ for a fed-batch reactor.

The concentration of ammonium is affected, in addition to convection, by the process of nitrogen uptake of the cells, so the balance for the ammonia-ammonium ion invariant during the first phase of a pH cycle when no ammonium is being added can be written as:

$$\dot{c_a} = D(c_{af} - c_a) - cR \tag{5.10}$$

Equations (5.7)-(5.10) describe the invariants of an open system. They can be added to yield

$$\dot{w} = D(w_f - w) - cR \tag{5.11}$$

with w defined as:

$$w = c_i + c_j + c_a + y \tag{5.12}$$

Integration of Eq. (5.11) between point 0 and t_1 of Fig. 5.1 yields:

$$we^{Dt}\Big]_0^{t_1} = \frac{1}{D}(Dw_f - cR)e^{Dt}\Big]_0^{t_1}$$

or

$$w(t_1)e^{Dt_1} - w(0) = \left[w_f - \frac{cR}{D}\right]\left[e^{Dt_1} - 1\right] \tag{5.13}$$

In the second phase of a pH cycle, during which ammonium is being added, the equivalent of Eq. (5.10) is:

$$\dot{c_a} = D(c_{af} - c_a) - cR + R_a \tag{5.14}$$

which yields the following equation for w:

$$\dot{w} = D(w_f - w) - cR + R_a \tag{5.15}$$

Similarly, integration of Eq. (5.15) between time t_1 and t_2 yields:

$$w(t_2)e^{D(t_2-t_1)} - w(t_1) = \left[w_f - \frac{cR}{D} - \frac{R_a}{D}\right]\left[e^{D(t_2-t_1)} - 1\right] \tag{5.16}$$

and eliminating $w(t_1)$ between Eqs. (5.13) and (5.16) one obtains:

$$w(t_2)e^{D\Delta t_2} - w(0)e^{-D\Delta t_1} - \left[w_f - \frac{cR}{D}\right]\left[1 - e^{-D\Delta t_1}\right] + \left[1 - e^{D\Delta t_2}\right]\left[w_f - \frac{cR}{D} + \frac{R_a}{D}\right] = 0 \tag{5.17}$$

It will now be shown that the quantity w is a state function of the pH; so that $w(t_2) = w(0)$. Furthermore by preparing the feed medium at the pH of point 2, of Fig. 5.1, $w_f = w(t_2)$, so that:

$$w(0) = w(t_2) = w_f \tag{5.18}$$

To show this note that $\dot{c_i} = \dot{c_j} = \dot{y} = 0$ implies that the concentrations c_i, c_j, and y in the reactor are constant and equal to the corresponding concentrations in the feed. It should be noted that the above is true both at steady state and during a transient with respect to the bioreactor state variables such as biomass and substrate/product concentrations. Hence, in terms of the invariants c_i, c_j, and y, the situation in the bioreactor is the same as in the feed and not affected by convection or fermentation. With constant c_i, c_j and for $pH_2 = pH_0$, it follows from the equilibrium relations that the concentrations of the buffer components are restored at the end of a pH cycle to the same values at the beginning of the cycle. Furthermore, by invoking the electroneutrality invariant y, it follows that $[NH_4^+]_2 = [NH_4^+]_0$, and from the ammonia equilibrium, $[NH_3]_2 = [NH_3]_0$ so that finally $c_a(t_2) = c_a(0)$. Therefore $w(t_2) = w(0)$ since all the components of the quantity w have the same values at the beginning and the end of the pH cycle.

Invoking Eq. (5.18) , Eq. (5.17) is simplified to:

$$cR = R_a \frac{1 - e^{-D\Delta t_2}}{1 - e^{-D(\Delta t_1 + \Delta t_2)}} \tag{5.19}$$

which is the final result of the analysis. Equation (5.19) provides an an

additional relationship between the total growth rate and quantities such as the rate of ammonia addition for pH control, Δt_1 and Δt_2, which are monitored in most fermentations and can be easily interfaced to a computer. In this sense the result of Eq. (5.19) is useful for on-line bioreactor identification.

For the case of a batch reactor $D = 0$, the application of L'Hospital's rule to Eq. (5.19) yields:

$$cR = R_a \frac{\Delta t_1}{\Delta t_1 + \Delta t_2} \tag{5.20}$$

which is exactly the same as Eq. (5.5) arrived at by different arguments. Note that the same equation may also be applicable to a continuous fermentations when the rate of ammonium uptake is large such that the term $D(\Delta t_1 + \Delta t_2)$ is small. The above enables one to approximate the exponentials in Eq. (5.19) by:

$$e^{-D\,\Delta t_2} = 1 - D\,\Delta t_2$$

and

$$e^{D\,(\Delta t_1 + \Delta t_2)} = 1 - D(\Delta t_1 + \Delta t_2)$$

Eq. (5.19) reduces to that of Eq. (5.5) when the above approximations are valid.

5.6 FED-BATCH REACTORS

For the case of a fed-batch reactor, $D = \frac{\dot{V}}{V}$, and the analysis will be exactly the same as that of a continuous reactor, except for the fact that in Eq. (5.11) the dilution rate D is no longer a constant but is given by $\frac{\dot{V}}{V}$.

For the first half of the pH cycle, Eq. (5.11) has to be rewritten as:

$$\dot{w} = \frac{\dot{V}}{V}(w_f - w) - cR \qquad 0 \le t \le t_1 \qquad (5.21)$$

with w defined in Eq. (5.12). Integration of Eq. (5.21) between 0 and t_1 of Fig. 5.1 yields:

$$wV\Big]_0^{t_1} = w_f V\Big]_0^{t_1} - cR\int_0^{t_1} V\,dt$$

or

$$w(t_1)V(t_1) - w(0)V(0) = w_f V(t_1) - w_f V(0) - cR\int_0^{t_1} V\,dt \qquad (5.22)$$

In the second phase of the pH cycle, during which ammonium hydroxide is being added, the dynamic equation for w is similarly given by

$$\dot{w} = \frac{\dot{V}}{V}(w_f - w) - cR + R_a \qquad t_1 \le t \le t_2 \qquad (5.23)$$

Integration of Eq. (5.22) between times t_1 and t_2 yields:

$$w(t_2)V(t_2) - w(t_1)V(t_1) = w_f V(t_2) - w_f V(t_1) - cR\int_{t_1}^{t_2} V\,dt + R_a\int_{t_1}^{t_2} V\,dt \qquad (5.24)$$

For the case of $w(0) = W(t_2) = w_f$, eliminating $w(t_1)$ between Eqs. (5.22) and (5.24) yields:

$$cR\int_0^{t_2} V\,dt = R_a\int_{t_1}^{t_2} V\,dt \qquad (5.25)$$

If the feed rate is a constant then $\dot{V}$ is given

$$\dot{V} = F$$

where F is the flow rate. Eq. (5.25) can be further simplified into

$$cR = R_a \frac{V_{t0}\Delta t_2 + \frac{F}{2}(t_2^2 - t_1^2)}{V_{t0}(\Delta t_2 + \Delta t_1) + \frac{F}{2}(t_2^2 - t_0^2)} \qquad (5.26)$$

where V_{t0} is the volume at time t_0.

5.7 EXPERIMENTS

5.7.1 Verification of Equation (5.20)

Equations (5.19) and (5.20) were first tested with non-biological, continuous flow experiments simulating various fermentation situations. An NBS-Bioflow fermentor of 1.3 litre working volume was employed for this study. First, the reactor was filled with a phosphoric acid buffer solution, the pH of which was adjusted to 7 by adding KOH pellets and subsequently a continuous flow of a similar buffer solution but of lower pH (pH=1.7) was introduced through the fermentor. This acidized buffer was prepared by adding concentrated HCl to the phosphoric acid buffer and was used to simulate the effect of proton generation by the fermention process. The flow of the acidified buffer solution produced a decrease in the pH of the fermentor which was corrected by the addition of basic buffer solution. This basic buffer solution was prepared by adding pellets of KOH to the natural (pH = 2.4) phosphoric acid buffer yielding a basic solution of pH = 11.2. A Corning pH combination electrode was used for the measurement of the pH. The pH of the reactor was controlled between 6.98 and 7.00 by a Chemtrix pH controller. During the course of the experiment the amount of base added at each pH cycle and the time intervals Δt_1 and Δt_2 of Figure 5.1 were continuously monitored with the computer-based data acquisition system described previously.

By measuring the flow rate of the buffer solution of known acidity through the reactor the true rate of proton addition to the reactor can be directly

calculated. Also, this rate of proton addition can be determined from the measurement of the amount of KOH solution added for pH control, and Δt_1 and Δt_2 by using Eq. (5.19) for continuous reactors, Eq. (5.26) for fed-batch reactors, and Eq. (5.20) for batch reactors. A direct comparison between the predictions of the developed equations and the true values is thus available. Shown in Table 5.1 are the results of various runs in the form of dimensionless $D(\Delta t_1+\Delta t_2)$, versus the dimensionless ratio of the total proton addition over the total base addition during one pH cycle.

As indicated in Table 5.1 the predictions of Eq. (5.19) are in close agreement with the true values. For small values of $D(\Delta t_1+\Delta t_2)$ both Eqs. (5.19) and (5.20) yield similar predictions as it was demonstrated earlier analytically. To further demonstrate the effect of $D(\Delta t_1+\Delta t_2)$ another series of runs was carried out in which the flow of the acidified buffer solution was kept constant but the flow of buffer solution was varied over a wide range to produce different values of the dilution rate D and, with it, varying values of $D(\Delta t_1+\Delta t_2)$. The results are plotted in Figure 5.2. Since the flow rate of the acidified buffer was kept constant, the value of the ratio, (proton added)/(base added), was also constant, and this is indicated by the straight line in Figure 5.2. The calculated values of this ratio as obtained from Eqs. (5.19) and (5.20) are also shown. Each point shown is the average of many runs (pH cycle) performed under the same conditions, the corresponding error being about 5 percent. It can be seen that the predictions of Eq. (5.19) are in excellent agreement with the true values. However, as the value of $D(\Delta t_1+\Delta t_2)$ increases, the deviation between the true values and the predictions of Eq. (5.20) becomes larger, as expected. It should be pointed out that Eq. (5.20) is, essentially, a representation of a balance between the amount of ammonia added to the fermentor and the amount taken up by

the microorganisms during one pH cycle. Such a balance is true for a batch reactor. Its use, however, with a continuous flow reactor may introduce serious errors in the identification procedure as indicated by the results of Figure 5.2. Instead, equation (5.19) is the outcome of the correct accounting of all pH-affecting processes and should be always used with open fermentors when the pH-changing process is of the type considered in this chapter.

5.7.2 Application to Continuous Yeast Fermentation

After the validity of Eq. (5.19) was established with previously described experiments, the above correction for the total biomass growth rate was employed for the on-line identification of a continuous yeast fermentation of glucose to ethanol. As pointed out before, the simple correction of Eq. (5.5) is not valid with a continuous system. Instead, Eq. (5.19) is necessary, along with the RQ measurement and the elemental balances for C, H, O and N to close the system of equations for the six stoichiometric coefficients of Eq. (2.1). Furthermore, Eq. (5.19) is written in terms of rates, and it is , for this reason, especially suited for use within the on-line bioreactor identification framework presented in Chapter 2.

5.7.2.1 Experimental Procedure

Materials, and methods, and the general experimental methodology for these runs were similar to the fed-batch fermentations described in Chapter 3. The only difference was that a smaller size vessel, a 2-litre NBS Bioflow fermentor, was used for these fermentations. A 1.3-litre working volume fermentor was initially filled with medium, inoculated, and operated in a batch mode until significant amount of biomass had been formed. At that point, the flow of medium through the reactor was started at a rate of 160 ml/hr corresponding to a dilution rate of 0.123 hr^{-1} and was maintained at that level for 4.5 days.

(approximately 13 residence times) to insure that a steady state with respect to biomass, glucose and ethanol concentrations had been reached. Then a transient was introduced by increasing the dilution rate from 0.123 hr^{-1} to 0.258 hr^{-1}.

5.7.2.2 Data Analysis and Results

Data analysis was performed following the same procedure described in Chapter 3. The only difference was that Eq. (5.19) was now employed in the calculation of the total biomass growth rate R. The results are shown in Figures 5.3-5.8. The solid lines represent on-line estimates obtained by the proposed methodology; dashed lines indicate estimates obtained by simple averaging. Shown also are the data points of the corresponding quantities with the associated error bar. These points were obtained by sampling the fermentor every 1/2 hour and measuring, off-line, cell biomass, glucose, and ethanol concentrations following the same method as described in Chapter 3. A direct comparison between on-line estimates and direct, off-line measurements can thus be afforded.

There are several points worth mentioning in Figures 5.3-5.8. First, the agreement between the estimates of the proposed estimator and the direct measurements is remarkable. It should be pointed out that this agreement exists despite the transient (washout) nature of the experiment and the rather wide range of variation of the quantities estimated. Second, after following the process for approximately one hour, the RC estimates started deviating significantly from the true values. This drastic departure was due to an instantaneous malfunctioning of one of the probes or analyzers. It can be seen that the proposed estimator was successful in filtering out this perturbation as well as another one that occurred at about the fifth hour of operation. No such

capability exists in the structure of the RC filter, however, and inevitable errors or noises in the process, the probes, or the analyzers would tend to create large errors in the estimates, especially after a long period of operation. This is a major disadvantage of the RC filters which counterbalances the advantage of the relatively simple implementation.

After reviewing the raw data, the source of the above error was located on the pH controller which was turned on accidentally at about one hour, and this produced a large increase in the calculated total biomass growth rate. To provide a safeguard against such an accidental happening, a data window was added to the estimation algorithms. That is, if two successive data points differ by less than 30 percent the latter point is accepted and processed. However, if the latter point falls outside this range it is rejected and the previous point is used. Application of this addition filter to the algorithm yielded the results shown in Figures 5.9-5.12. It can be seen that the estimates of the proposed algorithm remained essentially unchanged but the RC estimates were significantly improved by the elimination of the grossly deviating measurements.

A third point is the smoothness of the estimates of the specific growth rate as opposed to the noisy estimates of the RC filter. Despite a rather extensive moving averaging, the RC estimates of μ remained noisy and did not improve by the addition of the above window filter. Since the specific growth rate is an important control variable, the proposed adaptive estimator must be employed in the construction of a stable and efficient control structure.

A final point concerns the dynamic features of the specific growth rate as observed in Figs. 5.6 and 5.12 of this washout experiment. For over one hour after the initiation of the step-up perturbation, the value of μ remained constant and equal to the dilution rate before the introduction of the transient,

$D = 0.123\ hr^{-1}$. This is so despite a marked increase in the value of glucose concentration of over 50 percent during the same period of time. One can conclude that a delay of approximately one hour exists in the cell's response to changing environmental conditions for the purpose of preparing the organism's enzymatic machinery ready for the new environment. Such delays are frequently present and must be accounted for in the design of the reactor control structure.

5.7.2.3 Discussion

The analysis that led to Eq. (5.19) and Eq. (5.26) not only yields an additional correlation for bioreactor identification but also provides the means of evaluating the effect of various other factors on the above result. The case of acidic/basic product formation, using a different neutralizing agent for pH control, or, providing a different nitrogen source to satisfy the nitrogen needs of the microorganisms, each have special features which are discussed below in more detail.

When a weak acid, AH, is formed in a fermentation, its dissociation and the subsequent effect on the pH must be taken into consideration. Following the analysis of the earlier section, a new invariant for the total acid concentration, c_p, must be introduced

$$[AH] + [A^-] = c_p \tag{5.27}$$

subject to the dynamics

$$\dot{c_p} = D(c_{pf} - c_p) + fR \tag{5.28}$$

Furthermore, the definition of the y invariant must now be modified to account for the new weak base present:

$$y = [H^+] + [NH_4^+] - [OH^-] - [A^-] - \sum_i [M_i^-] - \sum_j [B_j H^-] - 2\sum_j [B_j^{2-}] = constant \tag{5.29}$$

and the corresponding quantity w becomes:

$$w = c_i + c_j + c_a + c_p + y \tag{5.30}$$

subject to the dynamics:

$$\dot{w} = D(w_f - w) + (f - c)R \tag{5.31}$$

which is the result of adding Eqs. (5.7)-(5.10) and (5.28).

An analysis similar to that presented earlier can also be carried out for the two phases of a pH cycle. In the presence of the acid product AH, however, the quantity w is no longer a state function of the pH, and $w(t_2) \neq w(0)$ despite the fact that the pH is restored to its set point at the end of a cycle. Only when the fermentor operates at a steady state, the analysis can be carried through to yield the equivalent of Eq. (5.19), but with the LHS replaced by $(c - f)R$ to account for the formation of the acidic product. In other situations the following approximation can be employed.

Usually the duration of the cycle is short and the product formation rate is small, and one can assume that $c_p(t_2) \approx c_p(0)$, so that $w(t_2) \approx w(0)$. In doing so yields:

$$(c - f)R = R_a \frac{1 - e^{-D\Delta t_2}}{1 - e^{-D(\Delta t_1 + \Delta t_2)}} + D(w_o - w_f) \tag{5.32}$$

The above equation can be used with the described methodology for the determination of the stoichiometric coefficients and total biomass growth rate, R. Once f and R have been determined over a pH cycle, Eq. (5.28) can be

integrated for the same time interval with c_{p0} as initial condition to yield the concentration c_p at the end of the cycle, c_{p2}. Thus at the end of a pH cycle:

$$[A^-] + [AH] = c_{p2} \tag{5.33}$$

and from the invariant for the electroneutrality condition:

$$[NH_4^+] - [A^-] = constant \tag{5.34}$$

the constant in Eq. (5.34) being equal to the corresponding quantity at the beginning of the pH cycle.

Equations (5.33) and (5.34) can then be combined with the equilibrium equations for NH_3 and AH to determine the concentrations $[A^-]$, $[AH]$, $[NH_4^-]$ and $[NH_3]$ at the end of the pH cycle and used as the initial value $w(0)$ for a similar calculation in the subsequent cycle.

A variation of the above procedure is to integrate Eq. (5.28) from the beginning by using the values of the previous cycle for f and R in order to obtain c_{p2}. Then $w(t_{t_2})$ can be evaluated by a procedure similar to that described above and used directly in Eq. (5.17) to yield a more complicated expression for the net rate of proton generation during a cycle. After the values of f, c, and R have been determined for the current cycle, they can be compared to the ones used initially in the integration of Eq (5.28). A trial and error method can further be employed to insure that the initially assumed values of f and R agree with those determined at the end.

Clearly the methodology in the case of acid/base product formation is more involved. In addition to the increased complexity, the possibility of error accumulation resulting from the integration of Eq. (5.28) is significantly higher in the absence of a direct measurement of the product. It is recommended that the on-line estimates of the product concentration be compared periodically

with accurate off-line measurements of the same quantity and corrected accordingly whenever large discrepancies are detected. The frequency of correction depends, of course, on the dilution rate and total rate of product formation, but for most fermentations one measurement every few days, will be sufficient.

The above discussion is also indicative of the complications that will arise if a different base, such as KOH is used for pH control. In this case the electroneutrality invariant should be modified to read:

$$y = [H^+] + [NH_4^+] + [K^+] - [OH^-] - [A^-] - \sum_i [M_i^-] - \sum_j [B_j H^-] - 2\sum_j [B_j^{2-}] = constant \tag{5.35}$$

By the same arguments, the quantity w is not a state variable of the pH, $w(t_2) \neq w(0)$, and the amount of K^+ ions added and washed out must be carefully accounted for in order to be able to determine the value of $w(t_2)$ by a procedure simliar to the one outlined for the case of acid product formation. Similarly, if a different salt is used as nitrogen source, care must be taken to use the corresponding strong acid or base to control the pH in order to facilitate the use of a very useful measurement for the identification of the reactor and to avoid complicated and error prone data reduction procedure.

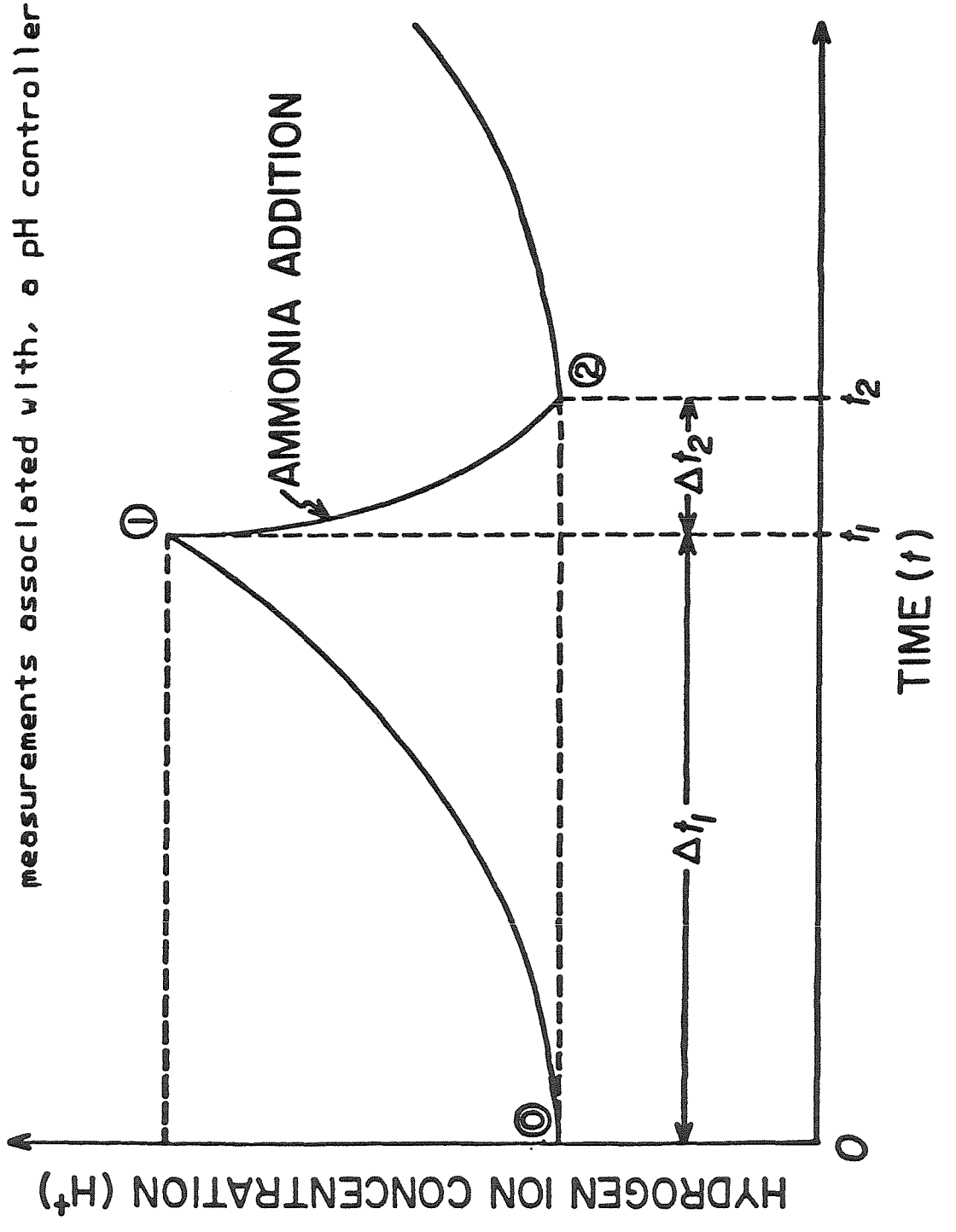

Fig. 5.1 Schematic representation of the function of, and measurements associated with, a pH controller

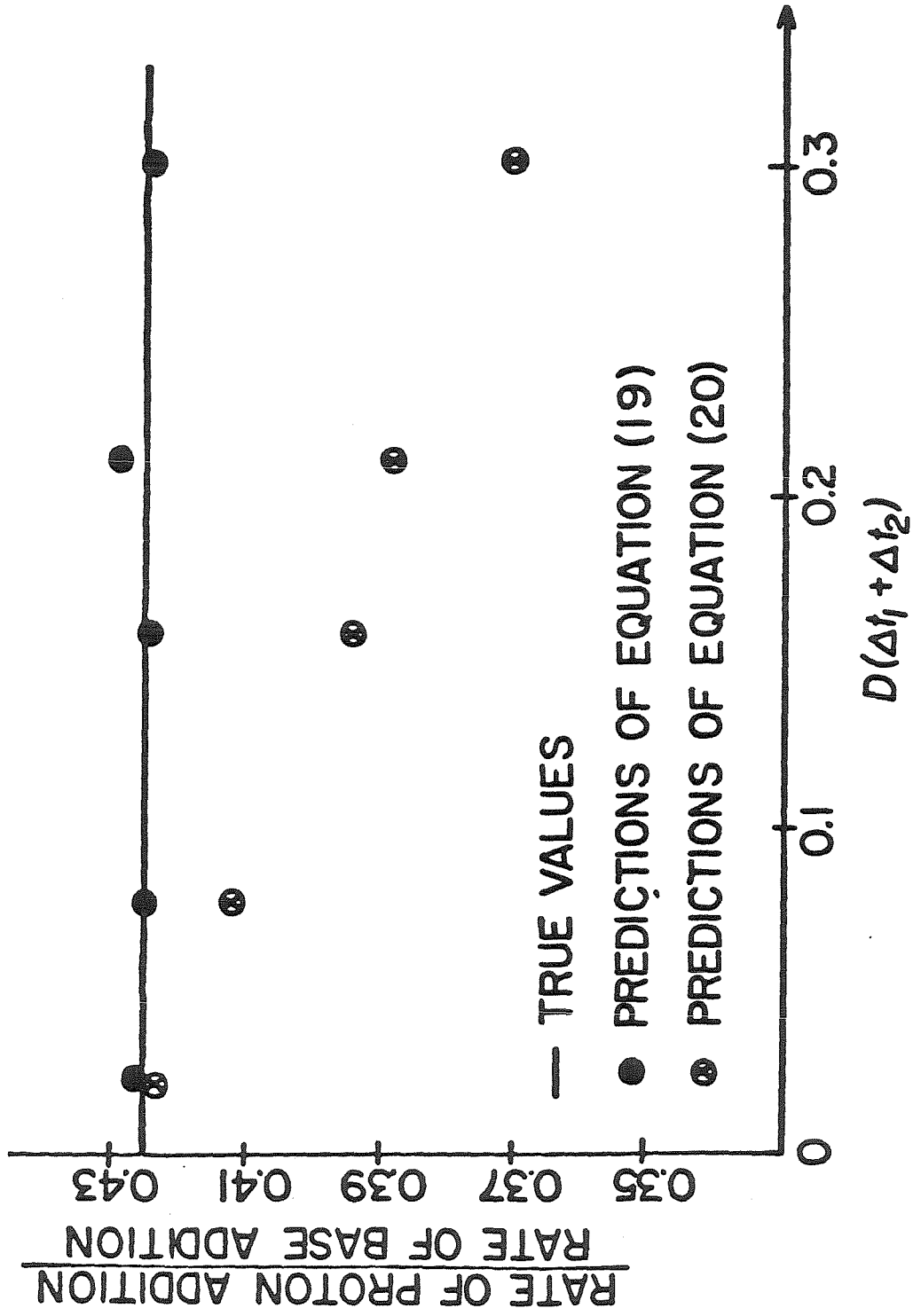

Fig. 5.2 Experimental verification of Eq. (5.19) with non-biological continuous flow, acid-base reaction system

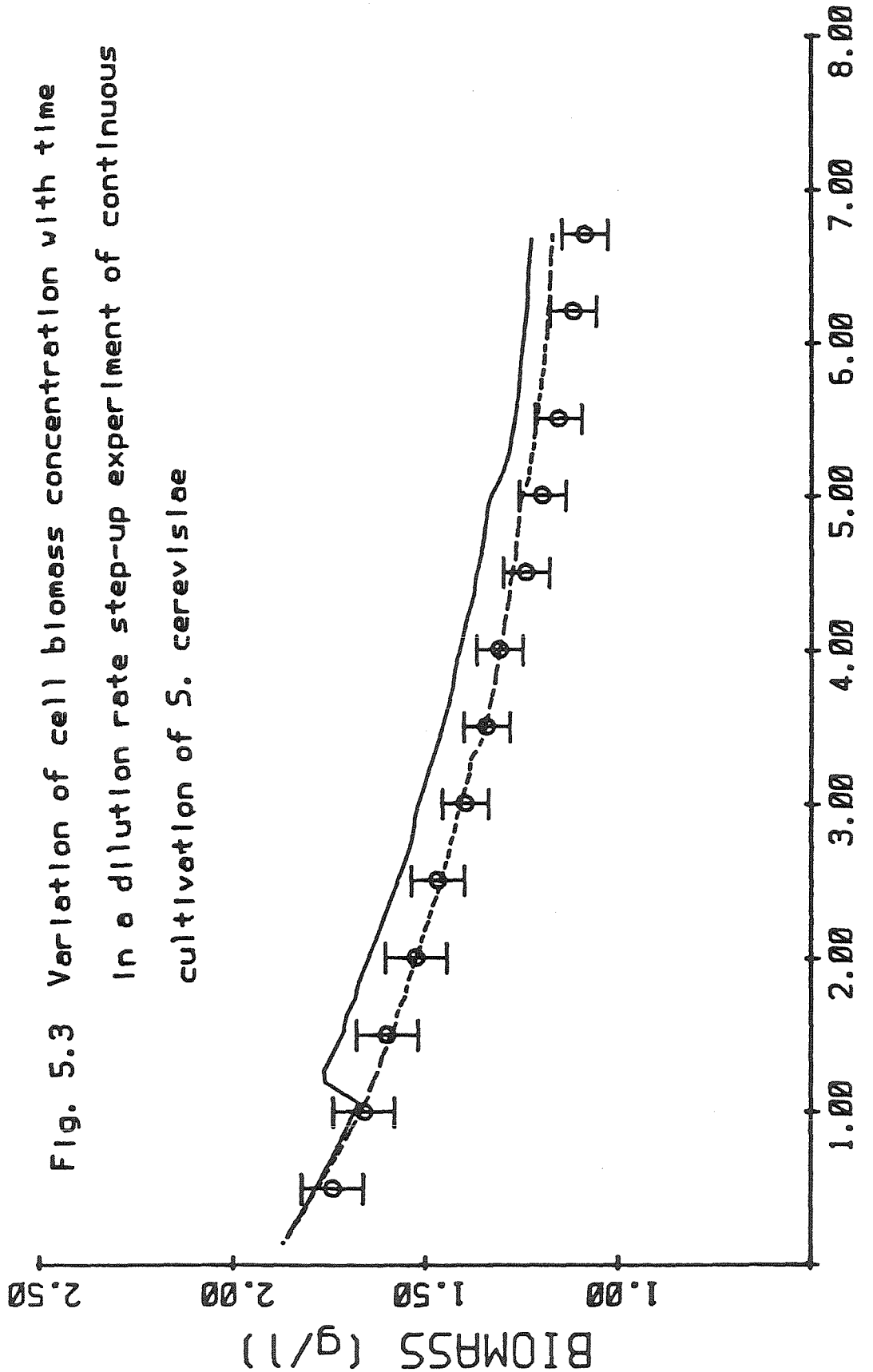

Fig. 5.3 Variation of cell biomass concentration with time in a dilution rate step-up experiment of continuous cultivation of S. cerevisiae

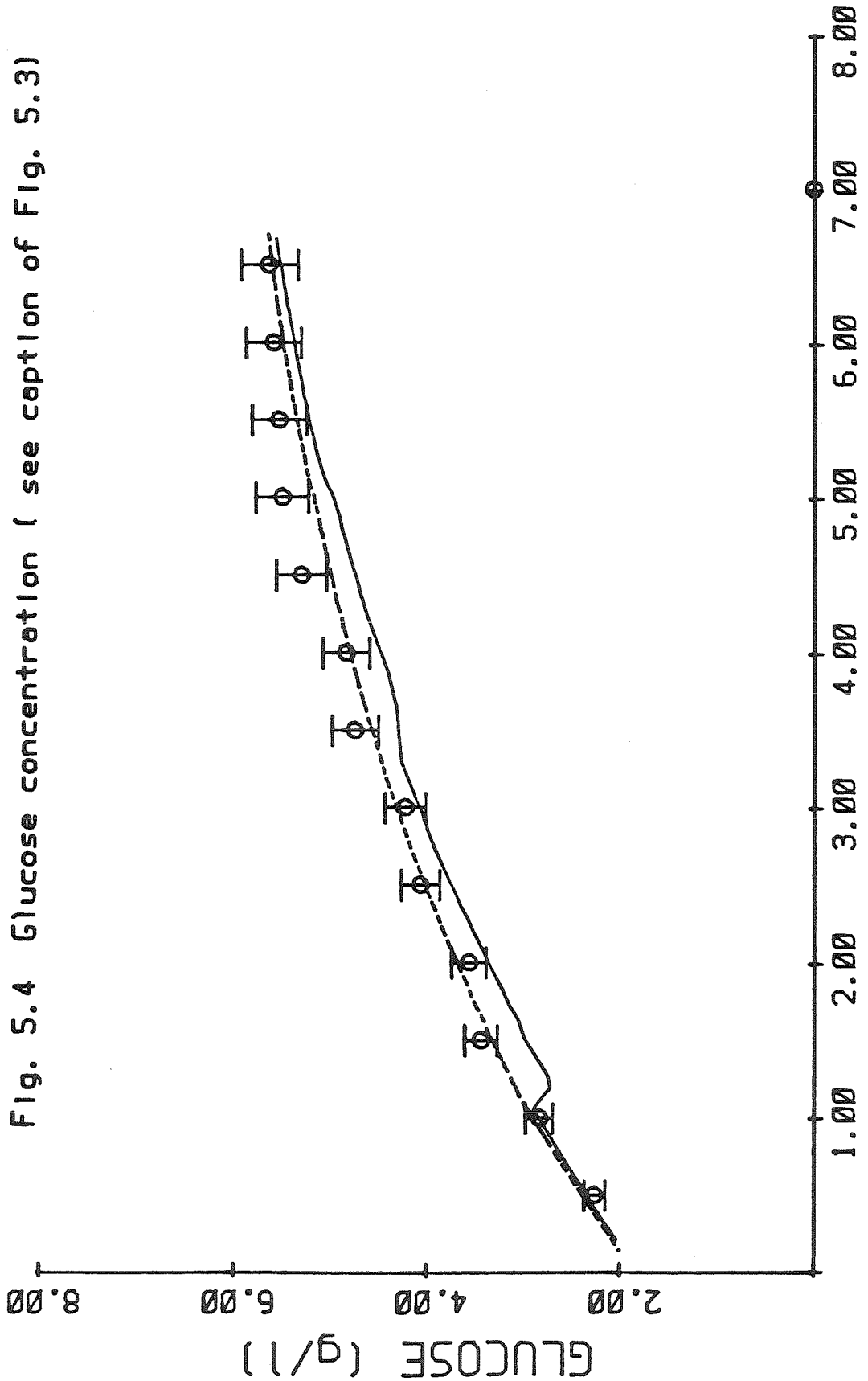

Fig. 5.4 Glucose concentration (see caption of Fig. 5.3)

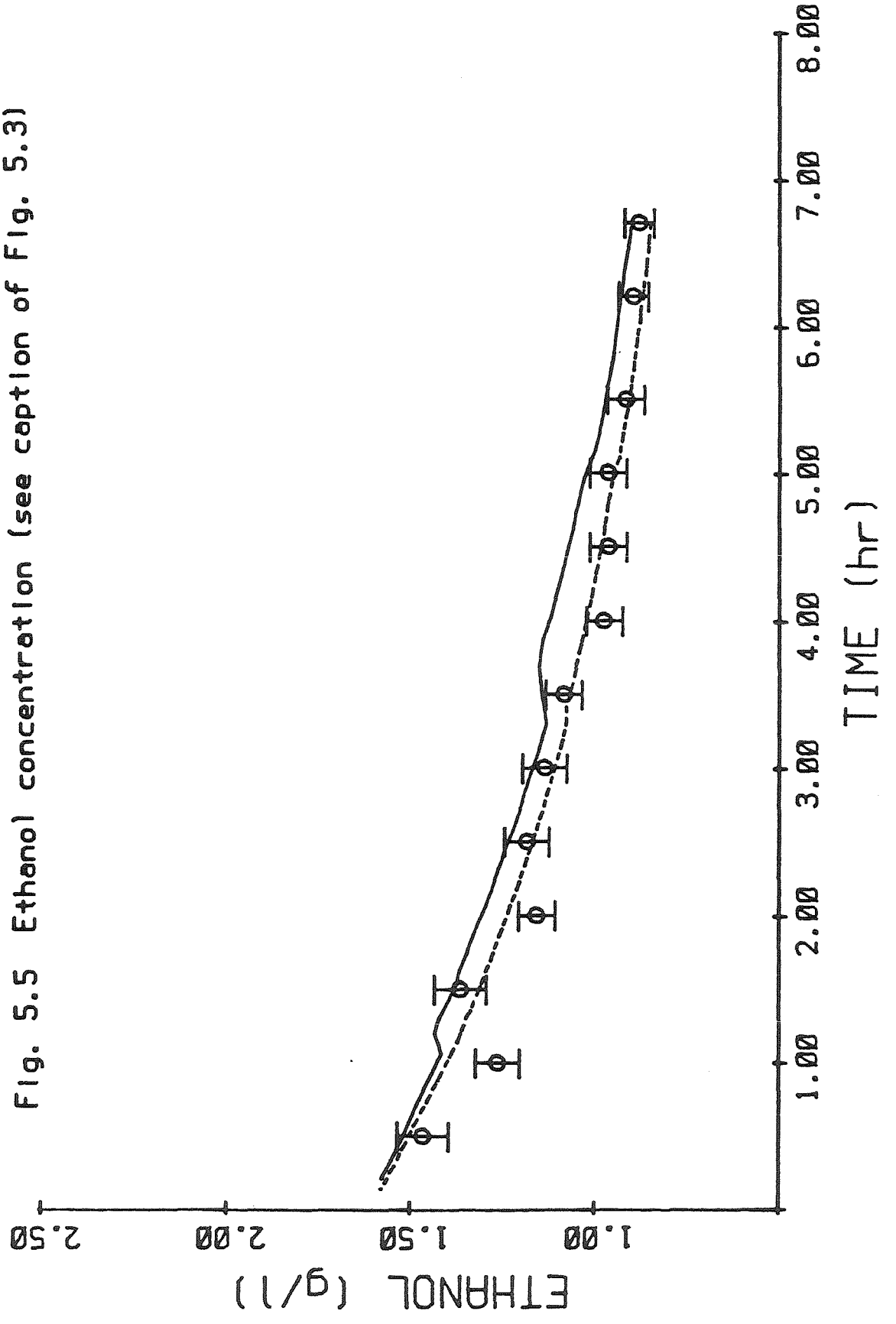

Fig. 5.5 Ethanol concentration (see caption of Fig. 5.3)

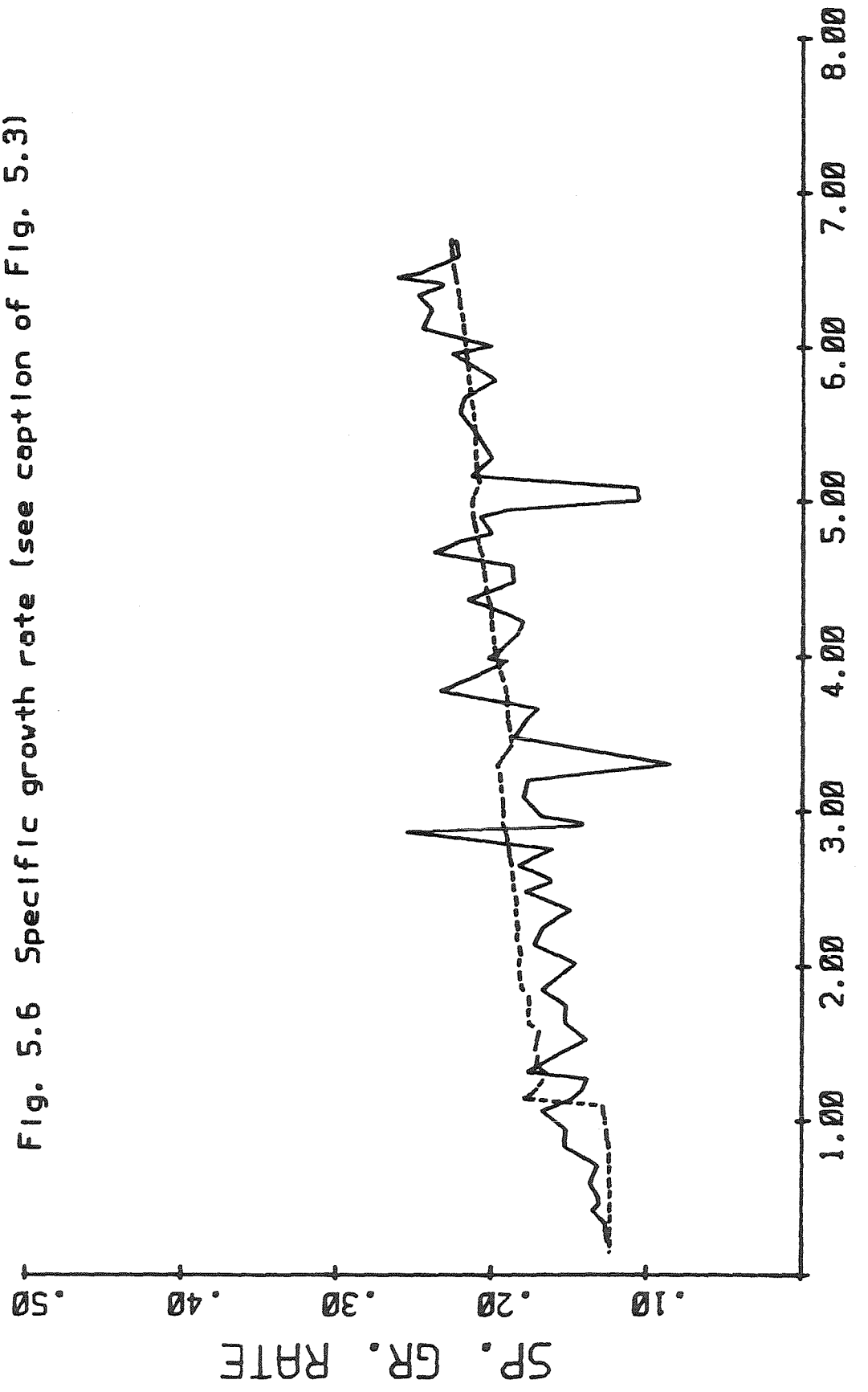

Fig. 5.6 Specific growth rate (see caption of Fig. 5.3)

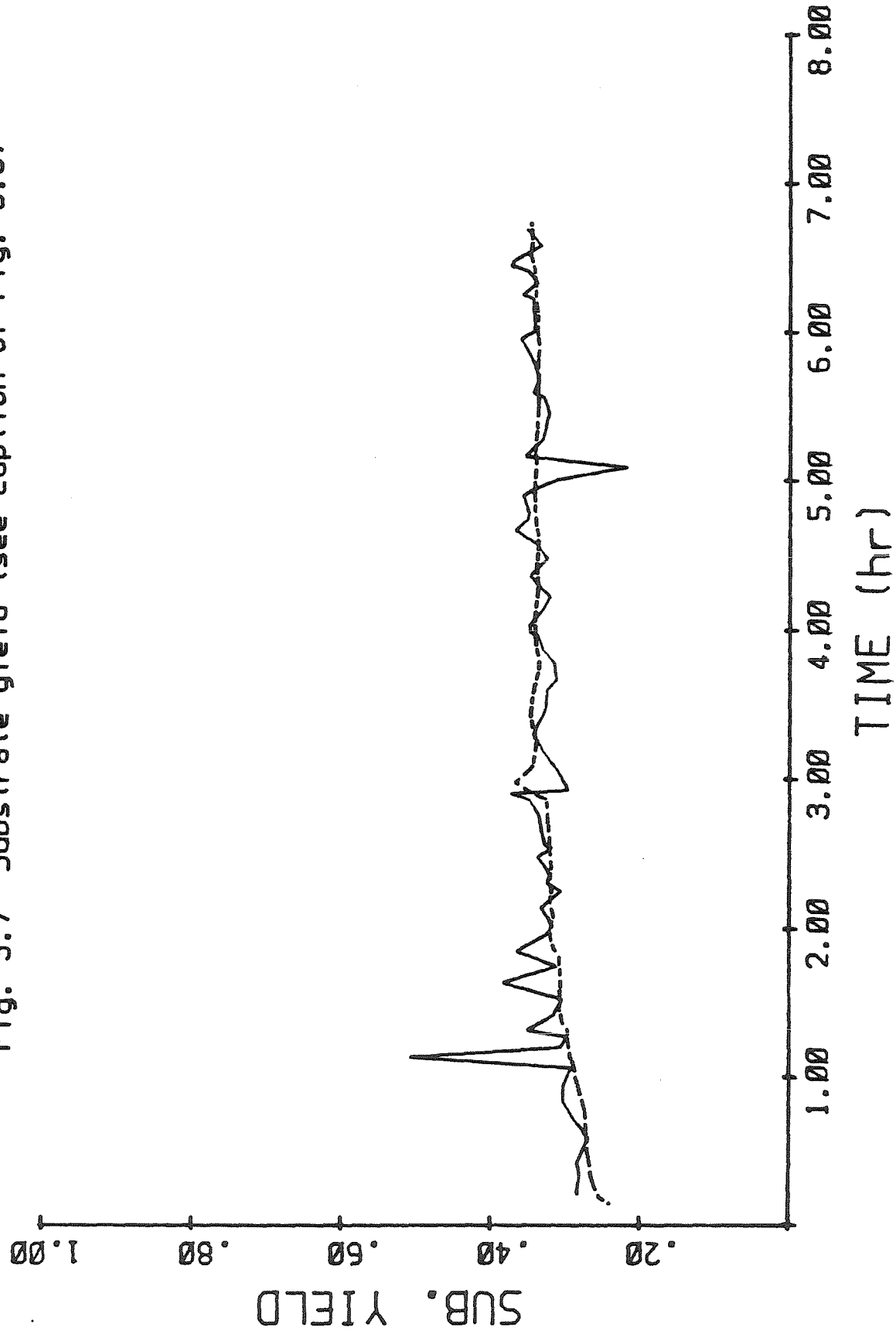

Fig. 5.7 Substrate yield (see caption of Fig. 5.3)

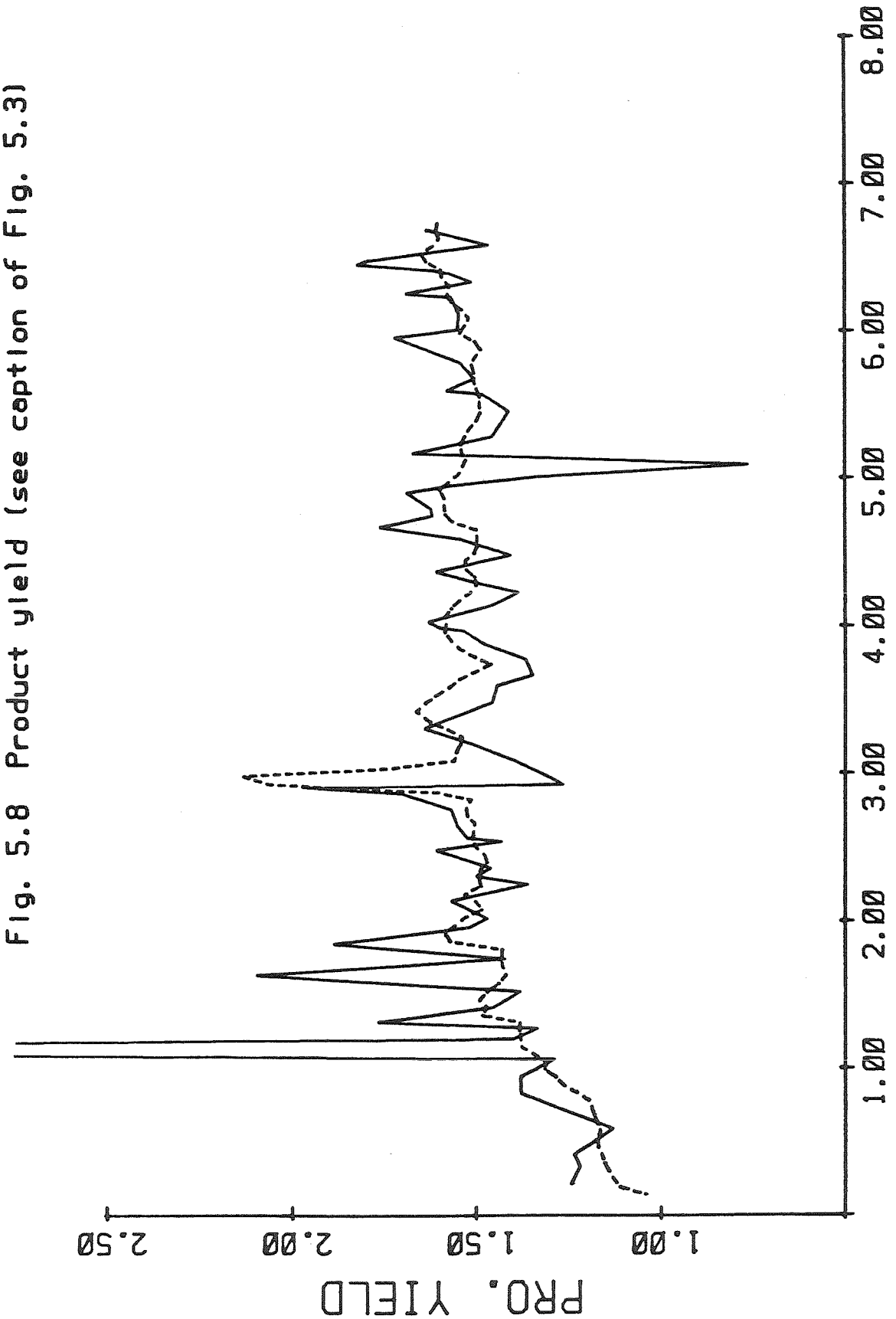

Fig. 5.8 Product yield (see caption of Fig. 5.3)

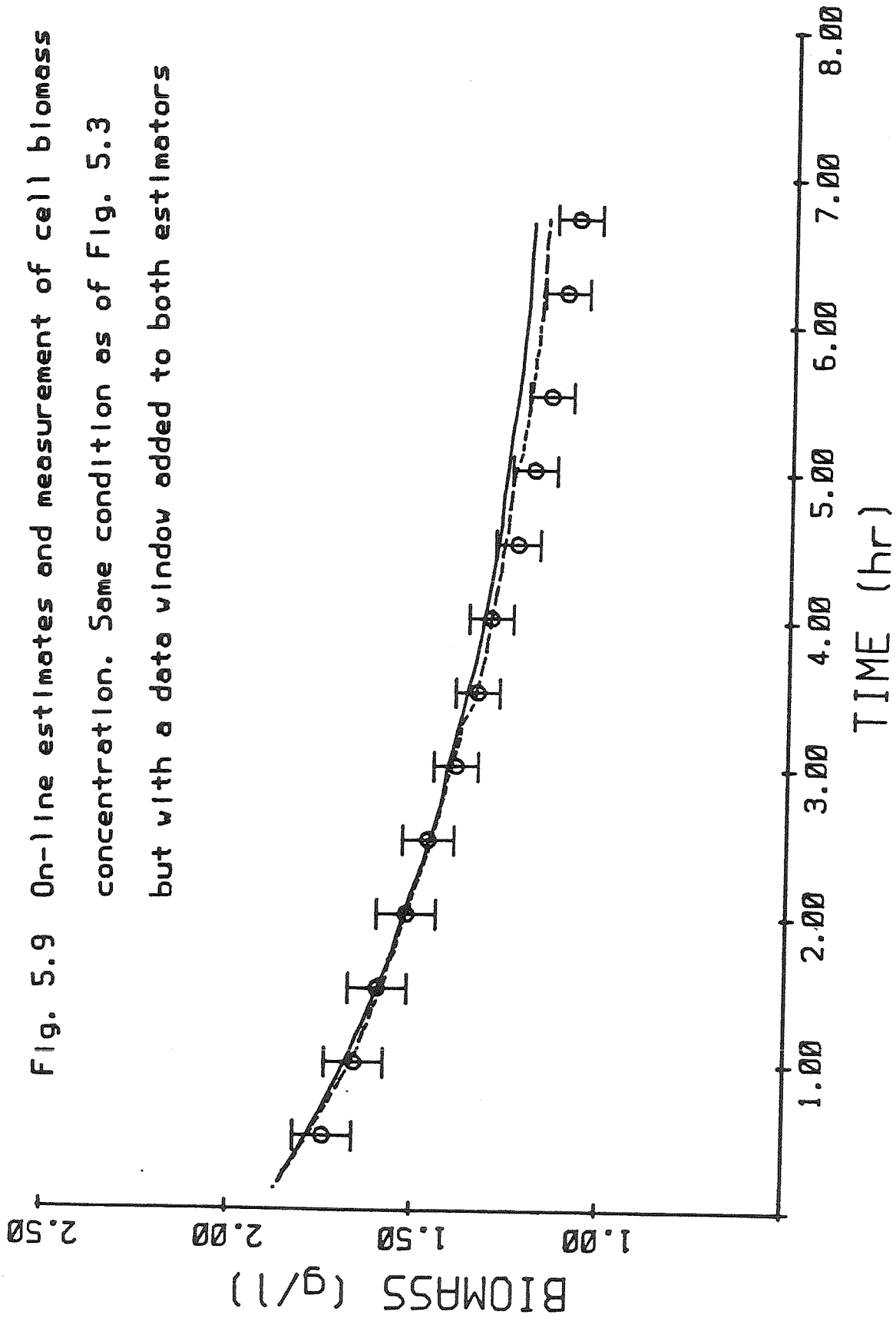

Fig. 5.9 On-line estimates and measurement of cell biomass concentration. Same condition as of Fig. 5.3 but with a data window added to both estimators

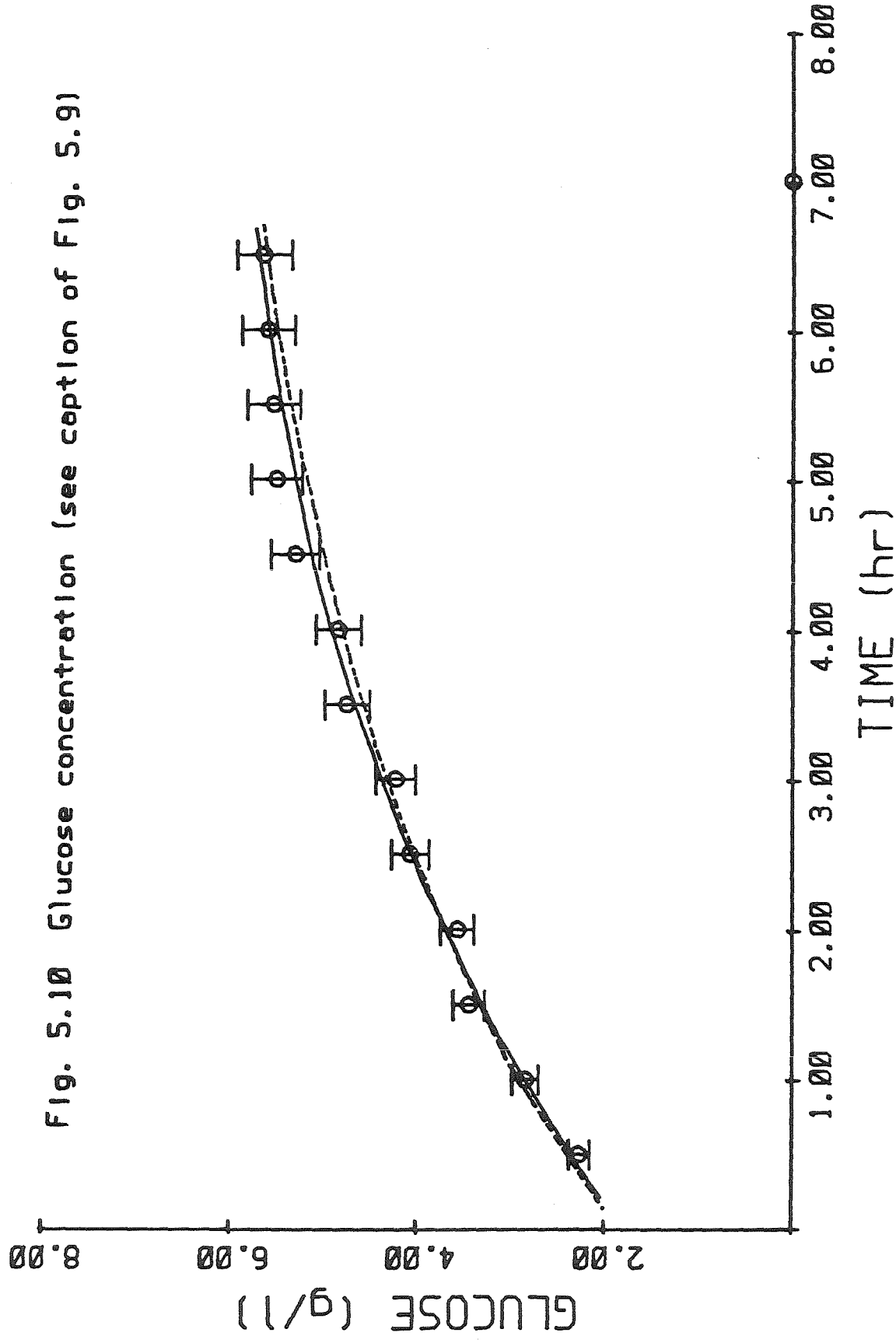

Fig. 5.10 Glucose concentration (see caption of Fig. 5.9)

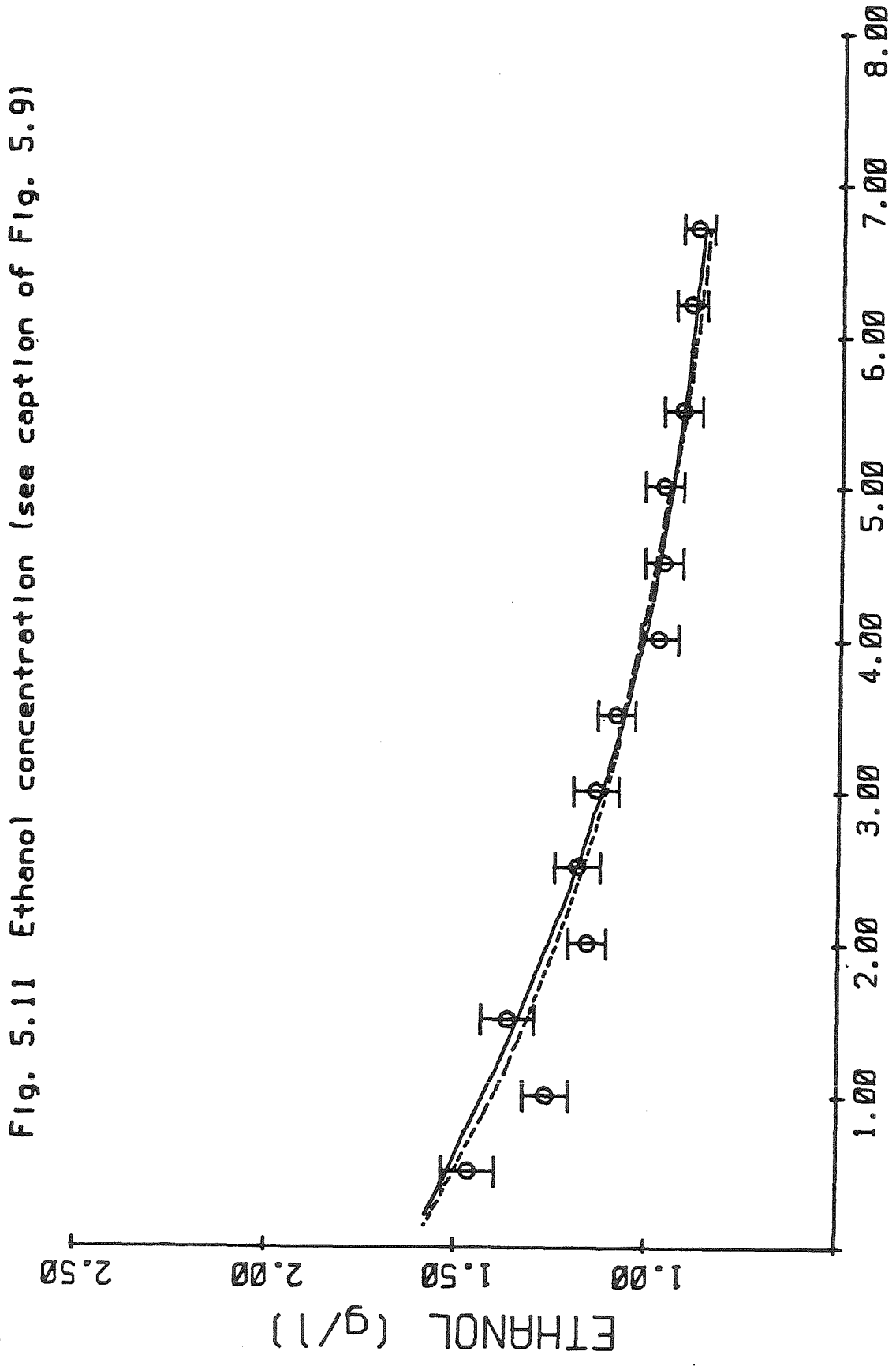

Fig. 5.11 Ethanol concentration (see caption of Fig. 5.9)

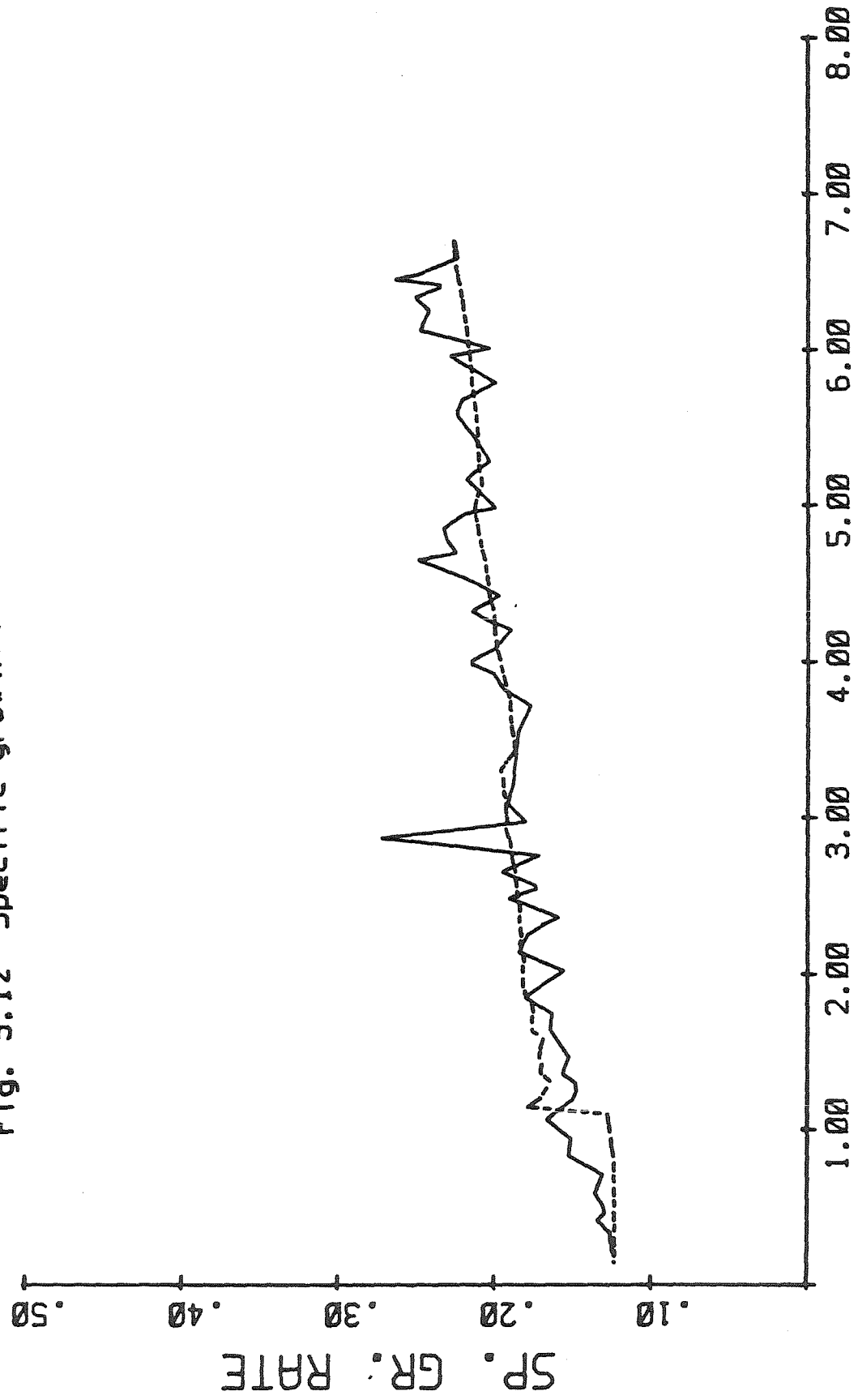

Fig. 5.12 Specific growth rate (see caption of Fig. 5.9)

$D(\Delta t_1+\Delta t_2)$	(rate of proton addition)/(rate of base addition)		
	True Value	Prediction 1	Prediction 2
0.245	0.0318 ± 0.0020	0.0295 ± 0.0013	0.0265 ± 0.0013
0.239	0.0458 ± 0.0010	0.0426 ± 0.0017	0.0372 ± 0.0017
0.216	0.0578 ± 0.0027	0.0573 ± 0.0021	0.0509 ± 0.0021
0.141	0.0436 ± 0.0020	0.0424 ± 0.0027	0.0399 ± 0.0027
0.089	0.0524 ± 0.0020	0.0522 ± 0.0022	0.0501 ± 0.0022

Prediction (1) using equation (19)

Prediction (2) using equation (20)

Table 5.1

NOTATION

a,b,c	gmole of carbon source, oxygen and ammonia, respectively, consumed per gmole of cell biomass produced
d,e,f	gmole of H_2O,CO_2 and product formed
c	stoichiometric coefficient for ammonia uptake
c_i	total concentration of monoacidic buffer component i
c_j	total concentration of biacidic buffer component j
c_p	total concentration of product
c_a	total concentration of ammonia and ammonium ion
c_{if}	feed concentration of component i
D	dilution rate
F	reactor flow rate
f	stoichiometric coefficient for product formation
K_i	equilibrium constant of dissociation reaction for component i
K_{kj}	equilibrium constant of K^{th} dissociation reaction for conponent j
K_A	equilibrium constant of ammonium dissociation
m	amount of ammonium hydroxide added during a pH cycle
R	total rate of growth per unit volume
R_a	rate of NH_4OH added for pH control per unit volume
RQ	respiration quotient
V	reactor volume
w	defined by equation 5.12
y	reaction invariant expressing the electroneutrality condition
Δt_1	time interval during which the pH controller is off
Δt_2	time interval during which the pH controller is on

CHEMICAL SYMBOL

AH	chemical symbol for the product during fermentation
A^-	cation of the product
B_jH_2	biacidic buffer system, component *j*
H^+	hydrogen ion
K^+	potassium ion
M_iH	monoacidic buffer system, component *i*
OH^-	hydroxide ion

PART II. SOME OPTIMAL CONTROL PROBLEMS OF BIOREACTOR

CHAPTER 1

OPTIMAL CONTROL POLICY FOR SUBSTRATE INHIBITED KINETICS WITH ENZYME DEACTIVATION IN AN ISOTHERMAL CSTR

1.1 INTRODUCTION

Immobilized enzymes suspended in a stirred tank or in a tubular reactor as a packed, moving or fluidized bed are being increasingly used in a variety of applications because of their high activity and specificity in catalysing useful reactions. An important consideration for the performance of immobilized enzyme reactor systems is the deactivation of the enzymes whereby they lose with use, some of their potency as catalysts. This decay of catalytic activity has serious consequences on the process economics, first because of the high cost of enzyme replacement and, second, because of a departure of the state of the reactor from the point of optimal operation.

Several aspects of enzyme deactivation have been addressed by previous studies. Among them, the interaction of physical and chemical factors that influence deactivation is discussed in Laidler and Bunting (1973). and the sequence of enzyme transformations that lead to deactivation in Reiner (1969). Expressions for the kinetics of enzyme decay that correspond to various deactivation mechanisms can be found also in Laidler and Bunting (1973). Other related problems have been examined by various investigators, such as the effect of enzyme decay on the effectiveness factor of a single pellet of immobilized enzyme (Korus and O'Driscoll, 1975,1976), and the effectiveness of several protective measures against the undesirable effects of enzyme decay in catalytic pellets (Lee and Reilly, 1978).

Further research into the mechanisms of enzyme action is expected to a

better understanding of the phenomenon of deactivation and more effective measures to prevent or slow down the rate at which it occurs. However, for as long as deactivation is taking place, it will be accompanied by an undesirable departure of the state of the reactor from the optimal point with the obvious consequences on the economics of the process. To better illustrate the point, consider the effect of enzyme deactivation on the performance of an isothermal CSTR with an enzyme immobilized in it that catalyzes the reaction $A \rightarrow B$. Assuming that external mass transfer resistance around the particles with immobilized enzymes is negligible and also neglecting intraparticle diffusion, the dynamics of this CSTR is described by

$$\dot{c_A} = \frac{F}{V}[c_{A0} - c_A] - a\,\frac{Kc_A}{c_A^2 + K_s c_A + K} \qquad (1)$$

For illustrative purposes only, substrate inhibited kinetics was assumed to describe the rate of reactant depletion in Eq. 1. If the enzyme activity a is constant, a steady state for c_A is obtained at the intersection of the curve $kc_A/(c_A^2 + K_s c_A + K)$ with the straight line $(\frac{F}{aV})(c_{A0}-c_A)$ representing, respectively, the rates of reactant consumption by reaction and the net rate of reactant addition by the feed (figure 1). If enzyme deactivation is taking place, a various with time, and Eq. 1 must be considered together with an equation that describes the change of the activity with time. No steady state exists in this case other than the trivial one obtained for $a = 0$ and $c_A = c_{A0}$.

However, as it is most often the case, the kinetics of the deactivation process is much slower than the kinetics of the main enzymatic reaction so that c_A can be considered to be at all times at a quasisteady state (QSS) obtained from Eq. 1 by setting $\dot{c_A} = 0$. This quasisteady state is obtained again as the intersection of the curve and the straight line is not constant but decreases as the

activity decreases with time. Therefore, the state of the reactor, initially at point A corresponding to activity equal to unity, will move progressively through a sequence of quasisteady states , B, C, *etc.*, Corresponding to decreasing values of the activity, as the enzyme deactivation process is occurring alongside with the main reaction (Figure 1a). Clearly, the initial point of operation, A, chosen to optimize certain performance criteria, cannot be maintained and the reactor will precipitate through a series of suboptimal states to truly uneconomical operation. If the curve for the main reaction kinetics has the shape shown in figure 1b, then multiple steady states are possible and in the succession of quasi-steady states a jump from a high conversion quasi-steady state (C) to a low conversion one (C') will take place. In this case, which is equivalent to reactor failure, the deactivation effects are more pronounced and a sudden drop in productivity will complicate the already undesirable departure from the optimal operating conditions.

There are various types of control that one can employ to counter the above effects of enzyme deactivation. Thus it is possible to cease operation when the enzyme activity falls below a low level or to add fresh enzyme to make up for the activity loss (Verhoff and Schlager, 1981), or, one can manipulate the temperature or the pH of the reactor to achieve an overall optimal operation (Chou *et al.*,1967; Szepe and Levenspiel, 1968; Ogunge and Ray, 1971; Hass *et al.*, 1974; Sadana, 1979: Park *et al.*, 1981). Although they produced definite improvements over the uncontrolled case, the above control scheme have various disadvantages. The first possibility is clearly not optimal, the second is suboptimal with respect to a combined performance index involving the cost of both the enzyme and the overall reactor volume, and the third is not very practical because of the narrow range within which temperature and pH can be varied

without causing denaturation of the enzyme. Furthermore, all alternatives require rather complicated schemes for their implementation and detailed knowledge of the kinetics of the main reaction and the deactivation process.

In this work another control possibility is examined, that of the flow rate manipulation. This type of control can be achieved with commercially available instruments and can be applied to existing reactors with minimal modification. The optimal control problem is formulated and solved using the Minimum Principle to give the variation of the flow rate with time that minimizes the performance index. Approximate solutions which utilize the concept of the quasi-steady state are also obtained and compared to the complete solution. These approximate solutions point to an interesting possibility of implementing the optimal control policy with a feedback scheme that requires minimal knowledge of the kinetics of the two processes and, finally, examples demonstrate the adequacy of the approximate solution and the improvements that can be achieved over the uncontrolled operation of the enzymatic CSTR.

1.2 FORMULATION OF THE PROBLEM

Consider the operation of a CSTR with an enzyme immobilized in it that catalyses the reaction $A \rightarrow B$. The reactor is initially charged with fresh enzyme and reactant A at a concentration equal to the concentration of the stream that will be used subsequently to feed the reactor during continuous operation. As it was discussed in the introduction, the quasi-steady state of operation changes continuously as a result of the continuous decline of the activity of the enzyme with time, thus making it impossible to maintain optimal operation. The objective of the present analysis is to derive a control policy for the flow rate of the reactor which counters the enzyme deactivation effects and yields an optimal

operation according to a performance index to be presented in the sequel.

Assuming negligible external mass transfer resistance and intraparticle diffusion, the reactor dynamics for the isothermal operation is described by the equation:

$$c_A = \frac{F}{V}[c_{A0} - c_A] - \alpha r(c_A, c_B, T) \quad ; \quad c_A(0) = c_{A0} \tag{2}$$

where r is the rate of depletion of reactant A or formation of product B per unit volume. Although a rate expression of the form

$$r = \frac{kc_A}{c_A^2 + K_s c_A + K} \tag{3}$$

corresponding to substrate inhibited kinetics was used in the numerical examples to be presented in later sections, the derived solution for the control is general and can be applied to any other type of functional relationship between the rate and the concentrations.

To complete the description one needs an expression for the time of change of the activity of the enzyme. Many previous works assumed an exponential decline of the activity taking place independently of the main reaction and various cases seem to be represented well in this way. However, if the deactivation is due to poisoning by the reactant or the product, different expressions for the change of the activity must be used. Such expressions have been developed by Do and Weiland(1980) who also point out that the deactivation rate expression can have only certain basic forms if it is to be consistent with rate expression of the main reaction. In particular, it must have the same denominator with the main kinetics. For kinetics similar to that of Eq. 3 the deactivation rate can be one of the following types:

$$-\dot{a} = r_d = \begin{cases} k_d c_A^n a / (c_A^2 + K_s c_A + K) \\ k_d c_A^{n-1} c_B a / (c_A^2 + K_s c_A + K) \end{cases}$$

Equations 4a and 4b corresponding to parallel and series poisoning mechanisms, respectively, and the exponent n may be taken on the value {1,2,3} depending in the exact steps of the poisoning mechanism. [See Do and Weiland (1980) for details.]

It should be noticed that when a general rate of the form indicated in Eq. 2 is used, or when a series poisoning mechanism is occuring, the rates r and r_d are functions of c_B as well as of c_A. An equation for the dynamics of c_B is obtained by making a balance on B over the reactor:

$$\dot{c_B} = \frac{F}{V} c_B + ar \quad ; \quad c_B(0) = 0 \tag{5}$$

Equations 2 and 5 can be combined to give

$$\frac{d}{dt}(c_A + c_B) = -\frac{F}{V}(c_A + c_B + c_{A0}) \quad ; \quad c_A(0) + c_B(0) = c_{A0}$$

the solution of which is $c_A + c_B = c_{A0}$ at all times. Therefore, a second equation for the dynamics for c_B is not needed but c_B can be substituted by

$$c_B = c_{A0} - c_A \tag{6}$$

in the differential equations for c_A and the activity.

The above conclusion is a consequence of the initial and the operating conditions that were chosen for this case, namely, the reactor being charged initially with pure A and the feed being free of B and of concentration equal to the initial concentration of A in the reactor. If any of the above conditions is not satisfied Eq. 6 can still be used except for an initial period of time during which

the existing variation between the initial condition for $(c_A + c_B)$ and its steady state is washed out and the steady-state plane (Eq. 6) is approached exponentially with a time constant F/V. Further details on the applicability of Eq. 6 can be found in Aris (1969) and Asbjornsen and Fjeld(1970).

A parallel poisoning mechanism directly by the reactant, (n=1), for the enzyme deactivation process, and substrate inhibited kinetics for main reaction of the type of Eq. 3 is first considered in this section. The treatment of this simpler case will thus serve as a vehicle in presenting the structure of the solution of the optimal control problem. The solution for the case of general kinetics for the main reaction and deactivation process will be presented in the following section.

The reactor dynamics for this case is described by Eqs 2 and 4a with Eq. 3 for the rate of the main reaction. Equations 2 and 4a can be rendered dimensionless by defining the following dimensionless variables.

$$\tau = \frac{kt}{c_{A0}^2} \quad ; \quad A = \frac{c_A}{c_{A0}} \quad ; \quad Q = \frac{Fc_{A0}^2}{kV}$$

$$\gamma = \frac{K_s}{c_{A0}} \quad ; \quad \beta = \frac{K}{c_{A0}^2} \quad ; \quad \varepsilon = \frac{k_d}{k} c_{A0} \tag{7}$$

With these dimensionless variables the reactor dynamics is described by the differential equations

$$\dot{A} = Q(1-A) - \alpha \frac{A}{A^2 + \gamma A + \beta} \tag{8a}$$

$$\dot{\alpha} = -\alpha \varepsilon \frac{A}{A^2 + \gamma A + \beta} \tag{8b}$$

and initial conditions:

$$A(0) = 1 \quad \text{and} \quad \alpha(0) = 1 \tag{8c}$$

where the dot is now taken to indicate differentiation with respect to the dimensionless time τ.

To complete the formulation of the optimal control problem one needs a performance index for the operation of the enzymatic CSTR. If the overall profit of the process is considered, then such index can have the form:

$$J' = \int_{a}^{t_f} [c_3'F(c_{A0}-c_A) - c_1' - c_2'Fc_{A0}]dt \tag{9}$$

where the three terms of the integrand represent revenues per unit time from the product, fixed costs per unit time and raw material cost per unit time, in this order. In the index of Eq. 9 it is assumed that no credit for the unreacted A is available, that is the reactant A cannot be recycled economically to the process after the product B has been separated from it. If this assumption is not made a credit for the unreacted A (equal to $c_2'Fc_A$) must be added to the integrand of Eq. 9 which is then reduced to the usual criterion of productivity:

$$J' = \int_{0}^{t_f} [Fc_B(c_3' - c_2') - c_1']dt \tag{10}$$

Both cases will be examined in the optimization problem. Using Eq. 7 and the following dimensionless groups

$$J = \frac{J'}{c_3'Vc_{A0}} \quad ; \quad c_1 = \frac{c_1'c_{A0}}{c_3'VK} \quad \text{and} \quad c_2 = \frac{c_2'}{c_3'} \tag{11}$$

the performance index can be written in dimensionless form as

$$J = \int_{0}^{\tau_f} [Q(1-A) - c_1 - c_2Q]d\tau \tag{12}$$

and the optimal control problem then is to find the flow rate Q that minimizes $(-J)$ subject to the system dynamics as given by Eq. 8.

It will be more convenient algebraically to define the fractional conversion of the reactant, ξ, as $\xi = 1-A$ and use ξ instead of A. The problem, then, can be stated in term of this variable as:

$$\min_{Q} (-J) = -\int_0^{\tau_f} [Q\xi - c_1 - c_2 Q]d\tau \tag{13}$$

subject to the following reactor dynamics:

$$\dot{\xi} = -Q\xi + a\frac{(1-\xi)}{\xi^2+\gamma'\xi+\beta'} \tag{14a}$$

$$\dot{a} = -a\varepsilon\frac{(1-\xi)}{\xi^2+\gamma'\xi+\beta'} \tag{14b}$$

and the constraint for the control:

$$Q_* \leq Q \leq Q^* \tag{15}$$

where Q^* and Q_* are the maximum and minimum, respectively, allowed space velocity. In this paper Q_* is taken to be zero.

1.3 THEORETICAL ANALYSIS

For the general optimal control problem:

$$\min_{u} J = \int_0^{\tau_f} L(\mathbf{x},\mathbf{u})d\tau; \quad u_{\min} \leq u \leq u_{\max} \tag{16}$$

subject to state dynamics

$$\dot{\mathbf{x}} = \mathbf{h}(\mathbf{x},\mathbf{u}) \tag{17}$$

the Hamiltonian is defined as

$$H = L(\mathbf{x},u) + \lambda^T\mathbf{h}(\mathbf{x},u) + \nu_1(u - u_{\max}) + \nu_2(u - u_{\min}) \tag{18a}$$

where the coefficient ν_1 is defined as $\nu_1=0$ if $u \neq u_{\max}$ and $\nu_1 \neq 0$ if $u = u_{\max}$. The coefficient ν_2 is defined in a similar manner. Equation 18a can be written in the

form

$$H = H^* + \nu_1(u - u_{max}) + \nu_2(u - u_{max}) \tag{18b}$$

with

$$H^* = L(\mathbf{x},u) + \lambda^T \mathbf{h}(\mathbf{x},u) \tag{18c}$$

and then the necessary condition for optimality is

$$\left[\frac{\partial H}{\partial u}\right]^T = \left[\frac{\partial \mathbf{h}}{\partial u}\right]^T \lambda + \left[\frac{\partial L}{\partial u}\right]^T = 0 \tag{19}$$

with the following equations for the state and adjoint variables:

$$\dot{\mathbf{x}} = \mathbf{h}(\mathbf{x},u) \tag{20}$$

$$\dot{\lambda} = -\left[\frac{\partial H}{\partial \mathbf{x}}\right]^T = -\left[\frac{\partial \mathbf{h}}{\partial \mathbf{x}}\right]^T \lambda - \left[\frac{\partial L}{\partial \mathbf{x}}\right]^T \tag{21}$$

For free time problems and autonomous systems, we have,in addition:

$$H = L + \lambda^T \mathbf{h} = 0 \tag{22}$$

A typical approach for the solution of this type of problem is to integrate Eqs. 20 and 21 with the proper boundary conditions (Koppel, 1968), evaluating the control at each time step as function of the state and adjoint variables from Eq. 19. For those systems, however, which are linear in the control, contributing thus to a special class of singular control problems. It can be shown (Bryson and Ho, 1969), that the solution in this case is that of a bang-bang control:

$$u^*(t) = \begin{cases} u_{min} & \text{if} \quad H_u^* > 0 \\ u_{max} & \text{if} \quad H_u^* < 0 \end{cases} \tag{23}$$

Thus, for a linear singular problem the control variable will take the extreme values allowed as long as $H_u^* \neq 0$. If $H_u^* = 0$, the minimum principle cannot tell what the control should be. However, if H_u^* is zero over a finite interval of

time, so must be its time derivatives and repeated differentiation of the relation $H_u^* = 0$ with respect to time will eventually yield an explicit relationship between the optimal control u^* and the state vector. The path followed by u during the time period over which u is not on the boundaries is often called singular arc. It turns out that an even number of differentiations with respect to time is always required to yield the relationship that gives u along the singular path; if two differentiations are required then the trajectory of u over the time interval is said to be a first order singular arc, *etc.* For such a singular arc a more general necessary condition for convexity has been derived and may be stated as:

$$(-1)^k \frac{\partial}{\partial u}\left[\left(\frac{\partial}{\partial t}\right)^k H_u\right] \geq 0 \tag{24}$$

where k is order of the singular arc.

Applying the above results to the the optimal control problems of Eqs. 13, 14 and 15 the following are obtained:

Hamiltonian:

$$0 = H = -(Q\xi - c_1 - c_2 Q) + \lambda_1(-Q\xi + af) + \lambda_2'(-a\varepsilon f) + \nu_1(Q-Q^*) + \nu_2(Q-Q_*)$$

where $\nu_1 = 0$ if $Q \neq Q^*$ and $\nu_1 \neq 0$ if $Q = Q^*$, and ν_2 is similarly defined. Setting $\lambda_2 = \varepsilon\lambda_2'$, the Hamiltonian can be written as:

$$0 = H = -(Q\xi - c_1 - c_2 Q) + \lambda_1(-Q\xi + af) + \lambda_2(-af) + \nu_1(Q-Q^*) + \nu_2(Q-Q_*) \tag{25}$$

State Equations: Changing the independent variable from τ to $\vartheta = \varepsilon\tau$ the equations for the state and adjoint variables become:

$$\varepsilon\frac{d\xi}{d\vartheta} = -Q\xi + af(\xi) \quad ; \quad \xi(0) = 0 \tag{26a}$$

$$\frac{da}{d\vartheta} = -af(\xi) \quad ; \quad a(0) = 1 \tag{26b}$$

where $f(\xi) = (1-\xi)/(\xi^2+\gamma'\xi + \beta')$, and

Adjoint Equations:

$$\varepsilon\frac{d\lambda_1}{d\vartheta} = (1 + \lambda_1)Q + (\varepsilon\lambda_2' - \lambda_1)af_\xi \quad ; \quad \lambda_1(\vartheta_f) = 0$$

$$\varepsilon\frac{d\lambda_2'}{d\vartheta} = (\varepsilon\lambda_2' - \lambda_1)f \quad ; \quad \lambda_2'(\vartheta_f) = 0$$

or in terms of λ_2:

$$\varepsilon\frac{d\lambda_1}{d\vartheta} = (1 + \lambda_1)Q + (\lambda_2 - \lambda_1)af_\xi \quad ; \quad \lambda_1(\vartheta_f) = 0 \tag{27a}$$

$$\frac{d\lambda_2}{d\vartheta} = (\lambda_2 - \lambda_1)f \quad ; \quad \lambda_2(\vartheta_f) = 0 \tag{27b}$$

In Eq. 27a. f_ξ means differentiation with respect to ξ.

Necessary Condition:

$$0 = \frac{\partial H^*}{\partial Q} = \frac{\partial H}{\partial Q} = -(1 + \lambda_1)\xi + c_2 \tag{28}$$

for the singular arc.

Since the Hamiltonian is linear in the control Q, The usual necessary condition $H_Q = 0$ does not contain the control variable and, therefore, cannot be used for the determination of the optimal control policy. Subsequent differentiation with respect to time, as discussed earlier in this section, yield:

$$0 = \frac{d}{d\vartheta}(H_Q) = -a[(1 + \lambda_1)f + (\lambda_2 - \lambda_1)\xi f_\xi] \tag{29}$$

$$\frac{d^2}{d\vartheta^2}(H_Q) = 0 \longrightarrow Q = \frac{2af f_\xi + a\xi f f_{\xi\xi} - 2a\xi f_\xi^2 + \varepsilon\xi f f_\xi}{2\xi f_\xi + \xi^2 f_\xi^2 - 2\xi^2 f_\xi^2/f}$$

$$= \frac{af}{\xi} + \frac{\varepsilon\xi f f_\xi}{2\xi f_\xi + \xi^2 f_\xi^2 - 2\xi^2 f_\xi^2 / f} \tag{30}$$

Then, combining the minimum principle and the result of Eq. 23, one can obtains for the optimal control:

$$Q = \begin{cases} Q_* = 0 & \text{if } -(1+\lambda_1)\xi + c_2 > 0 \\ Q^* & \text{if } -(1+\lambda_1)\xi + c_2 < 0 \\ \dfrac{af}{\xi} + \dfrac{\varepsilon\xi f f_\xi}{2\xi f_\xi + \xi^2 f_{\xi\xi} - s\xi^2 f_\xi^2 / f} & \text{if } -(1+\lambda_1)\xi + c_2 = 0 \end{cases} \tag{31}$$

Since the initial value of ξ is equal to zero and $c_2 > 0$, it can be seen from the above equation that $-(1 + \lambda_1)\xi + c_2 > 0$, so that the reactor is start with the minimal flow rate which is taken here to be zero. As the reaction progresses and the conversion increases, ξ also increases and at some point $-(1 + \lambda_1)\xi + c_2$ becomes equal to zero. At this point the flow rate enters the singular arc; it is raised to a value and subsequently follows the path indicated by the third of the Eqs. 31.

It will be useful to be able to predict the point at which the control enters the singular arc. This can be done by noting that during the initial phase of operation for which $Q = 0$, the state equations (Eqs. 26) can be integrated to yield an explicit relationship for the activity as a function of ξ, as follows:

$$\varepsilon \frac{d\xi}{d\vartheta} = af(\xi) \tag{32}$$

$$\frac{da}{d\vartheta} = -af(\xi) \tag{33}$$

and combining Eqs. 32 and 33:

$$\frac{da}{d\vartheta} = -\varepsilon \frac{d\xi}{d\vartheta}$$

which, when integrated with initial conditions $a(0) = 1$ and $\xi(0) = 0$, yields:

$$a(\vartheta) = 1 - \varepsilon\xi(\vartheta) \tag{34}$$

Equation 34 is valid during the startup period for which $Q = 0$. At the point of entrance in the singular arc, $H_Q = 0$ and also H and $dH_Q/d\vartheta$ are zero. Therefore,at that point, Eqs. 25, 28 and 29 are valid and can be used to eliminate λ_1 and λ_2 among them to obtain a relationship between the activity and ξ:

$$\frac{c_1}{c_2} = \frac{-af^2}{\xi^2 f_\xi} \tag{35}$$

or, after using Eq. 34 for a:

$$\frac{c_1}{c_2} = \frac{-(1-\varepsilon\xi)f^2(\xi)}{\xi^2 f_\xi} \tag{36}$$

Equation 36 involves ξ as the sole variable. If an expression for the kinetics, $f(\xi)$, is available, Eq. 36 can be used to determine the conversion point at which the flow rate enters the singular arc. By integrating Eq. 32 with 34 for $a(\vartheta)$, the time piont of entrance can also be determined. After the control has entered the singular arc it stays there for as long as the integrand of the performance index, Eq. 12 , remains positive, namely, for as long as the inequality $(Q(\xi)-c_2) > c_1$ is satisfied. This is so because, if the objective is to maximize J as defined in Eq. 12, the operation should cease when the net incremental return becomes nonpositive. the above requirement indicates that the operation cannot end on a singular arc because at the end point $\lambda_1(\vartheta_f) = 0$ and Eq. 28 gives $\xi(\vartheta_f) = c_2$ which is in violation of the above inequality, unless $c_1 = 0$. If $c_1 > 0$, the optimal control should stay on the singular arc till $Q(\xi - c_2) = c_1$ at which point it takes the maximum allowed value Q^* as indicated by Eq. 31 of $H_Q < 0$. The end of operation is determined again at the point at which $Q^*(\xi - c_2) = c_1$.

The above control policy was tested in a number of simulated operations presented in the following section. For a given initial condition of the state the

above control policy was applied and the final state condition determined. Using the so obtained final state, the known final conditions for the adjoint variables and the same control, the state and adjoints equations were integrated backwards and H_Q evaluated at each point. The very good agreement between these values and those obtained in the forward integration shows that the control described above is at least one optimal solution.

In conclusion, the optimal control law is to use the lowest(initially) and highest (finally) flow rate allowed, except along the singular arc. Provided that a reliable under dynamic conditions $f(\xi)$ function is available, the points of entrance and exit from the singular arc can be determined by integrating simultaneously the state and evaluating the control at each time step from Eq. 31. For the case considered in this work the numerical scheme required is quite simpler than those encountered in most optimal control problems because by substituting the control law of Eq. 31 in the state Eq. 26a the two state equations become uncoupled:

$$\frac{d\xi}{d\vartheta} = \frac{-\xi^2 f f_\xi}{2\xi f_\xi + \xi^2 f_{\xi\xi} - 2\xi^2 f_\xi^2 / f} \tag{37}$$

The above equation can be integrated with initial condition corresponding to the conversion at the entrance of the singular arc and the resulting $\xi(\vartheta)$ function be substituted into Eq. 26b the integration of which yields the variation of the activity along the singular path.

It is thus seen that the implementation of the control law (Eq. 31) is rather simple and also can be prescribed in advance for a particular operation. In some cases, however, much simpler solutions can be obtained and these possibilities are discussed below.

1.4 SPECIAL CASES

Case 1 : $\varepsilon << 1$

This case is equivalent to the deactivation process being much slower than the main reaction. Under this condition, the optimal control can be expressed in terms of a zeroth order solution plus other terms of first and higher orders in the small parameter ε. The smaller the value of the parameter ε the more the accurately the exact solution is approximated by the zeroth order solution. The latter is obtained by setting $\varepsilon = 0$ in the system equations and is actually the quasisteady state solution.

Returning to the original time varible τ and setting $\varepsilon = 0$ in Eq. 37 one obtains $d\xi/dt = 0$, i.e., the conversion at the QSS is constant. Also, for $\varepsilon = 0$, the state equation (Eq. 26a), or the control law (Eq. 31), yield for the control:

$$Q = a \frac{f(\xi)}{\xi} \tag{38}$$

Thus, by employing the QSS approximation, a control law is obtained according to which the flow rate decreases responding to the decay of activity and in such a way as to maintain the conversion at a quasi-steady level the optimal value of which, ξ^*, is determined below.

Optimal QSS Conversion

For $\varepsilon = 0$, Eq. 26a yields $af = Q\xi$, and substituting this relationship into Eq. 26b the dynamic equation for the activity becomes:

$$\frac{da}{d\tau} = -a\varepsilon f(\xi) = -\varepsilon Q\xi \tag{39}$$

Using the above equation for a change of independent variables from τ to a, neglecting the purging term, allows the performance index to be rewritten in

terms of a as:

$$(-J) = \int_{a_{en}}^{a_{min}} \frac{da}{\varepsilon} - \int_{a_{en}}^{a_{min}} \frac{c_2}{\varepsilon\xi} da + \int_0^{\tau_{en}} c_1 dt + \int_{\tau_{en}}^{\tau_f} c_1 dt$$

$$= \frac{1}{\varepsilon}\left\{\left[1 - \frac{c_2}{\xi}\right](a_{min} - a_{en}) + \varepsilon c_1 \tau_f\right\} \qquad (40)$$

In the above equation a_{en} is the activity of the catalyst when reactor enters QSS operation and τ_{en} the time of entrance into QSS operation. Also a_{min} is the activity at the end of the QSS operation which is given by $a_{min} = c_1\xi/(f\,\xi - f\,c_2)$. Noting that during start-up activity is given by

$$a = 1 - \varepsilon\xi$$

the following expressions can be obtained for the time of entrance into QSS operation, τ_{en}, and final time τ_f,

$$\tau_{en} = \int_0^{\xi} \frac{d\xi'}{(1 - \varepsilon\xi')(f(\xi')}$$

$$\tau_f = \tau_{en} + \frac{\ln(a_{en}/a_{min})}{\varepsilon f(\xi)} \qquad (41)$$

Substituting τ_f from Eq. 41 into Eq. 40 and minimizing $(-J)$ with respect to ξ by setting $d(-J)/d(\xi) = 0$ gives the desired equation for the optimal value of the conversion, ξ^*:

$$(a_{min} - 1)\frac{c_2}{\xi^{*2}} + \varepsilon + \frac{c_1 \ln\left[\dfrac{a_{min}}{1 - \varepsilon\xi^*}\right] f_\xi(\xi^*)}{f^2(\xi^*)} = 0 \qquad (42)$$

Equation 42 contains ξ^* as the sole unknown and be solved, once a *design* equation $f(\xi)$ is available to give the conversion of optimal optimal operation ξ^*. The control law of Eq. 38 can then be applied to maintain operation at ξ^* despite

changes in the activity. The use of the QSS approximation actually amounts to neglecting the effect of the activity changes on the conversion and varying the flow rate in response to activity changes only, as indicated by Eq. 38. By comparing the error involved with the use of the QSS is of the order of ε, i.e., minimal for small ε, and numerical calculations, discussed in the following section, confirm this observation. Figure 2 shows a convenient illustration of the reactor operation when the exact and the approximate solutions are employed for control. The reactor is initially at point A_0, corresponding to charging the reactor with reactant at concentration c_{A0}. During the start-up in which $Q = 0$, the state travels along the $f(c_A)$ curve till it enters the singular arc at point A_{in}. If the exact solution is applied, the state will move along the singular arc from A_{in} to A_{out} following the control law of Eq. 31. If the QSS solution is employed instead, the control law is given by Eq. 38 which indicates that the flow rate decreases as the activity decays in order to maintain the conversion at some optimal point A^* between A_{in} and A_{out} and determined by Eq. 42.

Case 2 : $c_2 = 0$

The cost of the reactant is negligible in this case and Eq. 28 indicates that $(1 + \lambda_1)\xi = 0$. This substituted into Eq. 29 yields $f_\xi = 0$. Therefor, when $c_2 = 0$ the QSS conversion for optimal operation is that for which $f(\xi)$ is maximum. The same conclusion is obtained if the productivity is used as the performance index, It is of interest to notice that when $f_\xi = 0$ the exact solution of the control law given by Eq. 31 reduces to $Q = \alpha f / \xi$ which is identical to that of the QSS solution of Eq. 37. Hence, the quasi-steady state solution is indeed the exact solution when $c_2 = 0$ and the kinetics of the deactivation and main reaction are as indicated in Eqs. 8.

1.5 GENERAL CASE

When the kinetics of the deactivation process and the main reaction are not of the form assumed in the previous section, Eqs. 26 are replaced by

$$\varepsilon \frac{d\xi}{d\vartheta} = -Q\xi + af(\xi) \qquad ; \qquad \xi(0) = 0 \tag{43a}$$

$$\frac{da}{d\vartheta} = -ag(\xi) \qquad ; \qquad a(0) = 1 \tag{43b}$$

where $f(\xi)$ and $g(\xi)$ are, respectively, the dimensionless form of the kinetics of the main and the deactivation process, as functions of the conversion ξ.

Following the exact same procedure described previously, one obtains the following expressions for the optimal flow rate:

$$Q = \begin{cases} Q_* = 0 & \text{if } -(1+\lambda_1)\xi + c_2 > 0 \\ Q^* & \text{if } -(1+\lambda_1)\xi + c_2 < 0 \\ \dfrac{af}{\xi} + \varepsilon \dfrac{g g_\xi \xi - \left[\dfrac{c_2 - \xi}{c_2 f}\right](g g_\xi f_\xi \xi^2 - f g_\xi^2 \xi^2)}{\kappa(\xi, g_\xi, g_{\xi\xi}, f, f_\xi, f_{\xi\xi}, c_2)} & \text{if } -(1+\lambda_1)\xi + c_2 = 0 \end{cases} \tag{44}$$

where

$$\kappa(\xi, g_\xi, g_{\xi\xi}, f, f_\xi, f_{\xi\xi}, c_2) = 2g_\xi \xi + \xi^2 g_{\xi\xi} - 2\xi^2 f_\xi g_\xi / f - [(c_2 - \xi)/c_2 f][f_\xi g_{\xi\xi}\xi^3 - g_\xi f_{\xi\xi}\xi^3]$$

Notice that when $f = g$, Eq. 44 reduces to the one previously derived for Q, Eq. 31.

The conversion, ξ_{en}, at which the reactor should enter the singular arc is similarly deduced. The same procedure yields the following algebraic equation for ξ_{en}:

$$a_{en} c_2 f g = c_1 \xi_{en}^2 g_\xi + (c_2 - \xi_{en})\xi_{en}(f g_\xi - g f_\xi) \tag{45}$$

with the activity, a_{en}, given by:

$$a_{en} = a(\xi_{en}) = 1 - \varepsilon \int_0^{\xi_{en}} \frac{g(\xi)}{f(\xi)} d\xi \tag{46}$$

during the start-up period and, therefore, at the entrance to the singular arc, as well. If the kinetics are known, the integral of Eq. 46 can be evaluated to yield a_{en} for use in the estimation of ξ_{en} from Eq. 45.

Finally, in the determination of the optimal QSS conversion the performance index is written as:

$$(-J) = \frac{1}{\varepsilon}\left\{\left[\frac{f}{g}\right](a_{\min} - a_{en})\left[1 - \frac{c_2}{\xi}\right] + \varepsilon c_1 \tau_f\right\} \tag{47}$$

with the final time, τ_f, given by:

$$\tau_f = \int_0^{\xi} \frac{d\xi'}{af} + \frac{\ln(a_{en}/a_{\min})}{\varepsilon g} \tag{48}$$

For known kinetics $f(\xi)$ and $g(\xi)$, the activity can be estimated as function of the conversion from Eq. 49 and then substituted into Eq. 48 and 47 to express the performance index as function of ξ. The optimal QSS conversion is then similarly obtained by setting $d(-J)/d\xi = 0$.

1.6 DISCUSSION

In order to assess the efficiency of the derived control law and evaluate the improvements over the uncontrolled operation, a test case with the kinetic parameters indicated in Figure 4 was simulated. The performance of the reactor when a constant flow rate is used is shown in Figure 3. When the flow rate varies with time according to the exact or approximate control laws of Eqs. 31 and 38 an improved performance is obtained and Figure 4 and 5, respectively, present the results for the progress of the flow rate, conversion and activity with time

for these two cases.

There are various points worth noticing in Figure 3-5. First, the structure of the control law: Initially the flow rate is zero and subsequently it is raised to a value given by Eq. 31 with ξ and a evaluated at the point of entrance to the singular arc as discussed in the previous section. The maximum flow rate Q^* is taken equal to unity and all the other flow rates are scaled accordingly. Secondly, the performance indices obtained for the exact and the QSS solution are remarkable close. Notice that when the exact solution is employed, the conversion decreases only by a very small amount during operation on the singular arc, thus verifying the validity of the QSS assumption according to which ξ is constant. (this is also reflected in the small difference between the values of the performance indices obtained for the two cases.) finally, the use of either kind of control law results in substantial improvement over the uncontrolled case. For the example considered, an improvement of 24 % is obtained over the case in which the flow is initially zero and is raised to a value equal to that given by Eq. 31. the improvement over the uncontrolled case depends on the rate of increase of $f(\xi)$ in the region to the left of the maximum. A relatively flat $f(\xi)$ curve produces rather modest decreases in the performance index when the optimal policy is applied for the flow rate.

The previous observations point to a very convenient control strategy for the enzymatic CSTR under examination: Using kinetic data for the main enzymatic reaction (such data must be available in one form or another for the design of the reactor), the conversion of optimal operation ξ^* is determined. Then the control consists of starting initially with a zero flow rate till a conversion equal to ξ^* is reached and subsequently manipulating the flow rate so that the optimal QSS conversion is maintained. This type of control action can be

achieved with simple existing instrumentation, requires the measurement of only one variable and can be incorporated in most operating reactors with minimal modifications. One disadvantage of the above scheme, namely, the variable flow rate which may be undesirable for various reasons can easily be avoided by having more than one reactor operating in parallel at the appropriate flow rates and phase lag among them.

The cost of enzyme c_E can be incorporated into the above scheme by redefining the time cost c_1 as $c_1 = c_T = c_{10} + c_E/\tau_f$ where c_{10} is the base daily operation cost and τ_f is the operating time for that particular c_T . QSS optimal operating profile for different c_1 can be obtained by using the method discussed earlier. This calculation also yields the optimal duration of operation, the QSS optimal conversion and the best value of the performance index. These results can be summarized conveniently in graphs similar to Figure 6 which was obtained by using the same kinetic data as before and a value of 0.402 for c_{10}. As expected, an increasing enzyme cost leads to shorter operating periods and smaller values for the performance index. Also notice that there is a small region in the values of the enzyme cost where multiple solutions for τ_f and J are possible.

It should also be pointed out that the obtained results are not dependent on the specific kinetics of the main reaction as indicated by Eq. 44 and 38 which give the control laws in terms of the functions $f(\xi)$ and $g(\xi)$. Any such functions can be used of this purpose and both parallel and series poisoning mechanisms can be treated for the deactivation process. A comparison between the variable flow rate and the other control possibilities mentioned in the introduction is not possible without referring to a specific case and optimizing the various operating parameters in each control mode. However, the simplicity of implementation

of the variable flow rate control mode is definitely a strong advantage which can lead to the preference of this control possibility over the others.

1.7 CONCLUSION

The optimal flow rate profile is derived for an immobilized enzyme CSTR with enzyme deactivation taking place in parallel with the main reaction. Although the various simulations were performed for the case of substrate inhibited kinetics, the obtained solutions are general enough to handle any other type of rate expression. For a reactor charged initially with reactant only, the structure of the solution of this singular problem consists of the flow rate set initially at the lower bound until the point of entrance to the singular arc. The variation of the flow rate along the singular arc is determined and this variation constitutes the optimal flow manipulation for as long as the operation is profitable (i.e. till the integrand of the performance index becomes zero). At that point the flow rate is increased to the upper bound to purge any remaining product out of the reactor, The point of entrance and exit from the singular arc are determined and expressions for the path along the singular arc are given. The application of the optimal flow rate results in significant improvements of the performance index over the uncontrolled case, and , furthermore, the derived control is very easy to implement in existing reactors. Both the complete solution and an approximate analytical solution based on the quasi-steady state approximation are derived and agreement between the two is shown to be excellent when the enzyme deactivation process is slow compared to the main reaction. The structure of the approximate solution indicates that optimal performance can be obtained by varying the flow rate so that the conversion remains constant at a predetermined level which minimizes the performance

index. Expressions for the optimal conversion levels are given. Such a policy is very easy to implement with a feedback control scheme that measures the current level of conversion at the predetermined level. No detailed knowledge of the kinetics is thus necessary and the control requires only the measurement of the current concentration of the main reactant.

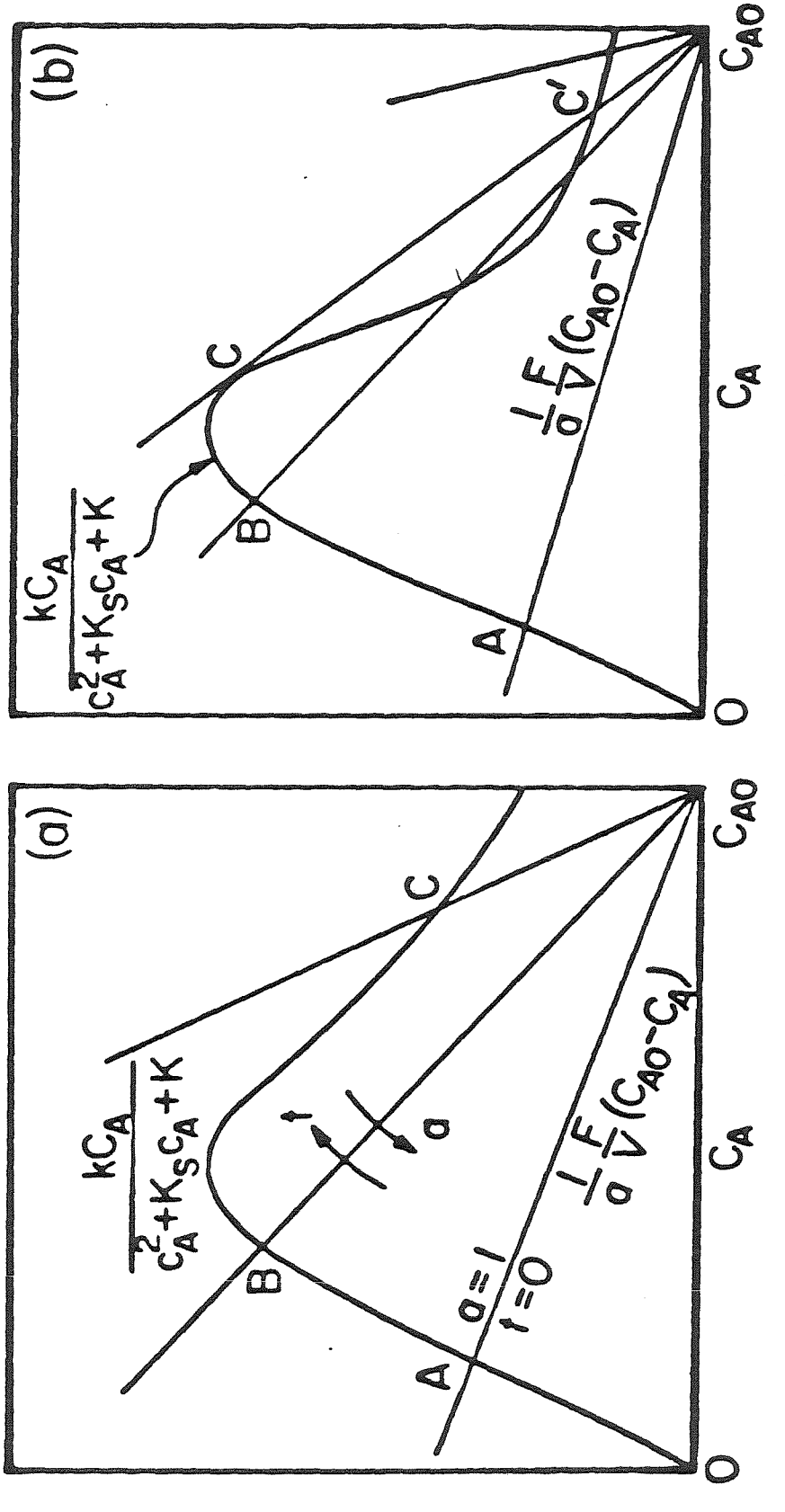

Fig. 2.1 Schematic of the movement of the quasi-steady of an enzymatic CSTR caused by a decline in the activity of enzyme (a) Single steady state, (b) Multiple steady state

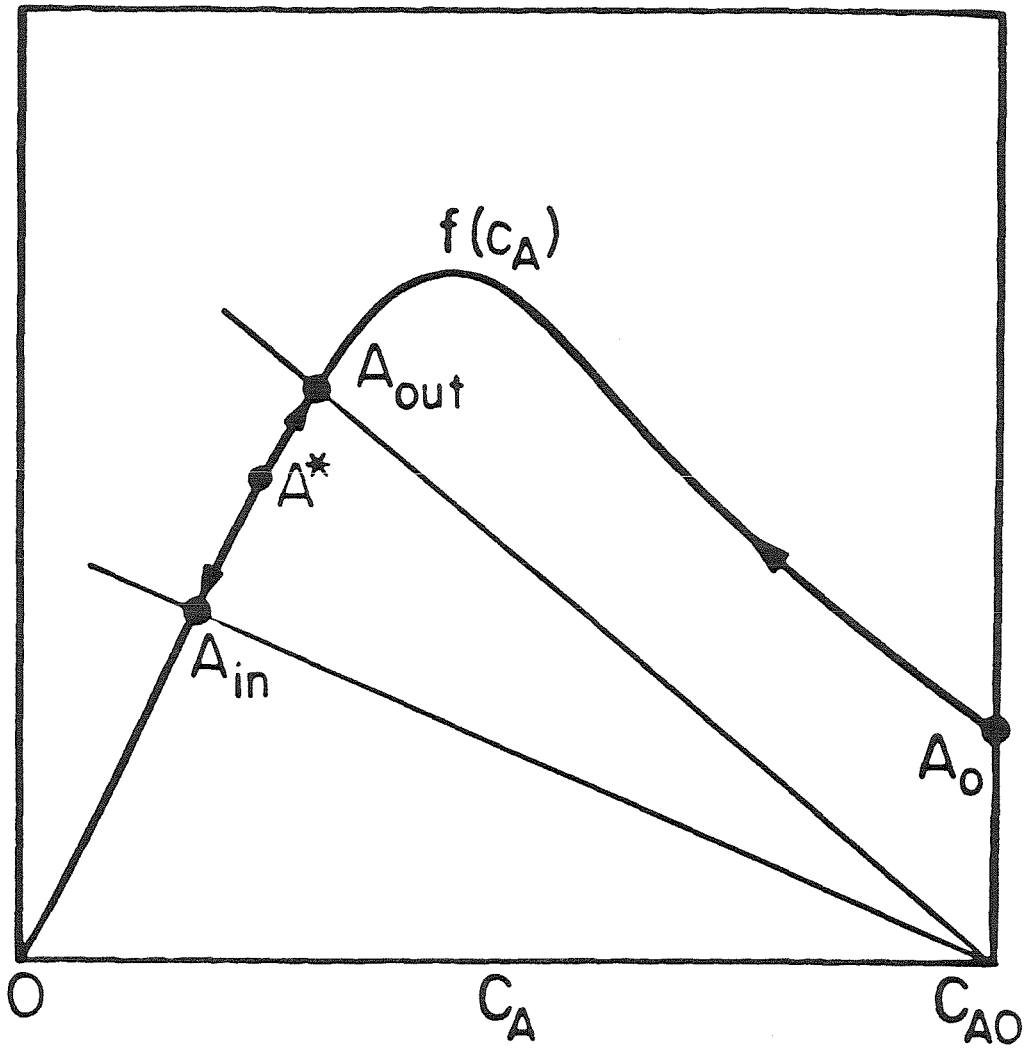

Fig. 2.2 Schematic representation of the operation of an enzymatic CSTR under the exact and the approx. control law for the flow rate

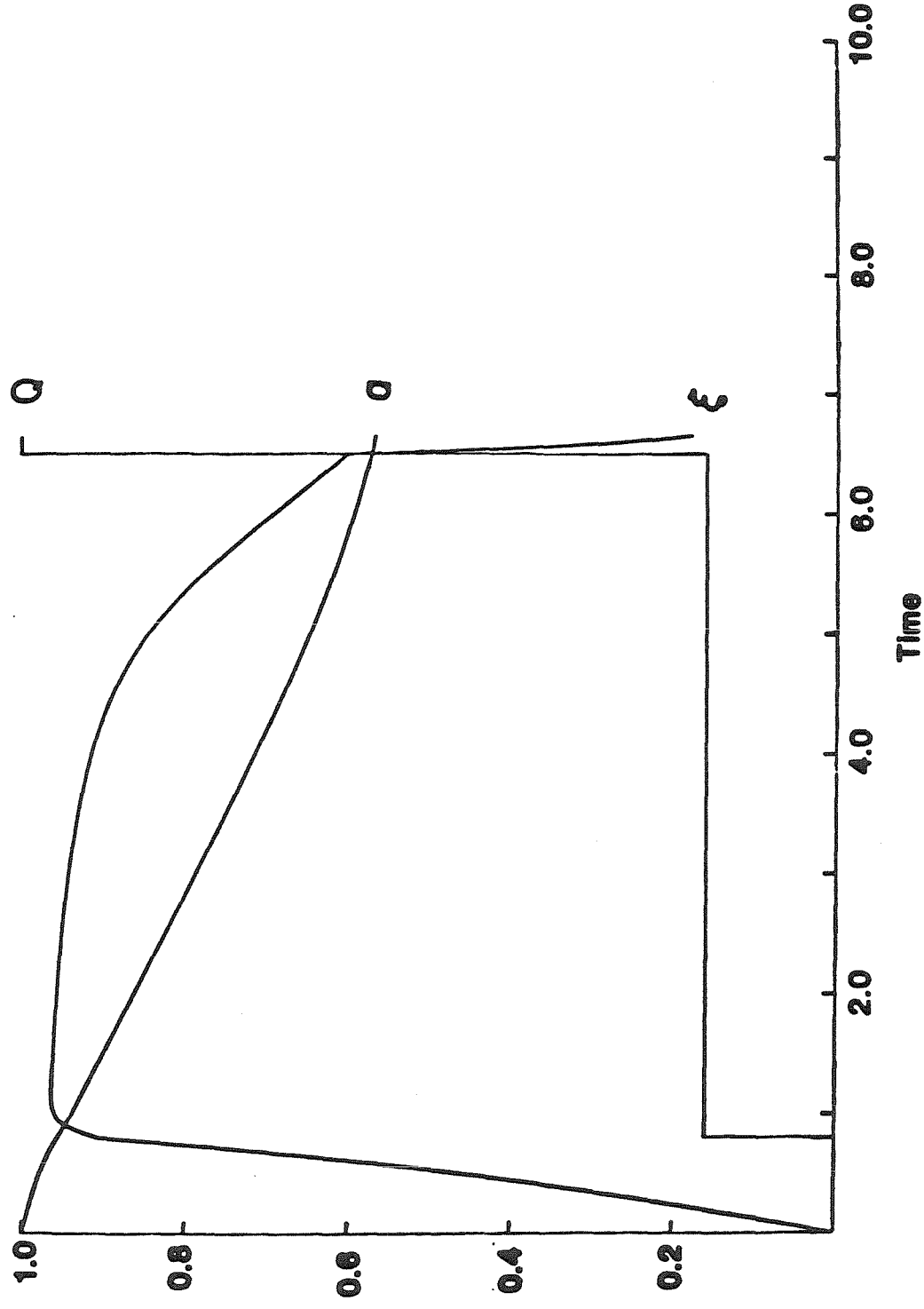

Fig. 2.3 The progress of the activity and conversion with dimensionless time of an enzymatic CSTR: Constant flow rate

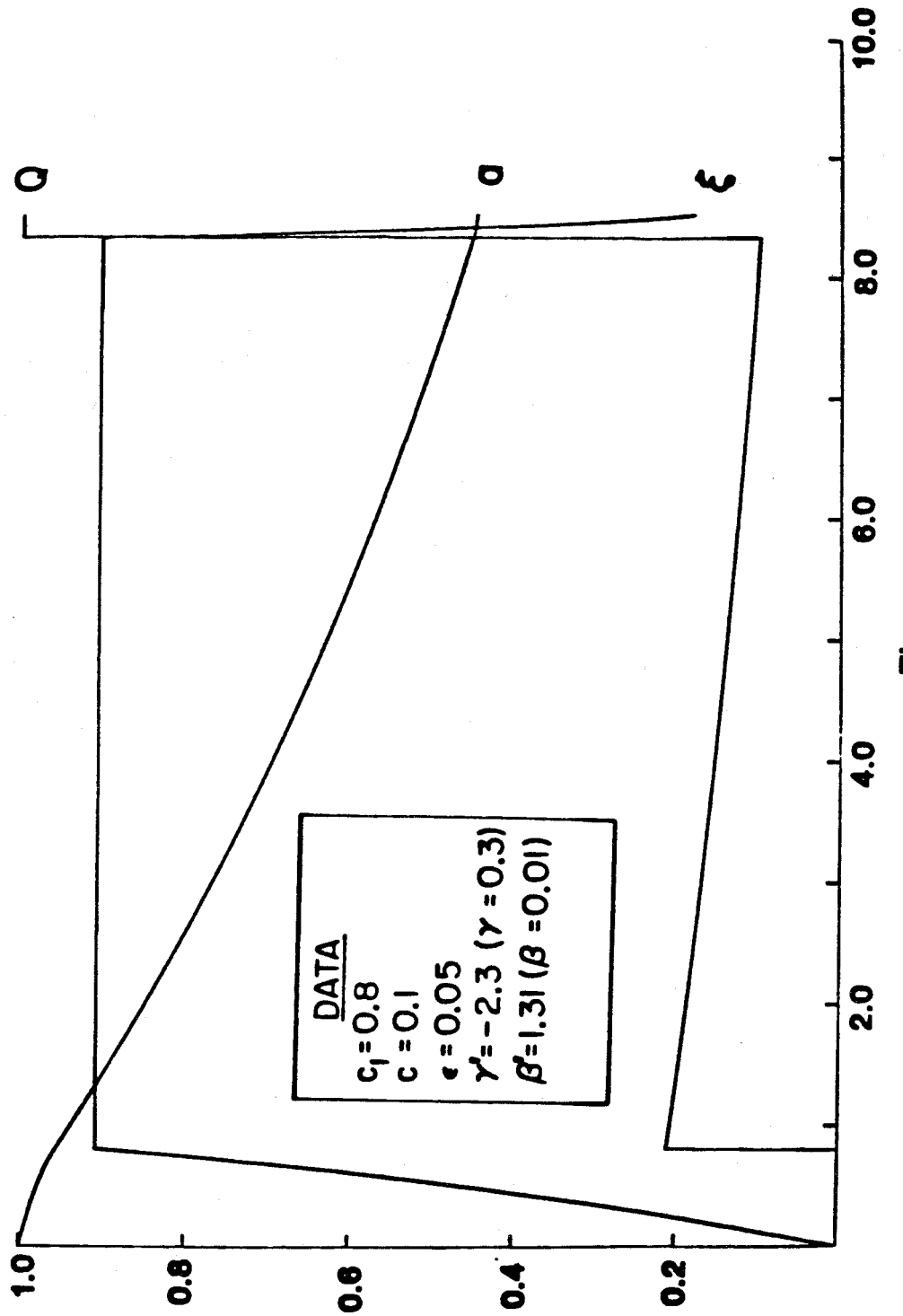

Fig. 2.4 The progress of the activity and conversion with dimensionless time of an enzymatic CSTR: the flow rate follows the exact solution of the optimal control problem

dimensionless time of enzymatic CSTR: the flow rate follows the solution of the QSS

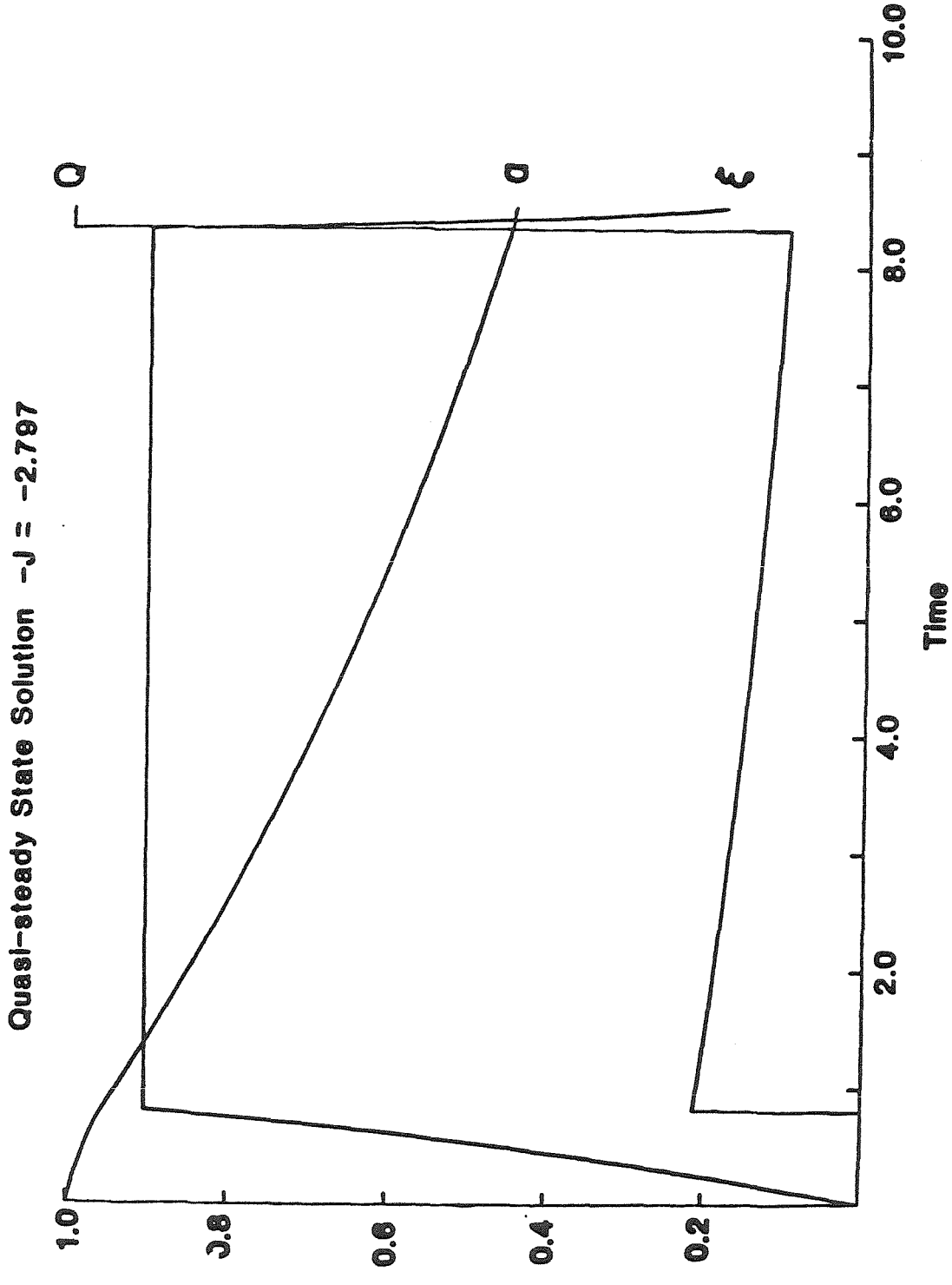

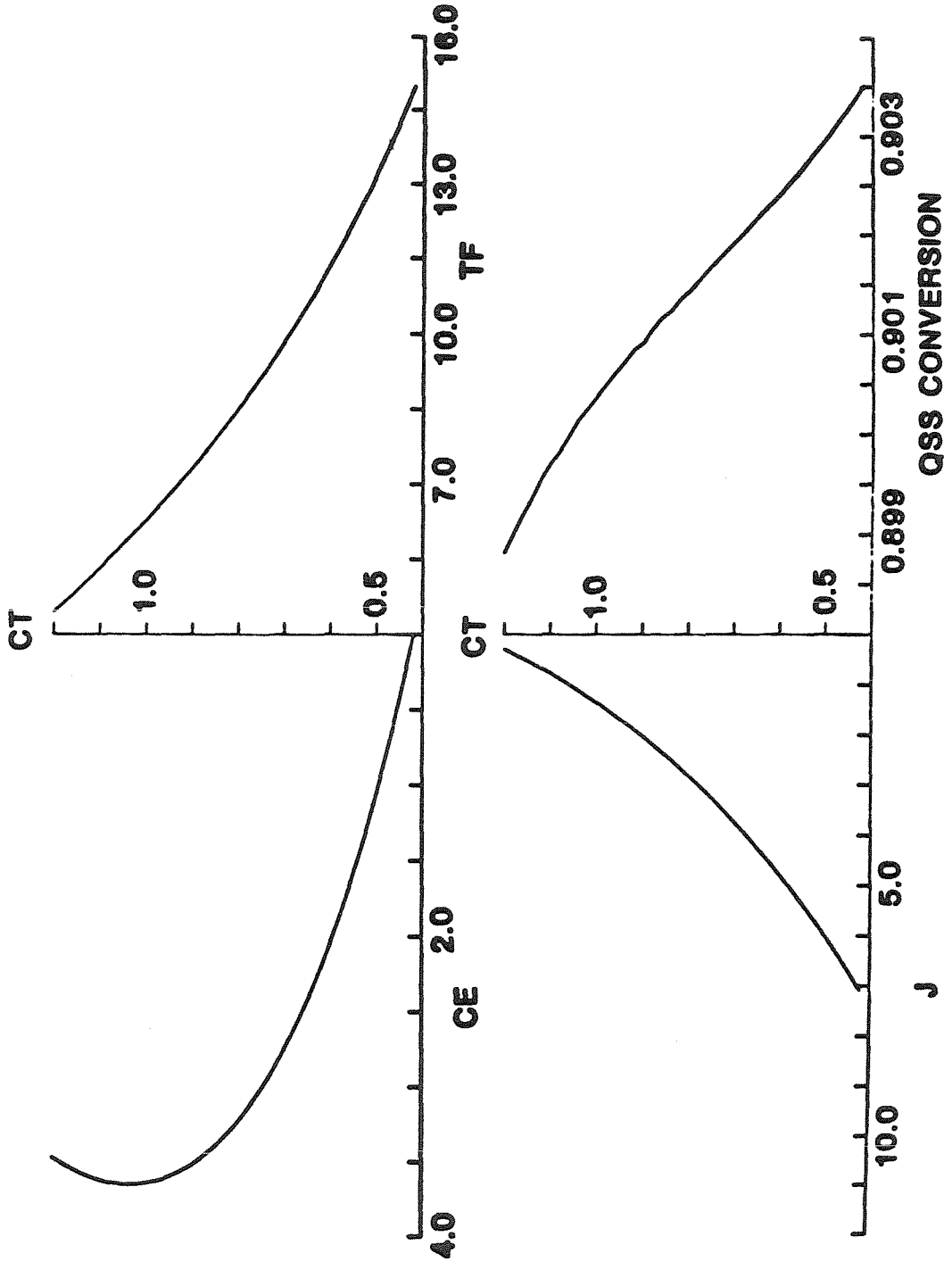

Fig. 2.6 The dependence of the optimal conversion, time of operation and performance index on the enzyme cost

NOTATION

a	enzyme activity
A	dimensionless concentration of A
c_A	concentration of reactant A
c_B	concentration of product B
c_1	dimensionless fixed cost
c_2	dimensionless reactant cost
c_1'	fixed cost per unit time
c_2'	cost per until gmol of reactant A
c_3'	selling price per gmol of product B
F	reactor flow rate
f	dimensionless rate equation of main reaction
f_ξ	derivative of $f(\xi)$ with respect to ξ
g	dimensionless rate equation for deactivation process
H	Hamiltonian function
J	dimensionless performance index
J'	dimensional performance index
k	rate constant of main enzymatic reaction
k_d	deactivation rate constant
K	constant in the reaction rate for substrate inhibited kinetics
K_s	constant in the reaction rate for substrate inhibited kinetics
Q	dimensionless flow rate
r	rate of reactant depletion by reaction per unit volume
r_d	rate of enzyme deactivation per unit volume
u	control variable in an optimal control problem
u^*	optimal value for the control variable
V	reactor volume

x state valuable in an optimal control problem

GREEK LETTERS

β dimensionless equivalent of K (Eq.7)

γ dimensionless equivalent of K_e (Eq.7)

δ defined by boundary condition of Eq. 27b

ε dimensionless ratio of deactivation and main reaction rate constants

ϑ new dimensionless time scale equal to $\tau\varepsilon$

λ adjoint variables in an optimal control problem

ν_i multipliers in the Hamiltonian Eqs. 18 and 25

ξ fractional conversion of the reactant

ξ^* optimal value of ξ at quasisteady state

τ dimensionless time

SUBSCRIPT

f final time

0 feed condition

en conditions of entrance to singular arc

CHAPTER 2

A NOTE ON THE OPTIMALITY CRITERIA FOR THE MAXIMUM BIOMASS PRODUCTION IN A FED-BATCH REACTOR

2.1 INTRODUCTION

Fed-batch fermentations are being introduced in increasing numbers during the past few years because of the increased productivity and, mainly, the enhanced control possibilities offered by these systems. several studies (D'Ans *et al.*, 1971; Yamane *et al.*, 1977; Ohno *et al.*, 1976; D'Ans *et al.*, 1972 ; Ohno *et al.*, 1978) in recent years have examined the problem of optimal operation of a fed-batch fermentor with respect to various objective functions and control variables. In some of these investigations the operation of batch and continuous systems was also considered and a variety of methods, such as the maximum principle and the use of Green's theorem, were employed for the solution of the corresponding optimization problem. Constantinides (1979) has provided and extensive review of this subject.

The most common control variable in these systems is the fermentor's flow rate and several studies in the past have addressed the problem of determining the optimal feeding strategy in order to optimize the performance of the fermentor. In the majority of the cases considered, the nature of the performance indices is such that the derived optimal control problem is singular. Various methods have been used for the solution of such problems. In their study on the optimization of product rate formation in a fed-batch fermentor with substrate feed as a control variable, Ohno *et al.* (1976) applied a method based on Green's theorem to generate the optimal feeding strategy. In a more recent communication Ohno *et al.* determined the optimal operating pattern, a combination of batch, fed-batch and continuous operation to maximize product

formation. In another series of studies, Weigand (1979,1981) studies the optimal feeding strategy which maximizes the repeated fed-batch reactor by employing the maximum principle.

The objective of this note is to complement the above studies by establishing the optimal start-up and final phase procedure in a fed-batch reactor through the formulation of the corresponding optimal control problem and the use of the maximum principle for its solution. Furthermore, useful criteria which signal the entrance of the optimal start-up trajectory to the singular arc are established. Also some intuitive notions about the nature of the conditions which must be satisfied along the singular arc and which have been employed in previous studies without justification are placed in the right perspective. The maximization of cell biomass produced in a fed-batch fermentor is used as a vehicle for presenting the above results and ideas. However, the same methodology can be applied to different performance indices that would be considered more appropriated in other fermentations.

2.2 DETERMINATION OF OPTIMAL START-UP POLICY

The optimal control problem for the maximization of cell biomass in a fed-batch fermentor is formulated as follows:

$$\underset{F}{MAX}\, J = V_f x_f - c_1 \int_0^{t_f} dt \tag{1}$$

subject to the dynamics of the fed-batch fermentor:

$$\dot{x} = \mu(s)x - \frac{F}{V}x \qquad ; \; x(0) = x_0 \tag{2a}$$

$$\dot{s} = \frac{F}{V}(s_f - s) - \frac{1}{Y}\mu x \qquad ; \; s(0) = s_0 \tag{2b}$$

$$\dot{V} = F \qquad ; \; V(0) = V_0 \,, \; V(t_f) = V_f \tag{2c}$$

The feed rate F is the control variable in the above scheme and c_1 is a composite overall cost in units of cell biomass per unit time. A constant biomass yield has been assumed. Two types of specific growth rate functional forms will be discussed in the sequel: a monotonic increasing function of the substrate concentration, (such as the Monod type), and one that exhibits a maximum, characteristic of substrate inhibition.

Due to the fact that the above is a free time problem and the Hamiltonian is autonomous, the Hamiltonian is set equal to zero:

$$0 = H = -c_1 + \lambda_x \left[\mu(s)x - \frac{F}{V}x \right] + \lambda_s \left[\frac{F}{V}(s_f - s) - \frac{1}{Y}\mu(s)x \right] + \lambda_v F \tag{3}$$

where λ_x, λ_s and λ_v are the adjoint variables for biomass, substrate and volume respectively, satisfying the dynamics:

$$\dot{\lambda_x} = -\frac{\partial H}{\partial x} = -\lambda_x \left[\mu(s) - \frac{F}{V} \right] + \lambda_s \mu(s) \frac{1}{Y} \qquad ; \; \lambda_x(t_f) = V_f \tag{4a}$$

$$\dot{\lambda_s} = -\frac{\partial H}{\partial s} = -\lambda_x \mu_s x + \lambda_s \left[\frac{F}{V} + \frac{\mu_s x}{Y} \right] \qquad ; \; \lambda_s(t_f) = 0 \tag{4b}$$

$$\dot{\lambda_V} = -\frac{\partial H}{\partial V} = -\lambda_x x \frac{F}{V^2} + \lambda_s (s_f - s) \frac{F}{V^2} \tag{4c}$$

The optimal control to the problem defined by Eqs. (1) and (2) is typically obtained by setting the partial derivative of H with respect to the control F equal to zero and solving the resulting equation for the optimal flow rate:

$$0 = \frac{\partial H}{\partial F} = -\lambda_x \frac{x}{V} + \lambda_s \frac{1}{V}(s_f - s) + \lambda_v \tag{5}$$

It can be seen, however, that for this particular system being linear in the control, Eq. (5) is independent of the flow rate and, hence cannot be used for the

determination of the optimal control. The solution in this case is that of bang-bang control (Bryson and Ho, 1969) :

$$F^*(t) = \begin{cases} F_{max} \text{ if } H_F = \dfrac{\partial H}{\partial F} = -\lambda_x \dfrac{x}{V} + \lambda_s \dfrac{1}{V}(s_f - s) + \lambda_v > 0 \\ F_{min} = 0 \text{ if } H_F < 0 \end{cases} \tag{6}$$

Thus, for this singular problem the flow rate should be set optimally at the extreme values allowed as long as $H_F \neq 0$. When $H_F = 0$ the optimal control cannot be determined from the maximum principle. However, if H_F is zero over a finite interval of time, so must be its time derivatives and repeated differentiation of $H_F = 0$ with respect to time will eventually yield an explicit relationship for the optimal flow rate. The trajectory followed by F during the time period over which H_F is zero and the control is not on the boundaries is often referred to as singular arc.

After a rather involved algebraic manipulation the derivative of H_F with respect to time, $\dot{H}_F$, can be written as:

$$\dot{H}_F = \frac{(s_f - s)}{V} \mu_s x \left(-\lambda_x + \frac{\lambda_s}{Y}\right) \tag{7}$$

A subsequent differentiation of $\dot{H}_F$ with respect to time yields a relationship from which the control can be determined along the singular arc as:

$$F_{sing} = \frac{\mu x V}{Y(s_f - s)} \tag{8}$$

Equations (6) and (8) determine the optimal feeding policy for this fed-batch fermentation.

In order to determine the feed rate during the start-up of the operation, the sign of H_F must be examined. For this purpose it is useful to note that the quantity $\left(-\lambda_x + \frac{\lambda_s}{Y}\right)$ remains negative during the course of the fermentation. To

show this Eq. (4b) is divided by Y and then added to Eq. (4a) to yield:

$$\frac{d}{dt}(-\lambda_x + \frac{\lambda_s}{Y}) = (-\lambda_x + \frac{\lambda_s}{Y})(\frac{F}{V} - \mu + \frac{\mu_s}{Y}x)$$

which can be integrated to give:

$$\left[-\lambda_x + \frac{\lambda_s}{Y}\right] = \left[-\lambda_x + \frac{\lambda_s}{Y}\right]_0 \exp\left[\int_0^t \left[\frac{F}{V} - \mu + \frac{\mu_s}{Y}x\right] dt\right] \tag{9}$$

From Eq. (9) it follows that the quantity $(-\lambda_x + \frac{\lambda_s}{Y})$ does not change sign, and, in view of the final conditions of Eqs (4), one can obtains that

$$-\lambda_x + \frac{\lambda_s}{Y} < 0 \quad \textit{at all time} \tag{10}$$

Two cases are now distinguished:

Case *I*: $\mu_s > 0$. Then $\dot{H}_F < 0$. If H_F is negative initially it remains negative at all times and Eq. (6) indicates that the flow rate should be always zero which cannot be optimal. If, on the other hand, H_F is initially positive, the fact that $\dot{H}_F < 0$ indicates that there may be a time at which H_F switches sign or becomes zero. Therefore, for μ_s initially positive the flow rate is set at the maximum allowed value during start-up and it follows Eq. (8) along the singular arc if H_F becomes zero. If H_F simply crosses from positive to negative values then the flow rate should be accordingly reduced from the maximum value to zero in response to this change.

Case *II*: $\mu_s < 0$. In this case $\dot{H}_F > 0$. IF H_F is initially positive it remains positive through the entire fermentation indicating that the reactor should be filled up with the maximum flow rate and then allowed to run in the batch mode. This is again not optimal because μ decreases during the start-up period resulting in

smaller overall productivity. This implies that H_F must be initially negative. Therefore, no substrate should be added after inoculation until H_F switches sign at which point the flow rate should be varied according to Eq. (8) or set to the maximum value allowed depending on whether H_F stays at zero for a prolong period of time or simply changes sign.

From the above analysis one may conclude that for Monod type kinetics, for which $\mu_s > 0$ always, the optimal policy is to fill the reactor as quickly as possible and let it run in the batch mode for a period of time until the final conditions on the adjoints are satisfied. If the biomass growth kinetics exhibits a maximum, either one of the above cases could be applicable. If, as is frequently the case, a small amount of inoculum is added to the reactor, the initial substrate concentration will be large indicating that μ_s is negative. In this case no substrate should be added to the reactor until H_F becomes zero and the singular arc is entered. The control follows Eq. (8) after this point and, when the final volume is reached, the reactor should run in the batch mode until the final adjoint constraints are satisfied.

2.3 CONDITION ALONG THE SINGULAR ARC

As indicated earlier, the singular arc is defined as the trajectory on which all three of H, H_F, and $\dot{H}_F$ vanish. These conditions form a set of linear equations in the adjoints that can be solved to determine the adjoint variable as functions of state variable:

$$\begin{bmatrix} \mu x - Fx/V & (s_f - s)F/V - \mu x/Y & F \\ -x/V & (s_f - s)/V & 1 \\ -\mu_s & \mu_s/Y & 0 \end{bmatrix} \begin{bmatrix} \lambda_x \\ \lambda_s \\ \lambda_V \end{bmatrix} = \begin{bmatrix} c_1 \\ 0 \\ 0 \end{bmatrix} \tag{11}$$

The determinant of the above matrix, however vanishes identically and a

condition for the existence of a non-trivial solution can be obtained by applying Fredholm's alternative, (or, the solvability condition), according to which: if det(**A**)=0, the condition for a non-trivial solution of $\mathbf{A}\,\boldsymbol{\lambda} = \mathbf{b}$ to exist is that

$$\mathbf{U}^T\,\mathbf{b} = 0 \tag{12}$$

where the vector **U** is determined as the solution of $\mathbf{A}^T\,\mathbf{U} = \mathbf{0}$.

For the problem in hand the above condition, $\mathbf{A}^T\,\mathbf{U} = \mathbf{0}$.

$$\begin{bmatrix} \mu x - Fx/V & -x/V & -\mu_s \\ (s_f - s)F/V - \mu x/V & (s_f - s)/V & \mu_s/Y \\ F & 1 & 0 \end{bmatrix} \begin{bmatrix} U_1 \\ U_2 \\ U_3 \end{bmatrix} = \begin{bmatrix} 0 \\ 0 \\ 0 \end{bmatrix} \tag{13}$$

yielding $U_2 = -FU_1$, $U_1 = \dfrac{\mu_s}{\mu x} U_3$. The vector **U** is then:

$$\mathbf{U} = \left[\frac{\mu_s}{\mu x}, \quad -\frac{F\mu_s}{\mu x}, \quad 1 \right]^T \tag{14}$$

and the solvability condition (12) is satisfied if:

$$\mu_s = 0 \tag{15}$$

It should be noted that the above is a necessary but not sufficient condition for the existence of a singular arc. For if $H_F \neq 0$ but condition (15) is satisfied, it can be seen that the solvability condition (12) is also satisfied despite the fact that no singular arc exists in this case ($H_F \neq 0$). In conclusion, it can be generally stated that when the system is on a singular arc, condition (15) is satisfied, but the latter condition alone cannot insure the existence of a singular arc.

For the particular problem under consideration it can be shown that condition (15) is necessary and sufficient for a singular arc. To show this the problem of Eq. (1) and (2) is recast in a new form with the volume as control vari-

able, and the total of biomass and the negative of the available substrate as state variables:

$$MAX\ J = y(t_f) - c_1 \int_0^{t_f} dt \tag{16}$$

subject to:

$$\dot{y} = \mu(Z,V)y \tag{17a}$$

$$\dot{Z} = -\frac{\mu(Z,V)y}{Y} \tag{17b}$$

with y and Z defined as:

$$y = xV, \qquad Z = (s - s_f)V \tag{18}$$

The volume is the new control variable subject to the constraints:

$$V(0) = V_0, \quad V(t_f) = V_f, \quad 0 \le \dot{V} \le F_{max} \tag{19}$$

the new Hamiltonian is :

$$0 = H = -c_1 + \lambda_y \mu(Z,V)y + \lambda_Z \frac{\mu(Z,V)y}{Y} \tag{20}$$

and the volume derivative:

$$0 = H_V = \left[\lambda_y + \frac{\lambda_Z}{Y}\right] y\,\mu_V \tag{21}$$

In view of Eq. (20), Eq. (21) can be satisfied if and only if

$$\mu_V = 0 \tag{22}$$

Condition (22) can written as:

$$0 = \mu_V = \frac{\partial \mu}{\partial V} = \frac{d\mu}{ds}\frac{\partial s}{\partial V} = \mu_s \left[\frac{-Z}{V^2}\right] \tag{23}$$

indicating that it will be satisfied if and only if Eq. (15) is true.

2.4 FINAL ARC

The control will follow the singular arc, Eq. (8), or, for Monod kinetics, will be maximum flow until the state constraint, in this case the final culture volume is reached. At that point the flow is stopped and the reactor runs in the batch mode. The stopping condition is found by substituting $F = 0$ and the final conditions for the adjoint variables into Eq. (3) for the Hamiltonian:

$$\mu(t_f) V_f = c_1 \tag{24}$$

2.5 CONCLUSION

If the biomass growth kinetics is of the Monod type, the optimal feeding strategy for the optimization of the final biomass produced in a fed-batch reactor is to fill the reactor after inoculation at the fastest possible rate and then run it in the batch mode until condition (24) is satisfied. If the biomass kinetics exhibits a maximum the optimal start-up feeding strategy is no flow if the initial substrate concentration is to the right of the maximum, and maximum flow if it is to the left. In both cases the substrate concentration tends towards the maximum and when Eq. (15) is satisfied this signals the entrance to the singular arc along which the optimal feed is given by Eq. (8). This flow pattern is maintained until $V = V_f$ after which the flow is stopped and the reactor runs as a batch until condition (24) is reached. It is pointed out that in this case $\mu_s = 0$ is a necessary and sufficient condition for operation along the singular arc. In general, however, the above is a necessary condition only.

NOTATION

c_1 overall time cost in unit of biomass per unit time

F reactor flow rate

H Hamiltonian

s substrate concentration

s_f feed substrate concentration

t time

x cell biomass concentration

Y biomass yield

y total biomass in the culture, defined by Eq. (18)

Z the negative of the total available substrate, defined by Eq. (18)

GREEK LETTERS

λ adjoint variable; λ_x for biomass, λ_s for substrate, λ_V for volume

μ specific growth rate

μ_s derivative of μ respect to s

μ_m maximum specific growth rate

SUBSCRIPT

o initial conditions

f final conditions

SUPERSCRIPT

* optimal trajectory

T transpose matrix

CHAPTER 3

A NOTE ON THE OPTIMAL CONTROL POLICY FOR THE MAXIMUM BIOMASS PRODUCTION IN A FED-BATCH REACTOR WITH TIME DELAY IN THE SPECIFIC GROWTH RATE

3.1 INTRODUCTION

In the past few years, increasing number of studies has been devoted to the theoretical and experimental investigation of the optimal control problems of fed-batch fermentation. There are two main advantages of such systems over the conventional batch or continuous mode of operations, namely, the enhanced control possibilities over the batch mode and the elimination of wash-out possibilities of the continuous mode. The kinetics models employed in almost all of these studies are lumped parameters models which express various rates as function of substrate concentration at that particular time. However, there are reasons to believe that there exists a lag between these rates and the instantaneous substrate concentration. Many justification or causes can be provided to explain the above phenomenon, such as the time required for the cells to generate other or more essential enzymes in response to a change in substrate concentration level or diffusion delay of substrate through the cell membrane, etc. Such delay effect has been observed and reported in several studies (San and Stepnanopoulos, 1983; Dairaku *et al*, 1982). Ignoring this delay may cause a lot of troubles in various control or dynamic problem. It is the purpose of this note to address this problem. The maximization of cell biomass produced in a fed-batch fermentation with delay in specific growth rate with respect to time is used as vehicle for presenting the ideas and results. The optimal control problem of such delay system is solved and a comparison is made with a feed-forward control strategy neglecting the delay effect.

3.2 FORMULATION OF THE OPTIMAL CONTROL PROBLEM

The optimal control problem for the maximization of cell biomass in a fed-batch fermentor with delay in specific growth rate is formulated as follows:

$$\underset{F}{MAX}\ J = V_f x_f - c_1 \int_0^{t_f} dt \tag{1}$$

subject to the dynamics of the fed-batch fermentor:

$$\dot{x} = \mu(y)x - \frac{F}{V}x \qquad ;\ x(0) = x_0 \tag{2a}$$

$$\dot{s} = \frac{F}{V}(s_f - s) - \frac{1}{Y}\mu(y)x \qquad ;\ s(0) = s_0 \tag{2b}$$

$$\dot{V} = F \qquad ;\ V(0) = V_0,\quad V(t_f) = V_f \tag{2c}$$

where $y = s(t-\vartheta)$ and

$$s(t) = \varphi(t) \qquad \text{for } -\vartheta \le t \le 0$$

In the above set of equations, the expression $\mu(s(t-\vartheta))$ is used as a model to account for the delay effect that has been discussed earlier. ϑ represents the amount of time which the cells require to adjust to any change in substrate concentration level, and is assumed to be a constant in this study. The feed rate F is the control variable in the above scheme and c_1 is a composite overall cost in units of cell biomass per unit time. A constant biomass yield has been assumed. Two types of specific growth rate functional forms will be discussed in the sequel: a monotonic increasing function of the substrate concentration, (of the Monod type), and one that exhibits a maximum, characteristic of substrate inhibition.

Due to the fact that the above is a free time problem and the Hamiltonian is autonomous, the Hamiltonian is set equal to zero:

$$0 = H = -c_1 + \lambda_x[x\mu(y) - \frac{F}{V}x] + \lambda_s[\frac{F}{V}(s_f - s) - \frac{1}{Y}\mu(y)x] + \lambda_V F \tag{3}$$

where λ_x, λ_s and λ_V are the adjoint variables satisfying the following equations:

$$\dot{\boldsymbol{\lambda}} = -\left[\frac{\partial H}{\partial \mathbf{x}}\right]^T \qquad \text{for } t_f - \vartheta \le t \le t_f$$

$$\dot{\boldsymbol{\lambda}} = -\left[\frac{\partial H}{\partial \mathbf{x}}\right]^T - \left[\frac{\partial H}{\partial \mathbf{y}}\right]^T_{t=t+\vartheta} \qquad \text{for } 0 \le t \le t_f - \vartheta \tag{4}$$

For the problem in hand, we have the following set of governing differential equations:

State equations:

$$\left.\begin{aligned} \dot{x} &= (\mu(\varphi(t-\vartheta)) - \frac{F}{V})x \\ \dot{s} &= \frac{F}{V}(s_f - s) - \frac{1}{Y}\mu(\varphi(t-\vartheta))x \\ \dot{V} &= F \end{aligned}\right\} \qquad \text{for } 0 \le t \le \vartheta \tag{5a}$$

$$\left.\begin{aligned} \dot{x} &= (\mu(y) - \frac{F}{V})x \\ \dot{s} &= \frac{F}{V}(s_f - s) - \frac{1}{Y}\mu(y)x \\ \dot{V} &= F \end{aligned}\right\} \qquad \text{for } \vartheta \le t \le t_f \tag{5b}$$

Adjoint equations:

$$\left.\begin{aligned} \dot{\lambda_x} &= -\lambda_x(\mu(y) - \frac{F}{V}) + \lambda_s \frac{(\mu(y))}{Y} \\ \dot{\lambda_s} &= -\lambda_s \frac{F}{V} - \overline{\lambda_x}\mu_s(s)\bar{x} + \overline{\lambda_s}\mu_s \frac{\bar{x}}{Y} \\ \dot{\lambda_V} &= -\lambda_x \frac{F}{V^2}x + \lambda_s \frac{F}{V^2}(s_f - s) \end{aligned}\right\} \qquad \text{for } 0 \le t \le t_f - \vartheta \tag{6a}$$

$$\left.\begin{aligned} \dot{\lambda_x} &= -\lambda_x(\mu(y) - \frac{F}{V}) + \lambda_s \frac{(\mu(y))}{Y} \\ \dot{\lambda_s} &= -\lambda_s \frac{F}{V} \\ \dot{\lambda_V} &= -\lambda_x \frac{F}{V^2}x + \lambda_s \frac{F}{V^2}(s_f - s) \end{aligned}\right\} \qquad \text{for } t_f - \vartheta \le t \le t_f \tag{6b}$$

where $\overline{\lambda_s}$ and $\bar{x}$ are the advanced variables, and are given by

$$\overline{\lambda_s} = \lambda_s(t + \vartheta) \qquad \overline{\lambda_x} = \lambda_x(t + \vartheta) \qquad \bar{x} = x(t + \vartheta)$$

The optimal control to the problem defined by Eqs. (1) and (2) is typically obtained by setting the partial derivative of H with respect to the control F equal to zero and solving the resulting equation for the optimal flow rate:

$$0 = \frac{\partial H}{\partial F} = -\lambda_x \frac{x}{V} + \lambda_s \frac{1}{V}(s_f - s) + \lambda_V \tag{7}$$

It can be seen, however, that for this particular system being linear in the control, Eq. (7) is independent of the flow rate and, hence cannot be used for the determination of the optimal control. The solution in this case is that of bang-bang control (Bryson and Ho, 1969) :

$$F^*(t) = \begin{cases} F_{\max} \text{ if } H_F = \dfrac{\partial H}{\partial F} = -\lambda_x \dfrac{x}{V} + \lambda_s \dfrac{1}{V}(s_f - s) + \lambda_V > 0 \\ F_{\min} = 0 \text{ if } H_F < 0 \end{cases} \tag{8}$$

Thus, for this singular problem the flow rate should be set optimally at the extreme values allowed as long as $H_F \neq 0$. When $H_F = 0$ the optimal control cannot be determined from the maximum principle. However, if H_F is zero over a finite interval of time, so must be its time derivatives and repeated differentiation of $H_F = 0$ with respect to time will eventually yield an explicit relationship for the optimal flow rate. The trajectory followed by F during the time period over which H_F is zero and the control is not on the boundaries is often referred to as singular arc.

After a rather involved algebraic manipulation the derivative of H_F with respect to time, $\dot{H}_F$, can be written as:

$$\dot{H}_F = \frac{(s_f - s)}{V} \mu_s x \left(-\overline{\lambda_x} + \frac{\overline{\lambda_s}}{Y}\right) \tag{9}$$

The above equation is valid only between $0 \leq t \leq t_f - \vartheta$, and $\dot{H}_F$ is identically equal to zero between $t_f - \vartheta \leq t \leq t_f$. One interesting point worth mentioning here is that if $\dot{H}_F$ is zero during this time period, then the control strategy cannot be determined by further differentiation of H_F with respect to time. In fact, in this particular case any control strategy which does not violate any state constraint will yield the optimal result because any subsequent control action on the flow rate will not affect the specific growth rate any more.

A subsequent differentiation of $\dot{H}_F$ with respect to time yields a relationship from which the control can be determined along the singular arc as:

$$F_{sing} = \frac{\mu(y)xV}{Y(s_f - s)} \tag{10}$$

Equations (8) and (10) determine the optimal feeding policy for this fed-batch fermentation.

3.3 CONCLUSION

It has been shown in previous note[2] that the initial control strategy can be obtained by noting that the quantity $-\lambda_x + \frac{\lambda_s}{Y}$ remains always negative during the course of fermentation. Following similar procedures, one can obtain the following conclusion about the control strategy.

If the biomass growth kinetics is of Monod type, the optimal feeding strategy for the optimization problem is to fill the reactor at the fastest possible rate after inoculation and then run it in batch mode until $\mu(t_f)V_f = c_1$ is satisfied. If the biomass kinetics exhibits a maximum the optimal start-up feeding strategy is no flow if the initial substrate concentration is to the right of the maximum, and maximum flow if it is to the left. The same strategy is followed until the substrate concentration satisfies $\mu_s(s) = 0$. This signals the entrance of the singular arc and the feeding rate is given by Eq. 10. The same pattern is

maintained until $V = V_f$, after which the flow is stop and the reactor is allowed to run in batch mode until the same condition $\mu(t_f)V_f = c_1$ is satisfied.

Results from the computer simulations which illustrate some of the problems with feed-forward control when there is a delay in the specific growth rate are shown in Fig. 3.1-3.4. Equations (5a) and (5b) were used to simulate the dynamics of the fermentor with substrate inhibited growth model. Details of the parameters employed in this simulation were listed in Fig. 3.1. Shown in these figures are results obtained from two different control strategies; the dashed line corresponded to the optimal control strategy with delay taking into account while the solid line corresponded to that neglecting the delay in the dynamic equations. It can be seen that the second control strategy resulted in a non-optimal solution; it requires twice as much time more than the optimal solution for the same biomass production.

One can conclude from the above simulations that by neglecting or using inaccurate delay parameters will result in departure from optimal solution for feed forward control. A good feedback control scheme is required to implement the optimal control strategy, in this case, a good substrate regulator is essential.

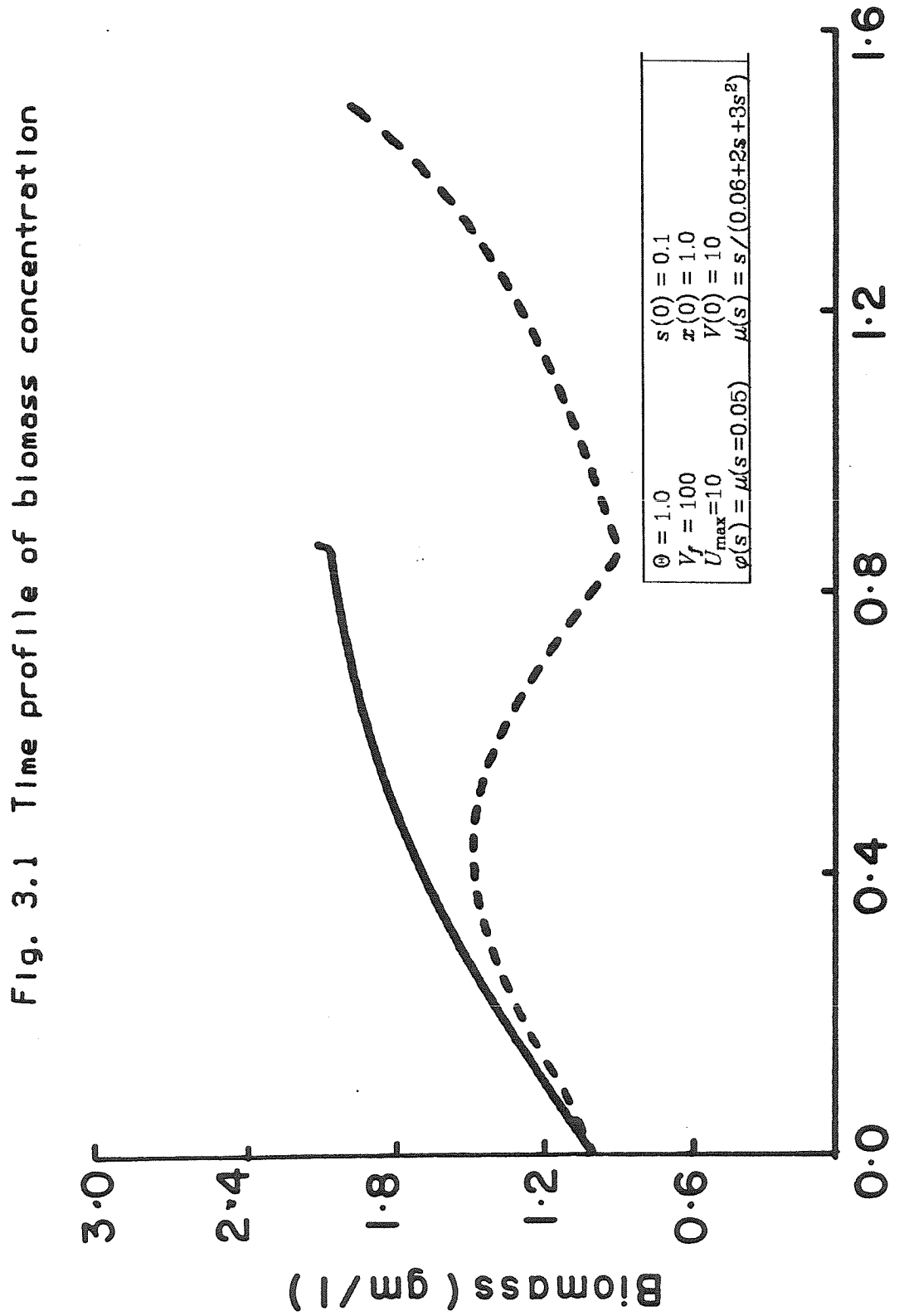

Fig. 3.1 Time profile of biomass concentration

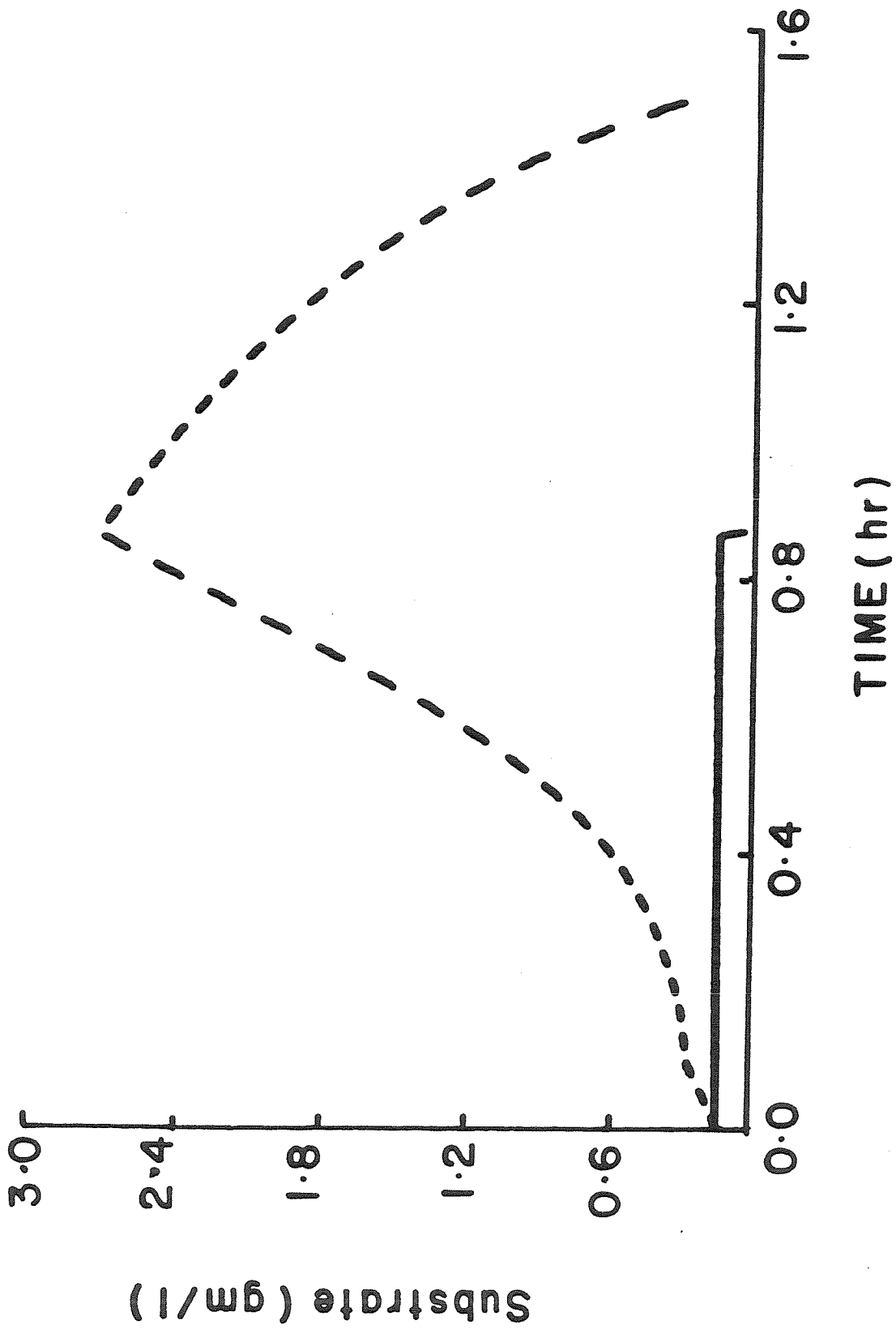

Fig. 3.2 Time profile of substrate concentration

NOTATION

c_1 overall time cost in unit of biomass per unit time

F reactor flow rate

H Hamiltonian

s substrate concentration

s_f feed substrate concentration

t time

x cell biomass concentration

$\bar{x}$ advanced variable defined as $x(t+\vartheta)$

y defined as $s(t-\vartheta)$

Y biomass yield

GREEK LETTERS

λ adjoint variable; λ_x for biomass, λ_s for substrate, λ_V for volume

$\overline{\lambda_s}$ advanced variable defined as $\lambda_s(t+\vartheta)$

$\overline{\lambda_x}$ advanced variable defined as $\lambda_x(t+\vartheta)$

μ specific growth rate

μ_s derivative of μ respect to s

μ_m maximum specific growth rate

ϑ delay time

φ substrate concentration for time between $-\vartheta$ and 0

SUBSCRIPT

o initial conditions

f final conditions

SUPERSCRIPT

* optimal trajectory

T transpose matrix

APPENDIX

Program for using the D/A converter

```
FUNCTION CONVERT(CHANNEL ,GAIN : INTEGER) : INTEGER;
  CONST    PORT = $B0;
           MASK = $01;

  BEGIN
  OUT[PORT]:=CHANNEL;
  OUT[(PORT+1)]:=0;          {start conversion}

  WAIT(PORT+1,MASK,FALSE);     {wait until the bit goes high}
                                {high implies conversion finished}
  CONVERT:=SWAP( INP[(PORT+3)] ) ! INP[(PORT+2)]
  END;
```

Program for setting the real-time-clock

```
PROGRAM STIME;
{ STIME -- set the time on the RTC-100 }
{    Written by K. Fickie          }

CONST    PORT0 = 24;     {base address}
         PORT1 = 25;
         PORT2 = 26;
         PORT3 = 27;


VAR        TIME : ARRAY[0..12] OF BYTE;
            YEAR : 1982..1990;
           MONTH : 1..12;
             DAY : 1..31;
            HOUR : 0..23;
          MINUTE : 0..59;
          SECOND : 0..59;
             DWK : 0..6;
                 I : INTEGER;


BEGIN
WRITE('Year (eg. 82): ');
READLN(YEAR);
TIME[12]:=SHL(YEAR DIV 10,4);
TIME[11]:=SHL(YEAR MOD 10,4);
WRITELN;

WRITE('Month: ');
```

```
READLN(MONTH);
TIME[10]:=SHL(MONTH DIV 10,4);
TIME[9]:=SHL(MONTH MOD 10,4);
WRITELN;

WRITE('Day: ');
READLN(DAY);
TIME[8]:=SHL(DAY DIV 10,4);
TIME[7]:=SHL(DAY MOD 10,4);
WRITELN;

WRITE('Day # of week (eg. Sunday ==> 0 ) : ');
READLN(DWK);
TIME[6]:=SHL(DWK,4);
WRITELN;

WRITE('Hour: ');
READLN(HOUR);
TIME[5]:=SHL(HOUR DIV 10,4);
TIME[4]:=SHL(HOUR MOD 10,4);
WRITELN;

WRITE('Minute: ');
READLN(MINUTE);
TIME[3]:=SHL(MINUTE DIV 10,4);
TIME[2]:=SHL(MINUTE MOD 10,4);
WRITELN;

TIME[1]:=0;
TIME[0]:=0;

OUT[PORT3]:=$F4;
OUT[PORT2]:=$FF;
OUT[PORT3]:=$F0;
OUT[PORT2]:=$FF;
OUT[PORT1]:=$F0;
OUT[PORT0]:=$FF;
OUT[PORT3]:=$F4;
OUT[PORT1]:=$F4;

FOR I:=0 TO 12 DO
  BEGIN
  OUT[PORT0]:=TIME[I] + I;
  OUT[PORT2]:=0;
  OUT[PORT2]:=1
  END;

OUT[PORT1]:=$F8;
OUT[PORT3]:=$F0
END.
```

Program to read the time

```
PROGRAM RTIME;
{ RTIME – reads the time from the RTC-100 }
{    Written by K. Fickie                 }
CONST    PORT0 = 24;
         PORT1 = 25;
         PORT2 = 26;
         PORT3 = 27;

     REVERSE = $12;
       QUIT = $11;
        CR = $0D;

TYPE   STRING9 = ARRAY[1..9] OF CHAR;

VAR        TIME : ARRAY[0..12] OF BYTE;
            DAYS : ARRAY[0..6] OF STRING9;
            YEAR : 1982..1990;
           MONTH : 1..12;
             DAY : 1..31;
            HOUR : 0..23;
          MINUTE : 0..59;
          SECOND : 0..59;
             DWK : 0..6;
         OLD_SEC : INTEGER;

PROCEDURE RTC_READ;

  VAR   I : INTEGER;
  BEGIN
  OUT[PORT1]:=$F0;
  OUT[PORT0]:=$0F;
  OUT[PORT3]:=$FC;
  OUT[PORT1]:=$F4;

  FOR I:=0 TO 12 DO
    BEGIN
    OUT[PORT0]:=I;
    TIME[I]:=SHR( INP[PORT0], 4)
    END;
  OUT[PORT1]:=$F8;
  OUT[PORT0]:=$0F;
  OUT[PORT3]:=$F8;
  OUT[PORT1]:=$FC;
  OUT[PORT0]:=$0F
  END;


PROCEDURE PRINT_TIME;
  BEGIN
  WRITE('The time is:  ',CHR(REVERSE),
       HOUR:2,':',MINUTE:2,':',SECOND:2,
```

```
      CHR(QUIT),CHR(CR),CHR($0B) );
  END;

BEGIN

DAYS[0]:='Sunday   ';
DAYS[1]:='Monday   ';
DAYS[2]:='Tuesday  ';
DAYS[3]:='Wednesday';
DAYS[4]:='Thursday ';
DAYS[5]:='Friday   ';
DAYS[6]:='Saturday ';

REPEAT
  RTC_READ;
  YEAR:=(TIME[12]*10) + TIME[11];
  MONTH:=( (TIME[10] & 3)*10 ) + TIME[9];
  DAY:=(TIME[8]*10) + TIME[7];
  DWK:=TIME[6];
  HOUR:=( (TIME[5] & 3)*10 ) + TIME[4];
  MINUTE:=(TIME[3]*10) + TIME[2];
  SECOND:=(TIME[1]*10) + TIME[0];

  IF SECOND< > OLD_SEC THEN
    BEGIN
    PRINT_TIME;
    OLD_SEC:=SECOND
    END
UNTIL FALSE;

END.
```

Program for data logging during experiment

```
PROGRAM EXPERIMENT;

CONST     PORT0 =24;
        PORT1 =25;
        PORT2 =26;
        PORT3 =27;

TYPE  STRING9 = ARRAY[1..9] OF CHAR;

VAR           F : TEXT;
            F_NAME : STRING;
          TIME : ARRAY[0..12] OF BYTE;
          DAYS : ARRAY[0..6] OF STRING9;
          YEAR : 1982..1990;
         MONTH : 1..12;
           DAY : 1..31;
          HOUR : 0..23;
```

```
      MINUTE : 0..59;
      SECOND : 0..59;
        DWK : 0..6;
      OLDSEC : INTEGER;
      DATE   : STRING;
    COMMENT  : STRING;
        F_RESULT : INTEGER;
         NUMBER : INTEGER;
        DELTA_T : INTEGER;
        CORRECT,TEMP,COUNT      : INTEGER;
    PTEMP,O2,CO2,OTEMP,CTEMP : REAL;
    O2C,CO2B,PH,PHCON,PPH    : REAL;
    PPTEMP,PCONV,PRE,PRES    : REAL;
    RES,PPRES,PTAKE,CO2C     : REAL;
        NN,I,J,TAKE          : INTEGER;
        CH9,CH10,CH11,CH12,CH13  : INTEGER;
    CH14,CH15                    : INTEGER;

EXTERNAL FUNCTION @BDOS(FUN, PARM : INTEGER) : INTEGER;

FUNCTION KEYPRESSED : BOOLEAN;
  BEGIN
  KEYPRESSED:=(@BDOS(11,0) <> 0)
  END;

 PROCEDURE CONV(VAR CO2,CO2C:REAL);
  CONST  A=-4.018189E-5;
         B=0.4052546;
         C=6.3770682E-2;
      D=1.0504625E-2;
         E=-3.8618033E-4;
  VAR   V:REAL;
  BEGIN
     V:=CO2;
        CO2C:=A+V*(B+V*(C+V*(D+V*E)));
  END;

PROCEDURE  ASK_QUESTIONS;
  BEGIN
  WRITE(' Enter the name of the data file:  ');
  READLN(F_NAME);  WRITELN;

  WRITE(' Enter to-days date');
  READLN(DATE);    WRITELN;

  WRITELN(' Enter any comment on this run');
  READLN(COMMENT);   WRITELN;

  WRITE(' Enter the number of data points you wish to take:  ');
  READLN(NUMBER);  WRITELN;

  WRITE(' Enter the # of seconds between sampling:  ');
  READLN(DELTA_T);  WRITELN;
  WRITE(' ENTER THE CHANNEL # FOR BAKGROUND');
```

```
  READLN(CH15);    WRITELN;

  WRITELN(' THE FOLLOWING ANALYSERS ARE ASSIGNED TO');
  WRITELN('  ANALYSER',' ':5,' CHANNEL #');
  WRITELN('  OXYGEN',' ':10,' 9');
  WRITELN('  CO2',' ':13,' 10');
  WRITELN('  PH-HIGH',' ':9,' 11');
  WRITELN('  PH-LOW',' ':10,' 12');
  WRITELN('  PRESSURE',' ':8,' 13');
  WRITELN('  PH-VALUE',' ':8,' 14');
  WRITELN(' BACKGROUND',' ':8,CH15:2);
  CH9 :=9    ;
  CH10 :=10   ;
  CH11 :=11   ;
  CH12 :=12   ;
  CH13 :=13   ;
  CH14 :=14   ;

  END;


FUNCTION CONVERT(CHANNEL : INTEGER) : INTEGER;
{ CONVERT – samples an analog signal the TECMAR 12 bit }
{         A/D converter.                               }

  CONST    PORT = $B0;
           MASK = $01;

  BEGIN
  OUT[PORT]:=CHANNEL;
  OUT[(PORT+1)]:=0;          {start conversion}

  WAIT(PORT+1,MASK,FALSE);     {wait until the bit goes higH}

  CONVERT:=SWAP( INP[(PORT+3)] ) ! INP[(PORT+2)]
  END;



PROCEDURE RTCREAD;

VAR I : INTEGER;

BEGIN
OUT[PORT1]:=$F0;
OUT[PORT0]:=$0F;
OUT[PORT3]:=$FC;
OUT[PORT1]:=$F4;

FOR  I:=0 TO 12 DO
   BEGIN
   OUT[PORT0]:=I;
   TIME[I]:=SHR( INP[PORT0], 4)
   END;
```

```
OUT[PORT1]:=$F8;
OUT[PORT0]:=$0F;
OUT[PORT3]:=$F8;
OUT[PORT1]:=$FC;
OUT[PORT0]:=$0F
END;

PROCEDURE DATATAKE( VAR CHANNEL : INTEGER;
                    VAR ANS :REAL);
VAR     II : INTEGER;
BEGIN
 II:=CONVERT(CH15);
 ANS:=10*(CONVERT(CHANNEL)-II)/2048.0;
END;

BEGIN  (* EXPERIMENT *)

ASK_QUESTIONS;
ASSIGN(F,F_NAME);
REWRITE(F);

 WRITELN(F,DATE);
 WRITELN(F,COMMENT);
 COUNT:=0;
 CO2:=0.093;
 CONV(CO2,CO2B);

WRITELN('Press any key when you are ready to start.');
REPEAT UNTIL KEYPRESSED;

FOR I:=1 TO NUMBER DO
  BEGIN
  NN:=0;
  TAKE:=0;
  WHILE ( DELTA_T >  NN ) DO
    BEGIN

    RTCREAD;
    HOUR:=( (TIME[5] & 3)*10) + TIME[4];
    MINUTE:=(TIME[3]*10) + TIME[2];
    SECOND:=(TIME[1]*10) + TIME[0];
    DATATAKE(CH9,O2);
    DATATAKE(CH10,CO2);
    DATATAKE(CH13,PTAKE);
    DATATAKE(CH14,PPH);
    OTEMP:=(OTEMP*TAKE + O2)/(TAKE+1);
    CTEMP:=(CTEMP*TAKE + CO2)/(TAKE+1);
    PTEMP:=(PTEMP*TAKE + PTAKE)/(TAKE+1);
    PPTEMP:=(PPTEMP*TAKE +PPH)/(TAKE+1);
    TAKE:=TAKE+1;
    IF SECOND< > OLDSEC THEN
     BEGIN
          OLDSEC:=SECOND;
```

```
        NN:=NN+1;
      TAKE:=0;
        DATATAKE(CH11,PH);
        DATATAKE(CH12,PHCON);
        IF (ABS(PHCON-PH)> 0.5)THEN COUNT:=COUNT+1;
  O2C:=19.0+0TEMP/2.5;
  CONV(CTEMP,CO2C);
  PPRES:=(CO2C-CO2B)/(20.93-O2C);
  PTEMP:=PTEMP*10/3.0;
  WRITE(I:6,'  ',HOUR:2,' ',MINUTE:2,' ',SECOND:2);
  WRITE(' ':5,OTEMP:6:3,'   ',CTEMP:6:3);
  WRITE(' ':3,PPRES:6:3,'   ',PPTEMP:6:3,'  ',PTEMP:6:3);
  WRITE(' ':2,COUNT:6);
  WRITELN;
  END;
  END;
  WRITE(F,I:6,'  ',HOUR:2,' ',MINUTE:2,' ',SECOND:2);
  WRITE(F , ' ':5, OTEMP : 6 : 3, CTEMP : 6 : 3);
  WRITE(F , ' ':5, PPRES : 6: 3,' ':5,PPTEMP:6:3);
  WRITE(F,' ':5,PTEMP:6:3,COUNT:6);
  WRITELN(F);
  IF ( (ABS(PHCON-PH)) <  0.5) THEN COUNT:=0;
  END;

CLOSE(F,F_RESULT);
WRITELN('SampliNg is completed')
END.
```

REFERENCES:

[1] Aris, R., *Elementary Chemical Reactor Analysis*, Prentice-Hall, Englewood Cliffs, NJ (1969).

[2] Aris, R. and R. H. S. Mah, " Independence of Chemical Reactions," *Ind. Engng. Chem. Fundl.*, **2**, 90 (1963).

[3] Asbjornsen, O.A. and M. Fjeld, " Response Modes of Continuous Stirred Tank Reactors," *Chem. Eng. Sci.*, **25**, 1627 (1970).

[4] Bailey, J. E. and D. F. Ollis, *Biochemical Engineering Fundamentals*, McGraw-Hill, New York (1977).

[5] Bravard, J. P., M. Cordonnier, J. P. Kernevez, and J. M. Lebault, " On Line Identification of Parameters in a Fermentation Process," *Biotechnol. Bioeng.*, **21**, 1487 (1979).

[6] Bryson, Jr., A. E. and Y. C. Ho, *Applied Optimal Control*, Blaisdell, Walthem, MA (1969).

[7] Burrill H., H. W. Doelle, and P. F. Greenfield, " The Inhibitory of Ethanol on Ethanol Production by *Zymomonas Mobilis*", *Biotechnology Letters*, **5**, 423 (1983).

[8] Chohji T., T. Sawada, and S. Kuno, " Analysis of the Growth-Inhibiting and Lethal Effects of Organic and Heavy-Metallic Compounds on Microorganisms" *International Chemical Engineering*, **21**, 501 (1981).

[9] Chou, A., W. H. Ray, and R. Aris, " Simple Control Policies for Reactors with Catalyst Decay," *Trans. Inst. Chem. Eng.*, **45**, 153 (1967).

[10] Constantinides, A., " Application of Rigorous Optimization Method to the Control and Operation of Fermentation Processes," *Annals of the New York*

Academy of Sciences, **326** 193 (1979).

[11] Constantinides, A., J. L. Spencer, and E. L. Gaden, " Optimization of Batch Fermentation Process. I. Development of Mathematical Models for Batch Penicillin Fermentation.," *Biotechnol. Bioeng.*, **12**, 803 (1970).

[12] Constantinides, A., Annals of the New York Academy of Sciences, *326*, 193 (1979).

[13] Cooney, C. L., H. Y. Wang, and D. I. C. Wang, " Computer-Aided Material Balancing for Prediction of Fermentation Parameters," *Biotechnol. Bioeng.*, **19**, 55 (1977).

[14] Crook, P. S., C. J. Wei, and R. D. Tanner, *Chem. Eng. Comm.*, (to appear).

[15] D'ans, G., P. Kokotovic and D. Gottlieb, *J. of Optimization Theory and Applications*, **7**, 61 (1971).

[16] D'ans, G., D. Gottlieb and P. Kokotovic, *Automatica*, **8**, 729 (1972).

[17] Dairaku, K., Y. Yamasaki, H. Morikowa, S. Shioya and T. Takamatsu, 'Experimental Study of Time-optimal Control in Fed-Batch Culture of Baker's Yeast," *J. Ferment. Technol.*, **60**, 67 (1982).

[18] Danielsson, B., B. Mattiason, R. Karlsson, and F. Winquist, " Use of an Enzyme Thermistor in Continuous Measurements and Enzyme Reactor Control," *Biotechnol. Bioeng.*, **21**, 1749 (1979).

[19] Do, D. D. and R. H. Weiland, " Consistency Between Rate Expressions for Enzyme Reactions and Deactivation," *Biotechnol. Bioeng.*, **22**, 1087 (1980).

[20] Erickson, L. E., S. E. Selga, and O. E. Viesturs, " Application of Mass and Energy Balance Regularities to Product Formation," *Biotech. and Bioeng.*, **20**, 1623 (1978).

[21] Fatima, M. de, V. de Queuroz, M. L. R. Vairo, and W. Borzani, " Influence of Initial Yeast and Sugar Concentrations on the Quantity of Yeast Produced in Batch Ethanol Fermentation of Sugar-Cane Blackstrap Molasses," *J. Ferment. Technol.*, **61**, 215 (1983).

[22] Fjeld, M., O. A. Asbjornsen, and K. J. Astom, " Reaction Invariants and Their Importance in the Analysis of Eigenvectors, State Observability and Controllability of the Continuous Stirred Tank Reactors," *Chem. Eng. Sci.*, **29**, 1917 (1974).

[23] Fredrickson, A. G. and H. M. Tsuchiya, " Microbial Kinetics and Dynamics," pp. 405-483 in *Chemical Reactor Theory, A Review.* L. Lapidus and N. R. Amundson (eds.), Prentice-Hall, Englewood Cliffs, N.J. (1980).

[24] Gelb, A. (eds.), *Applied Optimal Estimation*, written by the technical staff of Analytical Science Corp, MIT Press, Cambridge (1979).

[25] Gondo, S. M., M. Morishita, and T. Osaki, " Improvement of Glucose Sensor Performance with Immobilized Glucose Oxidase - Glucose Isomerase System," *Biotechnol. Bioeng.*, **22**, 1287 (1980).

[26] Grosz, R., K. Y. San, and G. N. Stephanopoulos, " Studies on the On-line Bioreactor Identification," *Biotech. and Bioeng.*, (submitted) (1983).

[27] Gustafsson, T. K. and K. V. Waller, " Dynamic Modelling and Reaction Invariant Control of pH," *Chem. Eng. Sci.*, **38**, 389 (1983).

[28] Haas, W. R., L. L. Tavlarides, and W. J. Wnek, " Optimal Temperature Policy for Reversible Reactions with Deactivation: Applied to Enzyme Reactors," *AIChE Journal*, **20**, 707 (1974).

[29] Heijnen, J.J. and J. A. Roels, " A Macroscopic Model Describing Yield and Maintenance Relationship in Aerobic Fermentation Process," *Biotechnol.*

Bioeng., **23**, 739 (1981).

[30] Hendy, N. A. and P. P. Gray , " Use of ATP as an Indicator of Biomass Concentration in the *Trichoderma* Fermentation," *Biotechnol. Bioeng.*, **21**, 153 (1979).

[31] Hikuma, M., T. Kubo, T. Yasuda, I. Karube, and S. Suzuki, " Microbial Electrode Sensor for Alcohol," *Biotechnol. Bioeng.*, **21**, 1845 (1979).

[32] Ho, L., " Process Analysis and Optimal Design of a Fermentation Process Based Upon Elemental Balance Equations: Generalized Semitheoretical Equations for Estimating Rates of Oxygen Demand and Heat Evolution," *Biotechnol. Bioeng.*, **21**, 1289 (1979).

[33] Hogan, T., *CP/M User Guide*, McGraw Hill (1969).

[34] Jazwinski, A. H., *Stochastic Processes and Filtering Theory*, Academic Press, New York (1970).

[35] Jefferis, R. P. and A. E. Humphrey, *Proceedings of GIAM-IV*, Sao-Paulo, Brazil, July 23-28, 767 (1979).

[36] Jones, R. P. and P. F. Greenfield, "Effect of Carbon Dioxide on Yeast Growth and Fermentation," *Enzyme Microb. Technol.*, **4**, 210 (1982).

[37] Kjellen, K. J. and H. Y. Neujahr, "Enzyme Electrode for Phenol," *Biotechnol. Bioeng.*, **22**, 299 (1980).

[38] Koppel, L. B., *Introduction to Control Theory with Applications to Process Control*, Prentice-Hall, Englewood Cliffs, NJ (1967).

[39] Korus, R. A. and K. F. O'Driscoll, "The Influence of Diffusion of the Apparent Rate of Denaturation of Gel Entrapped Enzymes," *Biotechnol. Bioeng.*, **17**, 441 (1975) and **18**, 1656 (1976).

[40] Kulys, J. and K. Kadziauskiene, "Yeast BOD Sensor" *Biotechnol. Bioeng.*, **22**, 221 (1980).

[41] Laidler, K. J., and P. S. Bunting, *The Chemical Kinetics of Enzyme Action*, 2nd ed., Oxford University, England (1973).

[42] Lamda, H. S. and M. P. Dudukovic, "Analysis of Reactors with Immobilized Enzymes Subject to Deactivation," p. 106 *Chemical Reaction Engineering--II*, H. M. Hulburt, ed., *Advances in Chemistry*, Series 133, ACS, Washington, DC (1974).

[43] Lee, C. and H. Lim, "New Device for Continuously Monitoring the Optical Density of Concentrated Microbial Culture," *Biotechnol. Bioeng.*, **22**, 639 (1980).

[44] Lee, G. k., and P. J. Reilly, "The Effect of Slow Pore Diffusion and Observed Immobilized Enzyme Stability," 84th AIChE National Meeting, Atlanta (1978).

[45] Maddron, F., "Material Balance Calculations of Fermentation Processes," *Biotechnol. Bioeng.*, **21**, 1487 (1979).

[46] Mori H., T. Kobayashi, and S. Shimizu, "Effect of Carbon Dioxide on Growth of Microorganisms in Fed-Batch Cultures," *J. Ferment. Technol.*, **61**, 211 (1983).

[47] Ogunye, A.F. and Q. H. Ray, "Optimal Control Policies for Tubular Reactors Experiencing Catalyst Decay," *AIChE Journal*, **17**, 43 (1971).

[48] Ohno H. and E. Nakanishi, "Optimal Control of a Semi-batch Fermentation," *Biotechnol. Bioeng.*, **18**, 847 (1976).

[49] Ohno H. E. Nakabishi and K. Takamatsu, *Biotechnol. Bioeng.*, **20**, 625

(1978).

[50] Osborne, A., *An Introduction to Microcomputers Vol I Basic Concepts*, Adam Osborne and Associates, Inc. (1977).

[51] Park, S. H., S. B. Lee, and D .D. Y. Ryu, "Optimization of Operating Temperature for Continuous Glucoic Isomerase System," *Biotechnol. Bioeng.*, **23**, 1237 (1982).

[52] Pelczar, M. J. and E. C. S. Chan " Laboratory Exercises in Microbiology " McGraw Hill,(1977).

[53] Reiner, J. M., *Behaviour of Enzyme Systems*, Van Nostrand-Reinhold, New York (1969).

[54] Roels, J. A., " Application of Macroscopic Principles to Microbial Metabolism," *Biotechnol. Bioeng.*, **22**, 2457 (1980).

[55] Sadana, A., "A Generalized Optimum Temperature Operations Criterion for a Deactivating Immobilized Enzyme Batch Reactor," *AIChE Journal*, **25**, 535 (1979).

[56] Sargent, M. III and R. L. Shoemaker, *Interfacing Microcomputers to the Real World*, Addison-Wesley (1981).

[57] San, K.Y. and G. Stephanopoulos " Studies on the On-line Bioreactor Identification," *Biotechnol. Bioeng.*, (submitted) (1983).

[58] Seinfeld, J. H., G. R. Gavalas, and M. Hwang, "Control of Nonlinear Stochastic System," *Ind. Eng. Chem. Fundamentals*, **8**, No. 2, 257 (1979).

[59] Seinfeld, J. H., " Optimal Stochastic Control of Nonlinear Systems," *AIChE J.*, **16**, No. 6, 1016 (1970).

[60] Stephanopoulos, G. N. and K. Y. San, " State Estimation for Computer Control of Biochemical Reactors," Proc. VIth Int. Ferm. Symposium, July 20-25, 1980, London, Canada, Vol I, 399 (1981).

[61] Strehaiano, P., M. Mota, and G. Goma, "Effect of Inoculum Level on Kinetics of Alcoholic Fermentation," *Biotechnology Letters*, **5**, 135 (1983).

[62] Szepe, S. and O. Levenspiel, " Optimal Temperature Policies for Reactors Subject to Catalyst Deactivation - I Batch Reactor," *Chem. Eng. Sci.*, 881 (1968).

[63] Vadehra D. V. and W. D. Bellamy, " The Inhibition of *Thermomonospora* by Heat Sterilized Lactose Broth" *Biotechnology Letters* **5**, 63 (1983).

[64] Verhoff, F. H. and S. T. Schlager, " Enzyme Activity Maintenance in Packed Bed Reactors via Continuous Enzyme Addition," *Biotechnol. Bioeng.*, **23**, 41 (1981).

[65] Wang, H. Y., C. L. Cooney, and D. I. C. Wang, " Computer-Aided Baker's Yeast Fermentation," *Biotechnol. Bioeng.*, **19**, 69 (1977).

[66] Wang, H. Y., C. L. Cooney, and D. I. C. Wang, " Computer Control of Baker's Yeast Production," *Biotechnol. Bioeng.*, **21**, 975 (1979).

[67] Weigand, W. A., " Maximum Cell Productivity by Repeated Fed-Batch Culture for Constant Yield Case," *Biotechnol. Bioeng.*, **18**, 249 (1978).

[68] Weigand, W. A., H. C. Lim, C. C. Creajam, and R. D. Mohler, *Biotechnol. Bioeng. Symp.*, **9**, 335 (1979).

[69] Yamane, T., T. Kume, E. Sada, and T. Takamatsu, Culture for Constant Yield Case," *J. Ferment. Technol.*, **55**, 587 (1977).

[70] Yamashito, S., H. Hishashi, and T. Inagaki, *Proc.* 4^{th} Inter. Ferm. Symp.,

Japan, 1969, 441 (1969)

[71] Ziegler, W. M. and A. E. Humphrey, Paper presented at the 178th Annual ACS Meeting, Washington, D. C., September 10-13, 1979 (1979)